(12) INTERNATIONAL APPLICATION PUBLISHED UNDER THE PATENT COOPERATION TREATY (PCT)

(19) World Intellectual Property Organization
International Bureau

(43) International Publication Date
13 February 2025 (13.02.2025)

(10) International Publication Number
WO 2025/035127 A2

(51) International Patent Classification: *B29C 35/02* (2006.01)

(21) International Application Number: PCT/US2024/041788

(22) International Filing Date: 09 August 2024 (09.08.2024)

(25) Filing Language: English

(26) Publication Language: English

(30) Priority Data:
63/518,662 10 August 2023 (10.08.2023) US

(71) Applicant: **UNIVERSITY OF VIRGINIA PATENT FOUNDATION** [US/US]; 722 Preston Avenue, Suite 107, Charlottesville, Virginia 22903 (US).

(72) Inventors: **XU, Baoxing**; 805 Gilliams Mountain Rd., Charlottesville, Virginia 22903 (US). **ZHANG, Yue**; 20 South 36th Street, Philadelphia, Pennsylvania 19104 (US). **YIN, Mengtian**; 725 Denali Way, Charlottesville, Virginia 22903 (US).

(74) Agent: **JOHNSON, R. Brian** et al.; Meunier Carlin & Curfman LLC, 999 Peachtree Street, NE, Suite 1300, Atlanta, Georgia 30309 (US).

(81) Designated States *(unless otherwise indicated, for every kind of national protection available)*: AE, AG, AL, AM, AO, AT, AU, AZ, BA, BB, BG, BH, BN, BR, BW, BY, BZ, CA, CH, CL, CN, CO, CR, CU, CV, CZ, DE, DJ, DK, DM, DO, DZ, EC, EE, EG, ES, FI, GB, GD, GE, GH, GM, GT, HN, HR, HU, ID, IL, IN, IQ, IR, IS, IT, JM, JO, JP, KE, KG, KH, KN, KP, KR, KW, KZ, LA, LC, LK, LR, LS, LU, LY, MA, MD, MG, MK, MN, MU, MW, MX, MY, MZ, NA, NG, NI, NO, NZ, OM, PA, PE, PG, PH, PL, PT, QA, RO, RS, RU, RW, SA, SC, SD, SE, SG, SK, SL, ST, SV, SY, TH,

(54) Title: SYSTEMS AND METHODS FOR USING ELASTO-CAPILLARY ROLLING TRANSFER TO FORM SPATIAL STRUCTURES

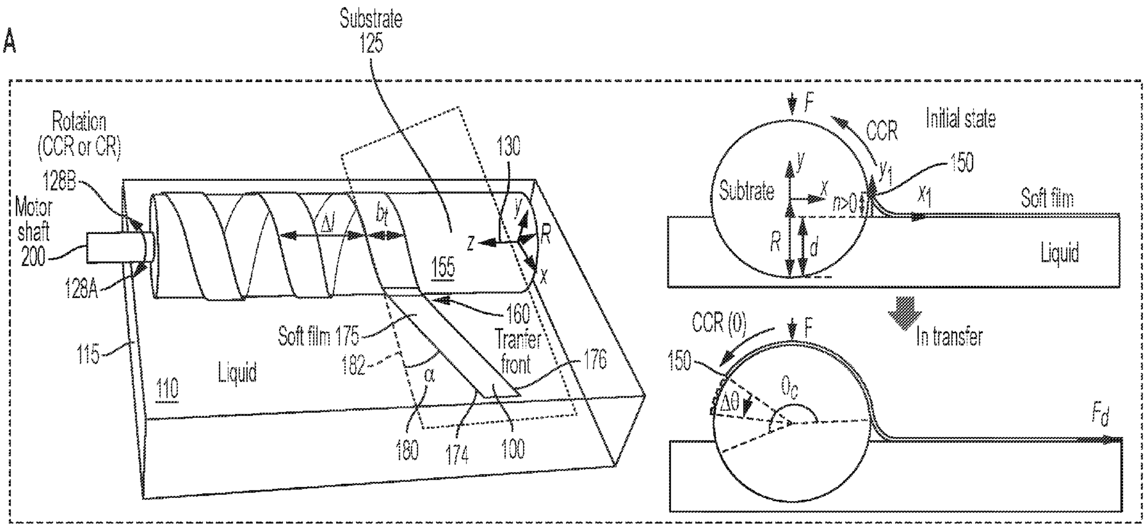

FIG. 1A

(57) Abstract: A system and method of forming an article include floating a pliable material onto a liquid held in a bath structure and placing a curvilinear substrate into the bath structure with the substrate having at least clockwise and counterclockwise rotational degrees of freedom, relative to a lengthwise axis of the substrate, within the liquid. A lateral edge of the pliable material is in contact with an outer surface of the curvilinear substrate to define a transfer front at an intersection of the lateral edge and the curvilinear substrate, and rotation of the curvilinear substrate advances a leading longitudinal edge of the pliable material onto the curvilinear substrate from the transfer front at an initial orientation angle, alpha (α), and an advanced orientation angle, beta (β), relative to the transfer front.

WO 2025/035127 A2

[Continued on next page]

TJ, TM, TN, TR, TT, TZ, UA, UG, US, UZ, VC, VN, WS, ZA, ZM, ZW.

(84) Designated States *(unless otherwise indicated, for every kind of regional protection available)*: ARIPO (BW, CV, GH, GM, KE, LR, LS, MW, MZ, NA, RW, SC, SD, SL, ST, SZ, TZ, UG, ZM, ZW), Eurasian (AM, AZ, BY, KG, KZ, RU, TJ, TM), European (AL, AT, BE, BG, CH, CY, CZ, DE, DK, EE, ES, FI, FR, GB, GR, HR, HU, IE, IS, IT, LT, LU, LV, MC, ME, MK, MT, NL, NO, PL, PT, RO, RS, SE, SI, SK, SM, TR), OAPI (BF, BJ, CF, CG, CI, CM, GA, GN, GQ, GW, KM, ML, MR, NE, SN, TD, TG).

Published:

— *without international search report and to be republished upon receipt of that report (Rule 48.2(g))*

SYSTEMS AND METHODS FOR USING ELASTO-CAPILLARY ROLLING TRANSFER TO FORM SPATIAL STRUCTURES

CROSS-REFERENCE TO RELATED APPLICATIONS

[0001] This application claims priority to and the benefit of U.S. provisional patent application No. 63/518,662, filed on August 10, 2023, and titled Elasto-Capillary Rolling Transfer Weaves Soft Materials to Spatial Structures, the disclosure of which is hereby incorporated by reference herein in its entirety.

STATEMENT OF GOVERNMENT RIGHTS

[0002] This invention was made with government support under Grant Nos. 1728149 and 1928788, awarded by The National Science Foundation. The government has certain rights in the invention.

BACKGROUND

[0003] Spatial structures of soft materials have attracted great interest because, by comparison to conventional planar counterparts, they not only inherit the unique properties of soft materials including low elastic modulus and high mechanical flexibility but also enrich a parameter control space of programing functionalities for a wide range of applications, such as soft robotics (1, 2), wearable electronics (3–6), micromachines (7, 8), microfluidic structures (9), and biomedical devices (10–12). Numerous approaches including direct three-dimensional (3D) printing (13–16) and electric (17), magnetic (18), thermal (19), and shape-memory (18)–driven assembly have been developed to fabricate the spatial structures of soft materials over the past years but usually suffer several practical constraints such as materials ink and printing resolution in 3D printing and intensity and control of exposures in environment stimuli-responsive assembly. As an alternative, mechanical programmable 3D assembly with the support of buckling mechanism is of particular interest because of their good compatibility with well-established planar fabrication processes and has been utilized to design spatial functional structures and devices with a broad variety of geometric morphologies (9, 20–23). Although shape memory materials, buckling modes, and bonding positions between the 2D precursors and pre-stretched soft substrate could be selected and controlled for obtaining desirable 3D structures including freestanding ones for robotic devices (24, 25), transferring the as-fabricated 3D structures onto a specific user set of substrates is challenging. Besides, it relies largely on 2D solid substrates with flat surfaces and requires ultrahigh mechanical stretchability that assists the achievement of large compressive buckling strain for pop-up 3D structures of 2D precursors. Compared with solid native substrates, liquid phase, an intrinsically mechanical strain-free substrate due to fluidity, could provide a unique and tactful platform that helps release rigid constraints for material fabrication, growth, self-assembly and also avoid residual stress or/and deformation mismatch with solid substrates and is considered an emerging host medium in the preparation of a wide variety of functional materials and devices. For example, liquid-assisted capillary peeling and transfer techniques have been recently developed to produce polymer/carbon nanotube composites–based flexible electronics (26), large-area 2D materials (27), patterned functional silicon membrane (28, 29), and biofilms (30), and the peeling can also help transform the 2D patterns to 3D shapes (31, 32). Liquid evaporation–induced folding and crumpling has also been designed in the assembly of 3D structures (33, 34). These liquid phase–assistant approaches are currently limited to generating or transferring material patterns and morphologies on a flat substrate and are of critical challenge to produce spatial structures with controllable geometries.

SUMMARY

[0004] A method of forming an article includes floating a pliable material onto a liquid held in a bath structure; placing a curvilinear substrate into the bath structure with the substrate having at least clockwise and counterclockwise rotational degrees of freedom, relative to a lengthwise axis of the substrate, within the liquid; placing a lateral edge of the pliable material in contact with an outer surface of the curvilinear substrate to define a transfer front at an intersection of the lateral edge and the curvilinear substrate, wherein rotation of the curvilinear substrate advances a leading longitudinal edge of the pliable material onto the curvilinear substrate from the transfer front; advancing the leading longitudinal edge onto the curvilinear substrate at an initial orientation angle, alpha (α), and an advanced orientation angle, beta (β), relative to the transfer front, wherein alpha is measured between a portion of the leading longitudinal edge of the pliable material floating on the liquid and a plane that is normal to both the outer surface of the curvilinear substrate and the lateral edge of the pliable material at the transfer front, and beta is measured between a second portion of the leading longitudinal edge of the pliable material that has advanced onto the curvilinear substrate and a plane extending vertically through both the curvilinear substrate and the second portion of the pliable material that has advanced onto the curvilinear substrate; and forming a pattern on the curvilinear substrate with the pliable material by advancing the pliable material onto the curvilinear substrate at the initial orientation angle and the advanced orientation angle.

[0005] A system for forming an article includes a bath structure containing a liquid for floating a pliable material onto the liquid; a curvilinear substrate in the bath structure with the substrate having at least clockwise and counterclockwise rotational degrees of freedom, relative to a lengthwise axis of the substrate, within the liquid; a power source connected to the longitudinal axis of the curvilinear substrate configured to rotate the curvilinear substrate in the clockwise direction and the counterclockwise direction; a lateral edge of the pliable material in contact with an outer surface of the curvilinear substrate to define a transfer front at an intersection of the lateral edge and the curvilinear substrate, wherein rotation of the curvilinear substrate advances a leading longitudinal edge of the pliable material onto the curvilinear substrate from the transfer front; wherein the pliable material comprises a leading longitudinal edge that intersects the curvilinear substrate at an initial orientation angle, alpha (α), and an advanced orientation angle, beta (β), relative to the transfer front, wherein alpha is measured between a portion of the leading longitudinal edge of the pliable material floating on the liquid and a plane that is normal to both the outer surface of the curvilinear substrate and the lateral edge of the pliable material at the transfer front; and beta is measured between a second portion of the leading longitudinal edge of the pliable material that has advanced onto the curvilinear substrate and a plane extending vertically through both the curvilinear substrate and the second portion of the pliable material that has advanced onto the curvilinear substrate.

BRIEF DESCRIPTION OF THE DRAWINGS

[0006] FIGS. 1A – 1E show schematic methods of elasto-capillary rolling transfer weaves soft film to spatial helical structure on curved substrates.

[0007] FIGS. 2A – 2E show schematic methods of weaving spatial structures with controllable ear-like local folded features by transfer.

[0008] FIG. 3A and 3B show schematic methods of weaving spatial structures with two soft films.

[0009] FIGS. 4A and 4B show schematic methods of transfer and assembly of multiple soft films (materials) without overlap onto a single substrate with the help of local folding deformation.

[0010] FIGS. 5A- 5C show application demonstrations of the woven freestanding spatial structure for thermal actuator with multimodal deformation.

[0011] FIG. 6A and FIG. 6B show a capillary-elastic theoretical analysis at the initial state of transfer.

[0012] FIG. 7 shows a schematic illustration (view in x-y plane) of the transfer process in CR rotation direction.

[0013] FIGS. 8A and 8B show theoretical calculations of the energy variation in the transfer process.

[0014] FIG. 9A and 9B show theoretical phase diagrams on the successful conditions of transfer.

[0015] FIG. 10 shows optical images (front view) of the rolling transfer experiment processes at a series of rotation circles in both CCR and CR rotation directions.

[0016] FIG. 11 shows optical images (front view) of the transferred film pattern after transfers with different alpha and rotation direction (CCR or CR).

[0017] FIG. 12 shows optical images (front view) of the transferred film pattern on substrate with different radius R for transfer in CCR direction.

[0018] FIG. 13 shows comparison between theoretical predictions and experimental measurements of the orientation angle beta and the normalized pitch.

[0019] FIGS. 14A and 14B show transfer of film with different thickness.

[0020] FIG. 15 shows optical images of the transferred film on curved substrates with various three dimensional geometry shapes.

[0021] FIGS. 16A , 16B, and 16C show theoretical analysis of the folding of film in dry air.

[0022] FIGS. 17A and 17B show theoretical analysis of the folding of film in liquid.

[0023] FIGS. 18A, 18B, and 18C show local fold structure for different film thickness.

[0024] FIG. 19 shows a schematic illustration (x-y plane view) of the transfer of spatial structure with multiple local ear-like folds onto substrate.

[0025] FIGS. 20A and 20B show a transferred pattern with different number of local folds.

[0026] FIGS. 21A and 21B show transfer in different starting rotation direction.

[0027] FIG. 22 shows transfer processes for the spatial structures with different distribution of local folds when the total number of folds n = 4.

[0028] FIG. 23 shows transfer processes for the spatial structures with different number of local folds embedded into the spatial layers when the total number n = 4.

[0029] FIG. 24 shows transfer processes for the spatial pattern with multiple local folds distributed in both angular and axial directions.

[0030] FIGS. 25A and 25B show a transfer with different rotation angles.

[0031] FIGS. 26A and 26B Transfer with different orientation angle alpha.

[0032] FIG. 27 shows optical images (front view and side view) of the transferred pattern distributed in a symmetrical way by the transfer with nonconstant rotation angles.

[0033] FIGS. 28A and 28B show weaving spatial structures with multiple soft films.

[0034] FIGS. 29A and 29B show transfer of multiple soft films with the help of local folding deformation.

[0035] FIGS. 30A, 30B and 30C show removal of the substrate for freestanding structures.

[0036] FIG. 31 shows pure torsion deformation of woven structure composed of PDMS/MWCNTs composite films with inclined weaving (intersection) positions in the pattern.

[0037] FIG. 32 shows PDMS/MWCNTs composite films-based spatial woven structure with two weaving order switch points (purple arrows in the schematic).

DETAILED DESCRIPTION

[0038] This disclosure reports on an elasto-capillary rolling transfer approach in a liquid substrate surface that enables a fast and facile weave and assembly of soft materials onto 3D curved substrate for spatial structures. The transfer could lead to spatial structures with desirable handedness, weaving orders, and arrangements on curved substrates with a broad diversity of geometry shapes including cylinder, sphere, and ones with changing curvature for single and multiple forms of soft wire, ribbon, and large-area film by controlling rolling direction and orientation and also could produce local structures with ear-like folded shapes by programming transfer directions. Applications on thermal actuation functionalities of freestanding spatial structures composed of thermal conductive soft films have been performed to demonstrate the weaving capability and robustness with well-designed controllability and programmability, potentially useful for mimicking soft and living matters and engineering soft functional devices with spatial structures.

[0039] Figs. 1 - 5 illustrate non-limiting embodiments of a method of forming an article that includes floating a pliable material 100 onto a liquid 110 held in a bath structure 115. The method includes placing a curvilinear substrate 125 into the bath structure with the substrate having at least clockwise 128A and counterclockwise 128B rotational degrees of freedom, relative to a lengthwise axis of the substrate, within the liquid. The method includes placing a lateral edge 150 of the pliable material in contact with an outer surface 155 of the curvilinear substrate to define a transfer front 160 at an intersection of the lateral edge and the curvilinear substrate, wherein rotation of the curvilinear substrate advances a leading longitudinal edge 175 of the pliable material onto the curvilinear substrate from the transfer front; advancing the leading longitudinal edge onto the curvilinear substrate at an initial orientation angle 180, alpha (α), and an advanced orientation angle 190, beta (β), relative to the transfer front, wherein alpha is measured between a portion 174 of the leading longitudinal edge 175 of the pliable material floating on the liquid and a plane 182 that is normal to both the outer surface of the curvilinear substrate and the lateral edge of the pliable material at the transfer front, and beta is measured between a second portion 179 of the leading longitudinal edge 175 of the pliable material that has advanced onto the curvilinear substrate and a different plane 173 extending vertically through both the curvilinear substrate and the second portion of the pliable material that has advanced onto the curvilinear substrate, and the method forms a pattern 187 on the curvilinear substrate with the pliable material by advancing the pliable material onto the curvilinear substrate at the initial orientation angle 180 and the advanced orientation angle 190.

[0040] The method further includes adjusting the initial orientation angle of the pliable material to form a weave pattern 250A, 250B on the curvilinear substrate, wherein the weave pattern comprises right-handed sections and left-handed sections of the pliable material overlapping on the curvilinear substrate.

[0041] The method further includes floating at least two pliable materials in the liquid and adjusting the respective initial orientation angles of the two pliable materials to form a weave pattern on the curvilinear substrate.

[0042] The method further includes floating at least two pliable materials in the liquid and adjusting the initial orientation angle of the two pliable materials to form a non-overlapping pattern of the pliable materials on the curvilinear substrate.

[0043] The method further includes adjusting the advanced orientation angle of the pliable material to change the pattern on the curvilinear substrate.

[0044] The method further includes adjusting the advanced orientation angle comprises moving the curvilinear substrate about a y axis that that is perpendicular to the longitudinal axis of the curvilinear substrate.

[0045] The method further includes adjusting the advanced orientation angle comprises moving a first portion of the pliable material that is floating in the liquid without changing the transfer front.

[0046] The method further includes changing the rotation direction of the curvilinear substrate to form folds 300 on the curvilinear substrate.

[0047] The method further includes removing the curvilinear substrate from the article.

[0048] In non-limiting embodiments, the curvilinear substrate defines a Cartesian coordinate system in which the longitudinal axis is a z axis, a y axis extends in a vertical direction that is perpendicular to the z axis, and an x axis extends in a horizontal direction that is perpendicular to the z axis.

[0049] A rotation direction of the curvilinear substrate may be either a clockwise rotation or a counterclockwise rotation of the curvilinear substrate about the z axis.

[0050] The rotation direction of the curvilinear substrate may include a first rotation angle 325, theta (ϑ) measured in a counterclockwise rotation direction from the x axis to the transfer front of the pliable material.

[0051] The rotation direction of the curvilinear substrate may include a second rotation 327 angle theta (ϑf) measured in a clockwise rotation direction from the transfer front of the pliable material to the x axis.

[0052] The curvilinear substrate defines a Cartesian coordinate system in which the longitudinal axis is a z axis, a y axis extends in a vertical direction that is perpendicular to the z axis, and an x axis extends in a horizontal direction that is perpendicular to the z axis, the method further comprising forming folds on the pliable material by changing a rotation direction of the curvilinear substrate at switch points on the second portion of the pliable material that has advanced onto the curvilinear substrate.

[0053] A changed rotation direction at a respective switch point includes a third rotation angle 329 (ϑc) measured as a third degree of rotation from a respective switch point to the x axis or from the x axis to the respective switch point for a respective clockwise rotation direction or counterclockwise rotation direction.

[0054] Floating the pliable material further comprises printing the pliable material onto the liquid in the bath structure.

[0055] The printing defines the initial orientation angle and the advanced orientation angle.

[0056] The printing changes the initial orientation angle or the advanced orientation angle while the pliable material advances onto the curvilinear substrate.

[0057] Forming folds on the pliable material may be accomplished by changing a rotation direction of the curvilinear substrate at switch points on the second portion of the pliable material that has advanced onto the curvilinear substrate, wherein the folds define a turn in the pliable material.

[0058] In non-limiting embodiments, the curvilinear substrate defines a Cartesian coordinate system in which the longitudinal axis is a z axis, a y axis extends in a vertical direction that is perpendicular to the z axis, and an x axis extends in a horizontal direction that is perpendicular to the z axis, wherein the turns in the pliable material are located at respective iterative angles measured from an initial x axis intersecting the transfer front and the turn.

[0059] The pliable material may include a first pliable material having a first transfer front on the curvilinear substrate and a second pliable material having a second transfer front on the curvilinear substrate, wherein the curvilinear substrate rotates to advance the first pliable material and the second pliable material into a weave pattern.

[0060] In another embodiment, a system for forming an article includes a bath structure containing a liquid for floating a pliable material onto the liquid. A curvilinear substrate is positioned in the bath structure with the substrate having at least clockwise and counterclockwise rotational degrees of freedom, relative to a lengthwise axis of the substrate, within the liquid. A power source, such as a motor connected to a computerized controller, may be connected to the longitudinal axis of the curvilinear substrate and configured to rotate the curvilinear substrate in the clockwise direction and the counterclockwise direction. A lateral edge of the pliable material is in contact with an outer surface of the curvilinear substrate to define a transfer front at an intersection of the lateral edge and the curvilinear substrate, wherein rotation of the curvilinear substrate advances a leading longitudinal edge of the pliable material onto the curvilinear substrate from the transfer front. The pliable material includes a leading longitudinal edge that intersects the curvilinear substrate at an initial orientation angle, alpha (α), and an advanced orientation angle, beta (β), relative to the transfer front, wherein alpha is measured between a portion of the leading longitudinal edge of the pliable material floating on the liquid and a plane that is normal to both the outer surface of the curvilinear substrate and the lateral edge of the pliable material at the transfer front; and beta is measured between a second portion of the leading longitudinal edge of the pliable material that has advanced onto the curvilinear substrate and a plane extending vertically through both the curvilinear substrate and the second portion of the pliable material that has advanced onto the curvilinear substrate.

[0061] In some embodiments, a computer having a processor and computer memory storing software controls the power source including but not limited to a motor that rotates the curvilinear substrate. The software implements computer commands that are configured to perform a method forming a pattern on the curvilinear substrate with the pliable material by advancing the pliable material onto the curvilinear substrate at the initial orientation angle and the advanced orientation angle. The method implemented by the software further includes adjusting the initial orientation angle of the pliable material to form a weave pattern on the curvilinear substrate, wherein the weave pattern comprises right-handed sections and left-handed sections of the pliable material overlapping on the curvilinear substrate. The method further includes changing the rotation direction of the curvilinear substrate to form folds on the curvilinear substrate. A printer such as a 3D printer may be used that prints the pliable material onto the liquid.

[0062] Figure 1A illustrates the working principle of the elasto-capillary rolling transfer. A cylinder substrate is partially submerged in the liquid bath with a certain depth, and the soft film is positioned onto the liquid surface near the substrate to form an initial contact line among substrate, film, and liquid, here referred to as the transfer front, with the direction of α relative to the perpendicular direction to the substrate (x-direction). Upon the sole rolling of the substrate in an either counterclockwise (CCR) or clockwise (CR) direction without translation motion, the film will detach from the liquid and gradually transits onto the substrate across the transfer front, until the entire film is wrapped around the curved surface of substrate. The transferred soft film will form a helical pattern on the substrate with a pitch length Δl. At the initial state of transfer, the soft film will be mechanically bent at the transfer front by the capillary force (top right schematic of Fig. 1A). With a negligible elongation and local deformation of the soft film at the transfer front (see note S1), our theoretical analysis shows that the transfer front must be above the liquid surface (i.e., $h > 0$ in Fig. 1A) to allow a pass of film moving upwards for the transfer along the CCR rotation direction; by contrast, the transfer along the CR direction requires the transfer front to be below the liquid surface with $h < 0$ (fig. S1A); $h = 0$ suggests that the capillary force is too small to bend the film and cannot drive the transfer of film onto the substrate, which can be used to determine the maximum flexural rigidity of film. In particular, to achieve a successful transfer of mechanically stiff films such as metal films, their thickness needs to be small enough to ensure that the bending stiffness of the films is below the maximum limit. Figure S1B summarizes the effect of the transfer conditions of liquid material phase, rolling velocity and surface wettability of substrate and film, and submerging depth of substrate into liquid on the selection of transfer directions. Once the rolling transfer direction of CCR or CR is determined, a successful transfer requires a continuous pass of film across the transfer front (Fig. 1A and 7) and can also be theoretically predicted by the energy-based model (note Fig. 6). In brief, the transfer process needs to be energy favorable with a decreased total energy with rotation in both transfer directions. In particular, when the viscosity of liquid is low, the mechanical tension energy associated with the stretching deformation of film can be neglected in comparison to its elastic bending energy (fig. S3A). This negligible tensile deformation suggests that no mechanical strain will be introduced to soft materials once transferred onto the substrate by the rolling transfer technique. Besides, a low level of rotation speed of substrate (<1 rev/s) will be used in the transfer to avoid the generation of liquid surface wave (*35*) and obtain a quasi-static stable transfer front. In addition, under a small rotation speed of substrate, our theoretical calculation (FIG. 8) shows that the energy dissipated because of the viscous drag force can be neglected. Besides, the selection of liquid substrate needs to satisfy a density requirement to ensure that the soft films stay on its surface to minimize the drag force of liquid and remain a stable transfer front during transfer. One should note that the transfer with the rotation angle $\theta \leq 360°$ (i.e., 1 revolution) is different from that with $\theta > 360°$ (i.e., multiple revolutions) for either CCR or CR rolling transfer, and Fig. 9 plots the theoretical phase diagrams of the criterion for a successful transfer of one and multiple revolutions on a wide variety of materials of soft films, transfer substrates, and liquid media and controlling parameters of rotation speed and orientation for both transfer directions of CCR and CR. The results indicate the transfer approach can be applied to materials with a broad range of properties and geometries.

[0063] Guided by the fundamental working principle and theoretical analysis, we conducted the rolling transfer experiments of a polydimethylsiloxane (PDMS) soft film (slightly dyed for vision, elastic modulus ~2 MPa) from a liquid water bath onto a cylinder substrate. With a rotation speed at 1 rpm, the film could be continuously transferred onto the substrate in either CCR or CR direction (fig. S5). In addition, guided by the theory, the initial orientation can be regulated to ensure that a long film can be fully wrapped onto the substrate. Figure 1B shows a spatial helical pattern of PDMS film on the substrate. With the CCR transfer, the helical pattern has a righthand "handedness," and with the CR transfer, the helical pattern has a left-hand "handedness." The initial orientation of film α could lead to different pitch Δl and orientation angle β of the transferred helix pattern, which can all be predicted in theory for both CR and CCR transfers (note S1). Figure 1C shows that at $\alpha \geq 0$, the orientation angle β is positive and increases with the increasing of α for CCR transfer, and the transferred pattern is right handed; the β is negative and decreases with the increasing of α for CR transfer, and the transferred pattern is left handed. Besides, the pitch normalized by width of soft film $\Delta l/b_t$ increases with the increasing of α and substrate radius R. By contrast, the β is independent of the R. The experimental measurements (Figs. 11 and 12) agree well with these theoretical calculations. Similar results are also obtained for $\alpha < 0$ (Fig. 13). In addition, at $\alpha = 0$, both the pitch and orientation angle become 0, and the transferred film will be fully overlapped at the same position on substrate for both CCR and CR transfer, as shown in Fig. 11.

[0064] Figure 1D shows that the normalized pitch decreases with the increasing of *bt/t* with remarkable consistency with theoretical predictions, where *bt* and *t* are width and thickness of film, respectively. At $\Delta l/bt < 1$, the transferred pattern shows an overlap, and vice visa. In particular, at bt/t approximately equal to 1, the soft film becomes a wire, and at $bt/t > 100$, the soft film can be considered a large-area film, indicating that this rolling transfer technique can be used to transfer soft materials with a broad variety of geometric shapes into desired patterns precisely in a well-controlled manner. Similar to that of Fig. 1C, the β of transferred patterns is independent of the geometry shapes of soft materials and the thickness (i.e., *bt/t*) even down to a few micrometers (Fig. 14). In addition, a series of successful transfer experiments of soft films onto 3D substrates with a diversity of geometry including cone, sphere, and saddle shapes confirm the robustness of this rolling transfer technique for potential complex spatial structures, as shown in Fig. 1E and Fig. S15. It should be noted that for transferring a large-area wide film onto a nondevelopable substrate counterpart, the films need to be carefully optimized in dimensions to achieve a conformal contact after transfer (*36*, *37*). The optimization design via structural meshing or network design (*38*, *39*) will help introduce extra degrees of freedom on films and relieve the geometric mismatch induced strain after transfer, and the basic size of each piece of optimized film elements could also be similar to the film dimensions that we demonstrated.

[0065] Different from a continuous unidirectional rotation for weaving structures of soft film with uniform spatial chirality, when the rotation direction switches during transfer, ear-like folded features can be achieved in the woven structures, as illustrated in Fig. 2A. Similar to that of weaving global spatial structures on the substrates in Fig. 1, the formation of these local morphologies is also an energy favorable process and can be predicted in theory (note FIG. 7). Figures 16 and 17 plot the theoretical predictions of minimum rotation angle θ required for successful folding and the radius of formed fold *r* fold for both dry-air and liquid conditions, and they both agree well with experiment measurements from Fig. 18.

[0066] Figure 2B shows the optical images (side view) of the transferred PDMS patterns with local folds. When the number of rolling direction switch *N*switch increases from one to four during transfer, the corresponding number of folds *n* will increase from one to four (Fig. 2B), in good agreement with the theoretical analysis (Fig. 19). When multiple folds are formed, they could be concentrated in a certain region with a very nonuniform distribution (Fig. 2B). In particular, they could be embedded into the spatial layers of the woven structures (Fig. 2Bc). The location and dimensional size of these folds can be well controlled by controlling the transfer direction and order and interval of switch (Figs. 20 to 23). Figure 2C shows the schematic illustration of woven structures with *n* local folds formed at $\alpha = 0$, where the folds are only located in angular (θ) direction. Both the location and size of folds can be predicted in theory (note Fig. 7 and Fig. 19), and agree very well with experimental measurements for different *N*switch and transfer directions, as shown in Fig. 2C.

[0067] When the initial orientation of film α is set to nonzero in the transfer, the fold could also be formed along the axial (*z*-) direction of the substrate, allowing to weave soft films onto a certain partial region of substrate, as illustrated in Fig. 24. With rolling transfer in CCR direction, $\alpha = 20°$, and periodic switch angle θf, Fig. 2D and Fig. 25 show the optical images of uniformly woven PDMS film on the cylinder substrate in both axial direction [front (*xz* plane) view] and angular direction [side (*xy* plane) view]. When the switch angle changes during the transfer, e.g., increases from 90° to 360°, the resultant woven pattern will also change, covering an increased angular area of the substrate from 90° to 360°. Because of its periodicity, the folds are formed in symmetry on the spatial cylinder substrate with angular spacing equal to θf, as shown in the schematic of Fig. 2E. Similar to that of folds at $\alpha = 0$ in Fig. 2C, the total number of formed folds and their dimensional size and angular spacing can also be theoretically predicted, as shown in Fig. 2E.

[0068] Besides, the axial spacing of folds Δ*Lf* is dependent on the switch angle and initial orientation as indicated in theory (note FIG. 7) and experiments (FIG. 26). Further, when the switch angle does not switch periodically with a sudden change, the woven patterns of film on the substrate will vary. For example, when a transition of 360° is introduced to the transfer, weaving the film on the cylinder substrate will change from one side to the opposite side, as shown in Fig. 2D.Weaving films on a desirable region onto the substrate with controllable spacing could also be achieved by programming the switch angle and transfer directions, as shown in FIG. 27. It should be noted that the local folds are helpful for weaving soft films to diverse and complex spatial patterns on partial regions of curved substrate because of their close association with necessary turning of weaving during transfer. Moreover, this fold feature could potentially be used as step increase of the *r* axis in the 3D manufacturing based on a cylindrical coordinate system (*r*-θ-*z*).

[0069] In addition, these folds offer an expandable operation space of woven films in response to external stimuli. For example, when an expansion of substrate occurs, the folds could be adjusted with spontaneous releasing to accommodate the mechanical expansion of the substrate, thereby providing mechanical protection to functionality and mechanical integrality of woven spatial structures of films, potentially useful in design of functional 3D structures and devices (*40*).

[0070] Figure 3A shows the optical images of two soft films transferred onto the cylinder. The same handedness for both of them is obtained because of the same rolling direction in transfer, leading to non-interlocked woven helical patterns. When their initial orientations (α) on liquid surface vary, the resultant pattern spacing will change, even becomes negative because of generation of the overlaps between them, as shown in Fig. 28. In particular, when their initial orientations are different, their handedness remain the same with non-interlocked woven patterns, in good consistency with theoretical predictions in Fig. 1C and Fig. 13. By contrast, when their transfer directions are opposite, they will be woven together with opposite handedness and orientation, forming an interlocked woven pattern, as shown in Fig. 3B. By controlling their initial orientations, different woven patterns on the substrate can be achieved.

[0071] For example, the same initial orientation leads to a symmetrically woven pattern (Fig. 3Ba), and the weaving (intersection) positions fall into a horizontal line at the center of the pattern. This symmetrically woven pattern is independent of the magnitudes of their initial orientations (FIG. 28A). The asymmetrically woven patterns can be obtained when the initial orientation of both films is different. The weaving positions can be also well controlled along an inclined line as shown in Fig. 3Bb. In addition to the regulation to the weaving patterns, we further conducted the experiments and obtained the interlocked woven patterns with different weaving orders. For example, Fig. 3Bc shows that the weaving order could change with the switch of relative positions between the red and blue films. Besides, both the number and location of the switch could be well controlled. When multiple films are transferred, diverse and complex weaving patterns can be obtained (Fig. 28B).

[0072] When local folding deformation is introduced by switching the rolling direction during transfer, the transfer of multiple films onto the cylinder substrate could be not interfered by each other without any overlap. Figure 4A shows the multiple PDMS films transferred on a single cylinder. In particular, when the number of transferred films N increases from two to four, the rolling angle θf during the transfer of each film needs to decrease from 180° to 90° to ensure no overlap among films. Further experiments show that the positions of films on the substrate can also be controlled well (Fig. 29A). In addition, by regulating the transition rolling angle during the transfer process, the films can be transferred to multiple positions on the substrate. For instance, with the transition angle 360°, for the transfer of two films (Fig. 4A), the film (dyed in blue) can be transferred from as-planned on the bottom (front view) and left (side view) part of the substrate at the beginning to the top (front view) and right (side view) part of the substrate. Similar results yet rich patterns are obtained when multiple films are transferred, as shown in Fig. 29.

[0073] When the folding is introduced along with the switch of rolling direction, a minimum rolling angle is required for a successful transfer (Fig. 16B and Fig. 7). As a result, there is a maximum capacity (Nmax) that allows to transfer the number of soft films onto substrate without overlap between each other (note Fig. 7). Figure 4B shows its theoretical predictions as a function of normalized film stiffness by liquid surface tension B/γl for different radius R of cylinder substrate. It suggests that for the thinner films with lower elastic modulus, the larger number of films could be allowed to transfer onto substrates with larger radius.

[0074] Once the transferred substrate is removed, spatial structures with programmable weaving orders and patterns suggest potential applications in mimicking living structures and systems in response to an external stimulus. The removal of the substrate can be conducted in liquid with the help of capillary interactions (Fig. 29). Figure 30B shows the comparison of both lengths and diameters at different intersection nodes of the structure measured before and after removal of the substrate. The nearly unchanged structure demonstrates a stable removal process without introduction of potential mechanical strain. For the substrate with a complex geometry shape and curvature, the removal could be performed with the aid of etching of sacrificial layer (*29*). Figure 30B also proves that the films in the freestanding woven structure can maintain the wrapped shape after the removal of substrate because of the adhesion in the woven overlap between films. Both theory and experiment in good agreement show that the freestanding structures could remain stable, and the stability depends on the balance between the gravity and stiffness (note FIG. 8and Fig. 30C). The spatial woven structure composed of two PDMS/multiwalled carbon nanotube (MWCNT) composite films, which have fast response to external heat (*41*), was taken as an example to demonstrate its function for desirable thermal actuation performance by programming the weaving patterns and orders of films. Depending on weaving patterns of spatial structures, bending, torsion, and their mixed mode of mechanical deformation can be achieved, as illustrated in Fig. 5A. Here, the on-demand weaving patterns can be realized by solely controlling the transfer conditions without the need of touching the properties and geometries of the film materials. For example, when one switch of weaving order is introduced to the spatial structures, bending deformation at the position of order switch will occur, and $c2 = 0$ (note Fig. 8). Therefore, the variation of energy ΔEs associated with bending deformation increases monotonically with the increasing of temperature ΔT as shown in Fig. 5A. In addition, this also indicates that the bending deformation of the structure is reversible when the temperature decreases because the bending deformation will not change the local weaving structure. For the woven structure with inclined weaving (intersection) positions (Fig. 5A, inset), the thermal expansion will lead to a torsion deformation of the structure. The energy associated with the torsion deformation increases with the increasing of temperature, and after the initial energy barrier it will decrease, as shown in Fig. 5A. This leads to irreversible torsion deformation when the temperature decreases. One should note that when the weaving order in the structures is uniform with weaving positions at the center, no mechanical deformation (i.e., bending and torsion) except for the symmetric expansion is expected (Fig. 5A), and therefore, there is no energy change due to mechanical deformation.

[0075] Figure 5B shows a series of experimental snapshots for spatial structures with bending deformation in response to 1 cycle of temperature increase and decrease, where the left end of the spatial structure was fixed to highlight the bending deformation. The structure is bent at the location of weaving order switch, and the bending angle increases with the increasing of time upon heating. Besides, when the temperature decreased back, the bending angle decreases until back to the original 0°, in a good consistency with the theoretical predictions. Similar results are also observed in experiment for torsion deformation of the woven structures, as shown in fig. S26. Different from the bending deformation, the local weaving positions were changed by torsion deformation, approaching to the center during the torsion deformation upon heating. Therefore, torsion deformation remains when the temperature decreases back. When multiple switches of weaving order are introduced in the woven structures, bending deformation at the corresponding locations are expected upon heating, suggesting the capability of programming modes of deformation. Figure 5C shows a variety of formed shapes. For example, when there are two switch points of weaving orders located at opposite sides of the structure, the woven structure will be bent at these two points, forming a C-shape pattern. When these two switch points are programmed to the same side, an L-shape pattern will be generated (Fig. 32).

[0076] When the switch points increase to four with uniform distance to opposite sides, an S-shape pattern can be obtained. Because the intersection positions of both films in these woven structures are located at the center, these shapes are all led by pure bending deformation and will be recovered to the original straight-line shape when the temperature decreases back, as shown in insets in Fig. 5C. By contrast, when a combination of bending and torsion deformation is involved, the programmed shape upon heating could remain. The formation of O-shape pattern involves five periodic switch points of weaving order that are distributed uniformly in the woven structure. Compared with the C-shape pattern, severe bending deformation occurs, indicating an O-shape pattern.

[0077] Besides, the torsion deformation occurred because of inclined intersection positions (highlight in green dash line) in the woven structure, and as a result, the shape will not recover when the temperature decreases. In addition, when the intersection positions are only inclined at the partial region of the structure, the woven structure could deform to a J-shape pattern upon heating. Upon cooling back to the original temperature, the partial pattern associated with pure bending deformation will recover, but that associated with combined bending and torsion deformation will remain, leading to a check mark–like shape. The achievements of these programmable shapes demonstrate potential applications of manipulating spatial soft structures, capable of mimicking response of living systems to environments and stimuli.

[0078] In summary, the elasto-capillary transfer technology with a rotational motion mode presented here introduces a weaving and assembly strategy for obtaining spatial structures of soft materials on curvilinear substrates. Fundamental studies of the rolling dynamics at the transfer front among soft material, curved substrate, and liquid surface and associated coupling of mechanical deformation of soft materials and fluid dynamics are conducted and establish the foundations for weaving soft materials with solid robustness and reliability. The achievements of woven spatial structures with controllable global weaving chirality, orders and arrangements, and local configurational features validate the feasibility of weaving soft materials into spatial structures by mechanical transfer. As application demonstrations, two thermally conductive films were woven into freestanding spatial structures with on-demand weaving patterns and orders. Their programmable robotic postures including bending, torsion, and their combination suggest potentials for broad applications.

[0079] Guided by theoretical analysis with the established parameter spaces of material selection and system control, integration of this technology with stimuli-responsive materials would help create future manufacturing technologies for fabricating a large diversity of active spatial structures with functionalities adaptive to application environments and could also invoke future exploration of unexpected properties of spatial structures woven by intrinsically planar nanomaterials.

[0080] In the fabrication of PDMS film, PDMS (Sylgard 184, Dow Corning Corp.) with 10:1 (otherwise stated) of base polymer to curing agent was first mixed and degassed. Small amount of dye (1.5% by weight) was also added in the mixture for visualization. The mixture was then poured into a Petri dish and placed in a 80°C oven for 2 hours to cure. In the fabrication of PDMS/MWCNT composite film, PDMS with 10:4 base polymer to hexane (n-Hexane, anhydrous, 95%, Sigma-Aldrich) was first mixed and then followed by the addition of MWCNTs (8 to 15 nm in diameter, 10 to 50 μm in length, 95%, NanoAmor Inc.). The PDMS-hexane/MWCNTs mixture was placed in an ultrasonicator for at least 12 hours with 40 kHz to achieve a homogeneous distribution of MWCNTs. Afterward, the PDMS curing agent was added to the mixture and then degassed before pouring into a glass tank mold. The mold was then delivered to a temperature control chamber to cure at 80°C for 1 hour. The characterization of the mechanical properties of the PDMS and PDMS/MWCNT films can be found in (*26*). Both PDMS and PDMS/MWCNT films were chosen in this work to represent a class of soft and composite materials, respectively. Cylindrical glass tubes with different radii were used as substrate in the transfer experiments, and the cylindrical substrates with several other kinds of geometric shapes (such as spherical and cone substrates) were fabricated using a 3D printer (Ultimaker 2+, Ultimaker). To adjust the surface wettability of cylinder substrate, a thin layer of PDMS (~100 μm in thickness) was coated onto the surface of substrates. PDMS (10:1 base polymer to curing agent) was mixed with n-Hexane in a 10:4 ratio and degassed. The mixture was then poured onto glass tubes to form a uniform layer of PDMS mixture. Coated glass tubes were then cured at 80°C for 2 hours.

[0081] In the rolling transfer experiments, a clean cylindrical substrate was first submerged in the liquid bath with a depth *d* and was in contact with one end of the desired film to form the contact line (referred to as the transfer front). The film was placed on the liquid surface with the help of soluble tape and could also be printed directly. The initial orientation between film and substrate is α as illustrated in Fig. 1A. One end of the horizontally oriented cylindrical substrate was fixed coaxially to the shaft of an electric motor. The substrate was driven by the motor to rotate in either clockwise (CR) or counterclockwise (CCR) direction (*35*, *42*). The rotation speed _θof the substrate could be well adjusted by the motor controller ranging from 1 up to 15 rpm. In each rotation, the overall rotation angle was calculated by θ ¼ _θ*T*, where *T* was the rotation time. During the rotation of substrate, if the transfer was successful, then the film would pass across the transfer front and would be gradually transferred onto the rotating substrate. If the transfer failed, then the film could not pass across the transfer front and would stay on the liquid surface. The rotation of substrate could be paused by the controller of motor at any rotation angle θ during the transfer process. Then, when the rotation direction was switched, the film would be folded on the substrate, and then transfer would continue in the new direction. However, if the folding failed, then the film would slide on the substrate and could not be transferred in the new direction. If the rotation direction was switched back and forth continuously in the transfer process, then film with multiple local folds could be transferred onto the substrate. The entire transfer process was recorded by the high-resolution camera placed near the liquid bath, and the image of the film pattern after transfer was also recorded by the high-resolution camera. The pitch Δl and orientation β of the transferred helical pattern were obtained using the image processing software as shown in Fig. 1B. The radius of the fold could also be obtained by the image processing as shown in Fig. 18. After a transfer, the substrate with film could be used as the substrate in the new transfer. In this way, multiple films could be transferred onto the substrate.

[0082] Besides, two films can also be transferred together at the same time to achieve woven pattern with desirable weaving orders. Initially, films 1 and 2 are placed at opposite side of the cylindrical substrate. In the first rotation, there can be a weaving order where film 2 (red) is on top of film 1 (blue). Then, to change this weaving order, a guidance of films 1 and 2 was required before next rotation, where films were to be pulled into the liquid, underneath the substrate, and out of the liquid to the opposite side of the substrate. The sequence of this guidance of films determines the desired weaving order. If film 2 was pulled first, then film 1 will be on top of film 2 instead in the next rotation, and then the woven pattern with a programmable weaving order can be achieved by repeating these processes.

[0083] At first, two PDMS/MWCNT composite films are used in the transfer considering the good thermal absorption behavior of MWCNTs (*41*). The diameter of the substrate was chosen as 6 mm to better maintain a stable spatial structure. The formation of spatial structure can be categorized into different types on the basis of the deformation mode (Fig. 5). Assembly of structure with bending mode started with the transfer of film 1 at α1 = 30° in CCR direction and film 2 at α2 = 30° in CR direction. Besides, the weaving order was changed at least once during the transfer process. Fabrication of structure with torsion mode was different in terms of the initial orientation α. While the initial orientation of film 1, α1, remained 30°, α2 became 27° to introduce the inclined weaving positions between films 1 and 2 in the pattern. After transfer, the woven spatial structure was made freestanding after taken off from the substrate with the help of capillary interaction (fig. S25A). Cylindrical substrate with transferred pattern was immersed into the liquid, and then the woven film structure can be easily pulled off from the substrate by hand. Freestanding structure was then carefully picked up from the liquid with a petri dish and then air-dried for further usage.

[0084] The woven spatial structure with on-demand weaving patterns and orders was first gently placed on the surface of the water bath and then both delivered to a temperature control chamber. Replacing conventional hard, solid substrate with water substrate helps reduce the friction force generated between films and solid substrate during actuation. One end of the structure was clamped for better imaging. Depending on different weaving patterns of structure, pure bending deformation, pure torsion deformation, and their combination in the structures can be realized by increasing the temperature in the chamber. After that, the temperature was decreased back to the original.

[0085] FIG. 6A and FIG. 6BG show a capillary-elastic theoretical analysis at the initial state of transfer. A, Schematic illustration (view in x-y plane) of the capillary-elastic analysis at the transfer front. For the transfer in clockwise (CR) rotation direction, the film needs to be bent downwards ($h < 0$) by the capillary force. $h = 0$ suggests the film cannot be transferred to the substrate. B, The theoretical phase diagram on the choice of the transfer direction with respect to materials (bending stiffness of soft film B, the static contact angle of substrate to the liquid θsl^s) and loading conditions (capillary number Ca and immerse displacement d), where $Ca* = 6 \times 10^{-5}$ (up), 2×10^{-4} (down), $d* = 1$ m . In the phase diagram, the blue and red area suggests conditions for the CR and CCR direction, respectively, the purple area is the condition where both directions are feasible, and the gray area is the condition where the film cannot be transferred.

[0086] FIG. 7 shows a schematic illustration (view in x-y plane) of the transfer process in CR rotation direction. The total rotation angle of substrate is θ . To ensure a continuous transfer, the process should be energy favorable in each increment of rotation angle $\Delta\theta$. θc is the angle corresponding to the part of substrate immersing in liquid.

[0087] FIGS. 8A and 8B show theoretical calculations of the energy variation in the transfer process. A, Theoretical calculations of the ratio of tension energy variation over bending energy variation $\Delta Etension/\Delta Ebending$ as a function of capillary number Ca for different type of liquid (low viscosity liquid water and high-viscosity liquid glycerol). B, Theoretical calculations of the ratio of viscous energy dissipation variation over surface energy variation $\Delta Eviscous/\Delta Esurface$ as a function of capillary number Ca for different type of liquid.

[0088] FIG. 9A and 9B show theoretical phase diagrams on the successful conditions of transfer. A, Theoretical phase diagrams on the successful conditions of continuous transfer, with respect to materials (bending stiffness of film B , liquid surface tension γl , static contact angle of film θtl and dynamic contact angle of substrate to the liquid $\theta sl\ d$), radius of substrate R and pitch distance Δl when the ratio of film/substrate adhesion energy over film/film adhesion energy Gts / $Gtt > 1$. In the theoretical diagram, the red and blue curves represent the theoretical predictions on critical condition of successful transfer for both CCR and CR directions. The orange area suggests conditions on successful transfer of 1 circle (nt=1) and purple area suggests conditions on successful transfer of multiple circles (nt>1), and the gray area is the condition where the film cannot be continuously transferred onto the substrate. B, Theoretical phase diagrams on the successful conditions of continuous transfer.

[0089] FIG. 10 shows optical images (front view) of the rolling transfer experiment processes at a series of rotation circles ($\boldsymbol{nt}$) in both CCR and CR rotation directions. In the experiments, the substrate is glass cylinder which is rotated by the electric motor, the liquid bath is water, and the film is PDMS film slightly dyed for visualization. In the CR transfer, the surface of glass cylinder is coated with a thin layer of PDMS to achieve the hydrophobic surface. The initial orientation is α. After the CCR transfer, the transferred film will form a right-handed helical pattern on the substrate when $\alpha > 0$. In contrast, the film will form a left-handed helical pattern for the CR transfer.

[0090] FIG. 11 shows optical images (front view) of the transferred film pattern after transfers with different $\boldsymbol{\alpha}$ and rotation direction (CCR or CR).

[0091] FIG. 12 shows optical images (front view) of the transferred film pattern on substrate with different radius R for transfer in CCR direction and $\boldsymbol{\alpha} = \mathbf{20}°$.

[0092] FIG. 13 shows comparison between theoretical predictions and experimental measurements of the orientation angle $\boldsymbol{\beta}$ and the normalized pitch $\boldsymbol{\Delta l/bt}$. Top figure: Theoretical predictions and experimental measurements of the orientation angle β of the transferred helical pattern for CCR and CR transfer directions when the initial orientation is negative ($\alpha < 0$). The orientation angle β is defined as positive when the helical pattern is right-handed and it's negative when the pattern is left-handed as shown in the insets. Bottom figure: Theoretical predictions and experimental measurements of the normalized pitch $\Delta l/bt$ of the transferred helical pattern for different substrate radius R when the initial orientation is negative ($\alpha < 0$). The error bar represents the standard deviation from the mean of 3 independent experiments.

[0093] FIGS. 14A and 14B show transfer of film with different thickness. A, Optical images (front view) of the transferred film with different thickness t. B, Comparison of the pitch distance $\Delta l/bt$ and orientation angle β of the transferred film pattern as a function of film thickness t between the theoretical calculations and experimental measurements. The error bar represents the standard deviation from the mean of 3 independent experiments.

[0094] FIG. 15 shows optical images of the transferred film on curved substrates with various three dimensional geometry shapes. A, Transfer of film onto spherical substrate by the transfer in CCR rotation direction. B, Transfer of film onto 3D curved substrates with different geometry shapes by the transfer in CR rotation direction.

[0095] FIGS. 16A , 16B, and 16C show theoretical analysis of the folding of film in dry air. A, Schematic illustration (xy plane view) of the folding of film through the switch of rotation direction in transfer. The soft film was first transferred onto the substrate with rotation angle θ in CCR direction, and then switch the transfer direction and rotates the substrate back for an angle θf , the film will be folded onto the substrate to form a local ear-like fold structure with radius r in the air. B, Theoretical phase diagrams on the successful conditions of folding of film. In the theoretical diagram, the red curves represent the minimum rotation angle θ required for successful folding of film as a function of $B/\gamma l$ for different initial angle α and film/film adhesion energy Gtt . C, Comparison of the radius of fold formed in the air r_{fold} (air) normalized by the radius of substrate R as a function of $B/\gamma l$ between the theoretical calculations and experimental measurements for different initial angle α and film/film adhesion energy Gtt . The error bar represents the standard deviation from the mean of 3 independent experiments.

[0096] FIGS. 17A and 17B show theoretical analysis of the folding of film in liquid. A, Schematic illustration (x-y plane view) of the folding of film through the switch of rotation direction in transfer. The soft film was first transferred onto the substrate with rotation angle θ in CR direction, and then switch the transfer direction and rotates the substrate back for an angle θf , the film will be folded onto the substrate to form a local ear-like fold structure with radius r in the liquid. B, Comparison of the radius of fold formed in the liquid $rfold$ $(liquid)$ normalized by the radius of substrate R as a function of $B/\gamma l$ between the theoretical calculations and experimental measurements for different initial angle α and film/film adhesion energy Gtt . The error bar represents the standard deviation from the mean of 3 independent experiments.

[0097] FIGS. 18A, 18B, and 18C show local fold structure for different film thickness. A, Optical images (side view) of the transferred pattern with a local fold structure for different film thickness t at $\alpha = 0°$ and $\alpha = 30°$, where the radius of fold $rfold$ can be obtained through image processing. B, Polar plot of the radius $rfold$ and position in θ-direction of the local fold for different thickness t at $\alpha = 0°$. C, Polar plot of the radius $rfold$ and position in θ -direction of the local fold for different thickness t at $\alpha = 30°$.

[0098] FIG. 19 shows a schematic illustration (x-y plane view) of the transfer of spatial structure with multiple local ear-like folds onto substrate. It's achieved by a series of direction switches (CCR to CR or CR to CCR) during the transfer process at $\alpha = 0$. The total number of folds n equals to the number of direction switch $Nswitch$. In these n folds, the ith ($1 \leq i \leq n$) fold is that formed in the ith direction switch. The position of the ith fold in the angular (θ) direction $\theta(i)$ can be controlled by adjusting the rotation angle $\theta f\ i$. And the fold can be formed in the air with radius $rfold\ (air)$ or in the liquid with radius $rfold\ (liquid)$.

[0099] FIGS. 20A and 20B show a transferred pattern with different number of local folds. A, Transfer processes for the spatial structures with different number n of local folds by using different $Nswitch$. B, Polar plot of the radius $rfold$ and position in θ direction of each fold in these transferred spatial structures.

[0100] FIGS. 21A and 21B show transfer in different starting rotation direction. A, Transfer processes using different starting rotation direction at $Nswitch = 4$. B, Polar plot of the radius $rfold$ and position in θ direction of folds in the transferred patterns.

[0101] FIG. 22 shows transfer processes for the spatial structures with different distribution of local folds when the total number of folds $\boldsymbol{n} = \mathbf{4}$.

[0102] FIG. 23 shows transfer processes for the spatial structures with different number of local folds embedded into the spatial layers when the total number $\boldsymbol{n} = \mathbf{4}$.

[0103] FIG. 24 shows transfer processes for the spatial pattern with multiple local folds distributed in both angular and axial directions. This is achieved by a series of direction switches (CCR to CR or CR to CCR) during the transfer process at a nonzero initial orientation α. The transferred film and local folds are distributed not only in the angular (θ) direction but also in the axial (z) direction. In the transferred pattern, the spacing angle between 2 neighboring folds in the angular (θ) direction can be controlled by the rotation angle θf.

[0104] FIGS. 25A and 25B show a transfer with different rotation angle $\boldsymbol{\theta f}$. A, Optical images (front view and side view) of the transferred pattern by the transfer with different rotation angle θf at $\alpha = 20°$, where the folds are distributed in both angular (θ) and axial (z) direction. B, Polar plot of the radius $rfold$ and position in θ direction of folds in these transferred patterns.

[0105] FIGS. 26A and 26B Transfer with different orientation angle $\boldsymbol{\alpha}$. A. Optical images (front view and side view) of the transferred pattern by the transfer with different α at $\theta f =$

180° . B, Optical images (front view and side view) of the transferred pattern by the transfer with different starting rotation direction at θf = 180°.

[0106] FIG. 27 shows optical images (front view and side view) of the transferred pattern distributed in a symmetrical way by the transfer with nonconstant rotation angles $\boldsymbol{\theta f i}$.

[0107] FIGS. 28A and 28B show weaving spatial structures with multiple soft films. A, Optical images of the noninterlocked woven and interlocked woven patterns assembled by the transfer of 2 films. The left 2 images are the non-interlocked woven patterns assembled by the transfer of 2 films in the same rotation direction. The right 2 images are the interlocked woven patterns assembled by the transfer of 2 films in the opposite rotation direction. B, Optical images of the woven patterns assembled by the transfer of 3 films. The left one is the non-interlocked woven pattern assembled by the transfer of 3 films in the same rotation direction. The right one is the pattern assembled by the transfer using different rotation directions.

[0108] FIGS. 29A and 29B show transfer of multiple soft films with the help of local folding deformation. A, Optical images (front and side views) of 2 PDMS films (dyed in different colors for visualization) transferred on a single glass cylinder, where the 1st transferred film (blue) is only woven on the top and right part of substrate and the 2nd transferred film (red) is only woven on the bottom and left part of substrate. B, Optical images (front, side and oblique views) of 3 PDMS films transferred on a single glass cylinder with transition rotation angle in the transfer. In the pattern, the 1st transferred film (blue) is originally woven on the top part of substrate. But with a transition rotation in the transfer, it becomes on the bottom part of substrate. The 3rd transferred film (purple) is arranged in the opposite way.

[0109] FIGS. 30A, 30B and 30C show removal of the substrate for freestanding structures. A, Schematic illustration of the processes for the fabrication of freestanding spatial woven structure. B, Experimental measurements of the lengths (L1, L2, L3, L4) and diameters (D1, D2, D3, D4) at different locations of the woven structure before and after removal of the substrate. C, Theoretical diagram on the required conditions to get stable freestanding structure, which was confirmed by experiment. The blue curve is the theoretical prediction on the critical radius R as a function of film stiffness $Et2$ for stable structure. The symbols and the optical images represent the experimental results, where the open symbol and its image denote an unstable structure, the solid symbol and its image denote a stable structure.

[0110] FIG. 31 shows pure torsion deformation of woven structure composed of PDMS/MWCNTs composite films with inclined weaving (intersection) positions in the pattern. Optical images at the center present the deformation state of the structure at different time during a temperature increase (heating)/temperature decrease (cooling) cycle in the experiment. The schematic indicates the weaving pattern of structure, where the green dash line highlights the weaving positions between 2 films. The green arrows indicate the torsion direction. The schematics indicate the local weaving positions in the structure were moved to the center (the green dash line becomes horizontal) due to torsion deformation upon heating. Therefore, there is no torsion anymore in the cooling process. Errors of the torsion angle ϕt measurement are 0.5°. Scale bar is 1cm.

[0111] FIG. 32 shows PDMS/MWCNTs composite films-based spatial woven structure with two weaving order switch points (purple arrows in the schematic). It will be bent to form the L-shape pattern upon heating in the experiment. Bottom optical images show the structure can return to its initial shape in the cooling process because there is only bending deformation. Scale bar is 5 cm.

[0112] Numerous other general purpose or special purpose computing devices environments or configurations may be used. Examples of well-known computing devices, environments, and/or configurations that may be suitable for use include, but are not limited to, personal computers, server computers, handheld or laptop devices, multiprocessor systems, microprocessor-based systems, GPU-based systems, network personal computers (PCs), minicomputers, mainframe computers, embedded systems, distributed computing environments that include any of the above systems or devices, and the like. Special purpose computing devices, environments, and/or configurations that may be suitable for use include, but are not limited to, digital circuits, analog circuits, photonics-based circuits, and quantum computer circuits inasmuch the neural network weights and connections can be represented and processed, either by direct means or by transformation to a different state space that can represent such computation.

[0113] Computer-executable instructions, such as program modules, being executed by a computer may be used. Generally, program modules include routines, programs, objects, components, data structures, etc. that perform particular tasks or implement particular abstract data types. Distributed computing environments may be used where tasks are performed by remote processing devices that are linked through a communications network or other data transmission medium. In a distributed computing environment, program modules and other data may be located in both local and remote computer storage media including memory storage devices.

[0114] Depending on the exact configuration and type of computing device, memory may be volatile (such as random-access memory (RAM)), non-volatile (such as read-only memory (ROM), flash memory, etc.), or some combination thereof.

[0115] Computing device may have additional features/functionality. For example, computing device may include additional storage (removable and/or non-removable) including, but not limited to, magnetic or optical disks or tape.

[0116] Computing devices typically include a variety of computer readable media. Computer readable media can be any available media that can be accessed by the device and includes both volatile and non-volatile media, removable and non-removable media.

[0117] Computer storage media include volatile and non-volatile, and removable and non-removable media implemented in any method or technology for storage of information such as computer readable instructions, data structures, program modules or other data. Memory, removable storage, and non-removable storage are all examples of computer storage media. Computer storage media include, but are not limited to, RAM, ROM, electrically erasable program read-only memory (EEPROM), flash memory or other memory technology, CD-ROM, digital versatile disks (DVD) or other optical storage, magnetic cassettes, magnetic tape, magnetic disk storage or other magnetic storage devices, or any other medium which can be used to store the desired information and which can be accessed by computing device.

[0118] Computing device 200 may contain communication connection(s) that allow the device to communicate with other devices. Computing device may also have input device(s) such as a keyboard, mouse, pen, voice input device, touch input device, etc. Output device(s) such as a display, speakers, printer, etc. may also be included. All these devices are well known in the art and need not be discussed at length here. For purposes herein, the computing devices of this disclosure may include a clock and a GPS or mapping system. The location of an original data source and the time of its acquisition can be used to authenticate the data and even play a role in data valuations according to this disclosure.

[0119] It should be understood that the various techniques described herein may be implemented in connection with hardware components or software components or, where appropriate, with a combination of both. Illustrative types of hardware components that can be used include Field-programmable Gate Arrays (FPGAs), Application-specific Integrated Circuits (ASICs), Application-specific Standard Products (ASSPs), System-on-a-chip systems (SOCs), Complex Programmable Logic Devices (CPLDs), etc. The methods and apparatus of the presently disclosed subject matter, or certain aspects or portions thereof, may take the form of program code (i.e., instructions) embodied in tangible media, such as floppy diskettes, CD-ROMs, hard drives, or any other machine-readable storage medium where, when the program code is loaded into and executed by a machine, such as a computer, the machine becomes an apparatus for practicing the presently disclosed subject matter.

[0120] Although exemplary implementations may refer to utilizing aspects of the presently disclosed subject matter in the context of one or more stand-alone computer systems, the subject matter is not so limited, but rather may be implemented in connection with any computing environment or other distributed computing environments. Still further, aspects of the presently disclosed subject matter may be implemented in or across a plurality of processing chips or devices, and storage may similarly be implemented across a plurality of devices. Such devices might include personal computers, network servers, and handheld devices, for example.

[0121]

References

1. T. Xu, J. Zhang, M. Salehizadeh, O. Onaizah, E. Diller, Millimeter-scale flexible robots with programmable three-dimensional magnetization and motions. *Sci. Robot.* 4, eaav4494 (2019).

2. W. Hu, G. Z. Lum, M. Mastrangeli, M. Sitti, Small-scale soft-bodied robot with multimodal

locomotion. *Nature* 554, 81–85 (2018).

3. J. H. Lee, C. Y. Koh, J. P. Singer, S. J. Jeon, M. Maldovan, O. Stein, E. L. Thomas, 25th anniversary

article: Ordered polymer structures for the engineering of photons and phonons. *Adv. Mater.* 26, 532–569 (2014).

4. C. Choi, M. K. Choi, S. Liu, M. S. Kim, O. K. Park, C. Im, J. Kim, X. Qin, G. J. Lee, K.W. Cho, M. Kim, E. Joh, J. Lee, D. Son, S.-H. Kwon, N. L. Jeon, Y. M. Song, N. Lu, D.-H. Kim, Human eye-inspired soft optoelectronic device using high-density MoS2-graphene curved image sensor array. *Nat. Commun.* 8, 1664 (2017).

5. M. Boncheva, S. A. Andreev, L. Mahadevan, A. Winkleman, D. R. Reichman, M. G. Prentiss, S. Whitesides, G. M. Whitesides, Magnetic self-assembly of three-dimensional surfaces from planar sheets. *Proc. Natl. Acad. Sci. U.S.A.* 102, 3924–3929 (2005).

6. K. Sim, S. Chen, Z. Li, Z. Rao, J. Liu, Y. Lu, S. Jang, F. Ershad, J. Chen, J. Xiao, C. Yu, Threedimensional curvy electronics created using conformal additive stamp printing. *Nat. Electron.* 2, 471–479 (2019).

7. J. Cui, T.-Y. Huang, Z. Luo, P. Testa, H. Gu, X.-Z. Chen, B. J. Nelson, L. J. Heyderman, Nanomagnetic encoding of shape-morphing micromachines. *Nature* 575, 164–168 (2019).

8. S. Fusco, M. S. Sakar, S. Kennedy, C. Peters, R. Bottani, F. Starsich, A. Mao, G. A. Sotiriou, S. Pane, S. E. Pratsinis, B. J. Nelson, An integrated microrobotic platform for on-demand, targeted therapeutic interventions. *Adv. Mater.* 26, 952–957 (2014).

9. H. Luan, Q. Zhang, T.-L. Liu, X. Wang, S. Zhao, H. Wang, S. Yao, Y. Xue, J. W. Kwak, W. Bai, Y. Xu, M. Han, K. Li, Z. Li, X. Ni, J. Ye, D. Choi, Q. Yang, J.-H. Kim, S. Li, S. Chen, C. Wu, D. Lu, J.-K. Chang, Z. Xie, Y. Huang, J. A. Rogers, Complex 3D microfluidic architectures formed by mechanically guided compressive buckling. *Sci. Adv.* 7, eabj3686 (2021).

10. X. Liu, H. Yuk, S. Lin, G. A. Parada, T. C. Tang, E. Tham, C. de la Fuente-Nunez, T. K. Lu, X. Zhao, 3D printing of living responsive materials and devices. *Adv. Mater.* 30, 1704821 (2018).

11. X. Zhao, J. Kim, C. A. Cezar, N. Huebsch, K. Lee, K. Bouhadir, D. J. Mooney, Active scaffolds for on-demand drug and cell delivery. *Proc. Natl. Acad. Sci. U.S.A.* 108, 67–72 (2011).

12. M. Sitti, Miniature soft robots—Road to the clinic. *Nat. Rev. Mater.* 3, 74–75 (2018).

13. X. Wang, M. Jiang, Z. Zhou, J. Gou, D. Hui, 3D printing of polymer matrix composites: A review and prospective. Compos. B Eng. 110, 442–458 (2017).

14. C. B. Dayan, S. Chun, N. Krishna-Subbaiah, D. M. Drotlef, M. B. Akolpoglu, M. Sitti, 3D printing of elastomeric bioinspired complex adhesive microstructures. Adv. Mater. 33, 2103826 (2021).

15. A. Kotikian, R. L. Truby, J. W. Boley, T. J. White, J. A. Lewis, 3D printing of liquid crystal elastomeric actuators with spatially programed nematic order. Adv. Mater. 30, 1706164 (2018).

16. Z. Wang, Z. Wang, Y. Zheng, Q. He, Y. Wang, S. Cai, Three-dimensional printing of functionally graded liquid crystal elastomer. Sci. Adv. 6, eabc0034 (2020).

17. M. K. Blees, A.W. Barnard, P. A. Rose, S. P. Roberts, K. L. McGill, P. Y. Huang, A. R. Ruyack, J.W. Kevek, B. Kobrin, D. A. Muller, P. L. McEuen, Graphene kirigami. Nature 524, 204–207 (2015).

18. Q. Zhao, W. Zou, Y. Luo, T. Xie, Shape memory polymer network with thermally distinct elasticity and plasticity. Sci. Adv. 2, e1501297 (2016).

19. M. Z. Miskin, K. J. Dorsey, B. Bircan, Y. Han, D. A. Muller, P. L. McEuen, I. Cohen, Graphene based bimorphs for micron-sized, autonomous origami machines. Proc. Natl. Acad. Sci. U.S.A. 115, 466–470 (2018).

20. H. Fu, K. Nan,W. Bai,W. Huang, K. Bai, L. Lu, C. Zhou, Y. Liu, F. Liu, J.Wang, M. Han, Z. Yan, H. Luan, Y. Zhang, Y. Zhang, J. Zhao, X. Cheng, M. Li, J.W. Lee, Y. Liu, D. Fang, X. Li, Y. Huang, Y. Zhang, J. A. Rogers, Morphable 3D mesostructures and microelectronic devices by multistable buckling mechanics. Nat. Mater. 17, 268–276 (2018).

21. Z. Yan, F. Zhang, J.Wang, F. Liu, X. Guo, K. Nan, Q. Lin, M. Gao, D. Xiao, Y. Shi, Y. Qiu, H. Luan, J. H. Kim, Y. Wang, H. Luo, M. Han, Y. Huang, Y. Zhang, J. A. Rogers, Controlled mechanical buckling for origami-inspired construction of 3D microstructures in advanced materials. Adv. Funct. Mater. 26, 2629–2639 (2016).

22. J. Shim, C. Perdigou, E. R. Chen, K. Bertoldi, P. M. Reis, Buckling-induced encapsulation of structured elastic shells under pressure. Proc. Natl. Acad. Sci. U.S.A. 109, 5978–5983 (2012).

23. Y. Li, H. Yu, K. Yu, X. Guo, X. Wang, Reconfigurable three-dimensional meso-structures of spatially programmed liquid crystal elastomers and their ferromagnetic composites. Adv. Funct. Mater. 31, 2100338 (2021).

24. W. Lee, Y. Liu, Y. Lee, B. K. Sharma, S. M. Shinde, S. D. Kim, K. Nan, Z. Yan, M. Han, Y. Huang, Y. Zhang, J.-H. Ahn, J. A. Rogers, Two-dimensional materials in functional three-dimensional architectures with applications in photodetection and imaging. Nat. Commun. 9, 1417 (2018).

25. S. Xu, Z. Yan, K.-I. Jang, W. Huang, H. Fu, J. Kim, Z. Wei, M. Flavin, J. McCracken, R. Wang, A. Badea, Y. Liu, D. Xiao, G. Zhou, J. Lee, H. U. Chung, H. Cheng, W. Ren, A. Banks, X. Li, U. Paik, R. G. Nuzzo, Y. Huang, Y. Zhang, J. A. Rogers, Assembly of

micro/nanomaterials into complex, three-dimensional architectures by compressive buckling. Science 347, 154–159 (2015).

26. Y. Zhang, M. Yin, Y. Baek, K. Lee, G. Zangari, L. Cai, B. Xu, Capillary transfer of soft films. Proc. Natl. Acad. Sci. U.S.A. 117, 5210–5216 (2020).

27. A. Okmi, X. Xiao, Y. Zhang, R. He, O. Olunloyo, S. B. Harris, T. Jabegu, N. Li, D. Maraba, Y. Sherif, O. Dyck, I. Vlassiouk, K. Xiao, P. Dong, B. Xu, S. Lei, Discovery of graphene-water membrane structure: Toward high-quality graphene process. Adv. Sci. 9, 2201336 (2022).

28. J. K. Park, Y. Zhang, B. Xu, S. Kim, Pattern transfer of large-scale thin membranes with controllable self-delamination interface for integrated functional systems. Nat. Commun. 12, 6882 (2021).

29. D. S. Wie, Y. Zhang, M. K. Kim, B. Kim, S. Park, Y.-J. Kim, P. P. Irazoqui, X. Zheng, B. Xu, C. H. Lee, Wafer-recyclable, environment-friendly transfer printing for large-scale thin-film nanoelectronics. Proc. Natl. Acad. Sci. U.S.A. 115, E7236–E7244 (2018).

30. J. Yan, A. Moreau, S. Khodaparast, A. Perazzo, J. Feng, C. Fei, S. Mao, S. Mukherjee, A. Košmrlj, N. S. Wingreen, B. L. Bassler, H. A. Stone, Bacterial biofilm material properties enable removal and transfer by capillary peeling. Adv. Mater. 30, 1804153 (2018).

31. S.W. Song, S. Lee, J. K. Choe, N.-H. Kim, J. Kang, A. C. Lee, Y. Choi, A. Choi, Y. Jeong,W. Lee, J.- Y. Kim, S. Kwon, J. Kim, Direct 2D-to-3D transformation of pen drawings. Sci. Adv. 7, eabf3804 (2021).

32. F. Zhang, D. Li, C.Wang, Z. Liu, M. Yang, Z. Cui, J. Yi, M.Wang, Y. Jiang, Z. Lv, S.Wang, H. Gao, X. Chen, Shape morphing of plastic films. Nat. Commun. 13, 7294 (2022).

33. C. Py, P. Reverdy, L. Doppler, J. Bico, B. Roman, C. N. Baroud, Capillary origami: Spontaneous wrapping of a droplet with an elastic sheet. Phys. Rev. Lett. 98, 156103 (2007).

34. J. Luo, H. D. Jang, T. Sun, L. Xiao, Z. He, A. P. Katsoulidis, M. G. Kanatzidis, J. M. Gibson, J. Huang, Compression and aggregation-resistant particles of crumpled soft sheets. ACS Nano 5, 8943–8949 (2011).

35. F. Henrich, D. Fell, D. Truszkowska, M. Weirich, M. Anyfantakis, T.-H. Nguyen, M. Wagner, G. K. Auernhammer, H.-J. Butt, Influence of surfactants in forced dynamic dewetting. Soft Matter 12, 7782–7791 (2016).

36. S. Liu, J. He, Y. Rao, Z. Dai, H. Ye, J. C. Tanir, Y. Li, N. Lu, Conformability of flexible sheets on spherical surfaces. Sci. Adv. 9, eadf2709 (2023).

37. Q. Liu, J. Huang, B. Xu, Evaporation-driven crumpling and assembling of two-dimensional (2D) materials: A rotational spring–mechanical slider model. *J. Mech. Phys. Solids* 133, 103722 (2019).

38. J. Liu, S. Jiang, W. Xiong, C. Zhu, K. Li, Y. Huang, Self-healing kirigami assembly strategy for conformal electronics. *Adv. Funct. Mater.* 32, 2109214 (2022).

39. Y.-K. Lee, Z. Xi, Y.-J. Lee, Y.-H. Kim, Y. Hao, H. Choi, M.-G. Lee, Y.-C. Joo, C. Kim, J.-M. Lien, I.-S. Choi, Computational wrapping: A universal method to wrap 3D-curved surfaces with nonstretchable materials for conformal devices. *Sci. Adv.* 6, eaax6212 (2020).

40. Y. Park, C. K. Franz, H. Ryu, H. Luan, K. Y. Cotton, J. U. Kim, T. S. Chung, S. Zhao, A. Vazquez-Guardado, D. S. Yang, K. Li, R. Avila, J. K. Phillips, M. J. Quezada, H. Jang, S. S. Kwak, S. M. Won, K. Kwon, H. Jeong, A. J. Bandodkar, M. Han, H. Zhao, G. R. Osher, H. Wang, K. H. Lee, Y. Zhang, Y. Huang, J. D. Finan, J. A. Rogers, Three-dimensional, multifunctional neural interfaces for cortical spheroids and engineered assembloids. *Sci. Adv.* 7, eabf9153 (2021).

41. L. Chen, C. Liu, K. Liu, C. Meng, C. Hu, J. Wang, S. Fan, High-performance, low-voltage, and easy-operable bending actuator based on aligned carbon nanotube/polymer composites. *ACS Nano* 5, 1588–1593 (2011).

42. B. A. Puthenveettil, V. K. Senthilkumar, E. Hopfinger, Motion of drops on inclined surfaces in the inertial regime. *J. Fluid Mech.* 726, 26–61 (2013)

CLAIMS

1. A method of forming an article, comprising:

floating a pliable material onto a liquid held in a bath structure;

placing a curvilinear substrate into the bath structure with the substrate having at least clockwise and counterclockwise rotational degrees of freedom, relative to a lengthwise axis of the substrate, within the liquid;

placing a lateral edge of the pliable material in contact with an outer surface of the curvilinear substrate to define a transfer front at an intersection of the lateral edge and the curvilinear substrate, wherein rotation of the curvilinear substrate advances a leading longitudinal edge of the pliable material onto the curvilinear substrate from the transfer front;

advancing the leading longitudinal edge onto the curvilinear substrate at an initial orientation angle, alpha (α), and an advanced orientation angle, beta (β), relative to the transfer front, wherein:

alpha is measured between a portion of the leading longitudinal edge of the pliable material floating on the liquid and a plane that is normal to both the outer surface of the curvilinear substrate and the lateral edge of the pliable material at the transfer front;

beta is measured between a second portion of the leading longitudinal edge of the pliable material that has advanced onto the curvilinear substrate and a plane extending vertically through both the curvilinear substrate and the second portion of the pliable material that has advanced onto the curvilinear substrate; and

forming a pattern on the curvilinear substrate with the pliable material by advancing the pliable material onto the curvilinear substrate at the initial orientation angle and the advanced orientation angle.

2. The method of Claim 1, further comprising adjusting the initial orientation angle of the pliable material to form a weave pattern on the curvilinear substrate, wherein the weave pattern comprises right-handed sections and left-handed sections of the pliable material overlapping on the curvilinear substrate.

3. The method of Claim 1, further comprising floating at least two pliable materials in the liquid and adjusting the respective initial orientation angles of the two pliable materials to form a weave pattern on the curvilinear substrate.

4. The method of Claim 1, further comprising floating at least two pliable materials in the liquid and adjusting the initial orientation angle of the two pliable materials to form a non-overlapping pattern of the pliable materials on the curvilinear substrate.

5. The method of Claim 1, further comprising adjusting the advanced orientation angle of the pliable material to change the pattern on the curvilinear substrate.

6. The method of Claim 5, wherein adjusting the advanced orientation angle comprises moving the curvilinear substrate about a y axis that that is perpendicular to the longitudinal axis of the curvilinear substrate.

7. The method of Claim 5, wherein adjusting the advanced orientation angle comprises moving a first portion of the pliable material that is floating in the liquid without changing the transfer front.

8. The method of Claim 1, further comprising changing the rotation direction of the curvilinear substrate to form folds on the curvilinear substrate.

9. The method of Claim 1, further comprising removing the curvilinear substrate from the article.

10. The method of Claim 1, wherein the curvilinear substrate defines a Cartesian coordinate system in which the longitudinal axis is a z axis, a y axis extends in a vertical

direction that is perpendicular to the z axis, and an x axis extends in a horizontal direction that is perpendicular to the z axis.

11. The method of Claim 10, wherein a rotation direction of the curvilinear substrate comprises either a clockwise rotation or a counterclockwise rotation of the curvilinear substrate about the z axis.

12. The method of Claim 10, wherein the rotation direction of the curvilinear substrate comprises a first rotation angle theta (ϑ) measured in a counterclockwise rotation direction from the x axis to the transfer front of the pliable material.

13. The method of Claim 10, wherein the rotation direction of the curvilinear substrate comprises a second rotation angle theta (ϑf) measured in a clockwise rotation direction from the transfer front of the pliable material to the x axis.

14. The method of Claim 1, wherein the curvilinear substrate defines a Cartesian coordinate system in which the longitudinal axis is a z axis, a y axis extends in a vertical direction that is perpendicular to the z axis, and an x axis extends in a horizontal direction that is perpendicular to the z axis, the method further comprising forming folds on the pliable material by changing a rotation direction of the curvilinear substrate at switch points on the second portion of the pliable material that has advanced onto the curvilinear substrate.

15. The method of Claim 14, wherein a changed rotation direction at a respective switch point comprises a third rotation angle (ϑc) measured as a third degree of rotation from a respective switch point to the x axis or from the x axis to the respective switch point for a respective clockwise rotation direction or counterclockwise rotation direction.

16. The method of Claim 1, wherein floating the pliable material further comprises printing the pliable material onto the liquid in the bath structure.

17. The method of Claim 16, wherein the printing defines the initial orientation angle and the advanced orientation angle.

18. The method of Claim 17, wherein the printing changes the initial orientation angle or the advanced orientation angle while the pliable material advances onto the curvilinear substrate.

19. The method of Claim 1, further comprising forming folds on the pliable material by changing a rotation direction of the curvilinear substrate at switch points on the second portion of the pliable material that has advanced onto the curvilinear substrate, wherein the folds define a turn in the pliable material.

20. The method of Claim 1, wherein the curvilinear substrate defines a Cartesian coordinate system in which the longitudinal axis is a z axis, a y axis extends in a vertical direction that is perpendicular to the z axis, and an x axis extends in a horizontal direction that is perpendicular to the z axis, wherein the turns in the pliable material are located at respective iterative angles measured from an initial x axis intersecting the transfer front and the turn.

21. The method of Claim 1, wherein the pliable material comprises a first pliable material having a first transfer front on the curvilinear substrate and a second pliable material having a second transfer front on the curvilinear substrate, wherein the curvilinear substrate rotates to advance the first pliable material and the second pliable material into a weave pattern.

22. A system for forming an article, comprising:

a bath structure containing a liquid for floating a pliable material onto the liquid;

a curvilinear substrate in the bath structure with the substrate having at least clockwise and counterclockwise rotational degrees of freedom, relative to a lengthwise axis of the substrate, within the liquid;

a power source connected to the longitudinal axis of the curvilinear substrate configured to rotate the curvilinear substrate in the clockwise direction and the counterclockwise direction;

a lateral edge of the pliable material in contact with an outer surface of the curvilinear substrate to define a transfer front at an intersection of the lateral edge and the curvilinear substrate, wherein rotation of the curvilinear substrate advances a leading longitudinal edge of the pliable material onto the curvilinear substrate from the transfer front;

wherein the pliable material comprises a leading longitudinal edge that intersects the curvilinear substrate at an initial orientation angle, alpha (α), and an advanced orientation angle, beta (β), relative to the transfer front, wherein:

alpha is measured between a portion of the leading longitudinal edge of the pliable material floating on the liquid and a plane that is normal to both the outer surface of the curvilinear substrate and the lateral edge of the pliable material at the transfer front; and

beta is measured between a second portion of the leading longitudinal edge of the pliable material that has advanced onto the curvilinear substrate and a plane extending vertically through both the curvilinear substrate and the second portion of the pliable material that has advanced onto the curvilinear substrate.

23. The system of Claim 22, further comprising a computer having a processor and computer memory storing software that controls the power source that rotates the curvilinear substrate, wherein the software implements computer commands that are configured to perform a method comprising:

forming a pattern on the curvilinear substrate with the pliable material by advancing the pliable material onto the curvilinear substrate at the initial orientation angle and the advanced orientation angle.

24. The system of Claim 23, wherein the method further comprises:

adjusting the initial orientation angle of the pliable material to form a weave pattern on the curvilinear substrate, wherein the weave pattern comprises right-handed sections and left-handed sections of the pliable material overlapping on the curvilinear substrate.

25. The system of Claim 23, wherein the method further comprises:

changing the rotation direction of the curvilinear substrate to form folds on the curvilinear substrate.

26. The system of Claim 23, further comprising a printer that prints the pliable material onto the liquid.

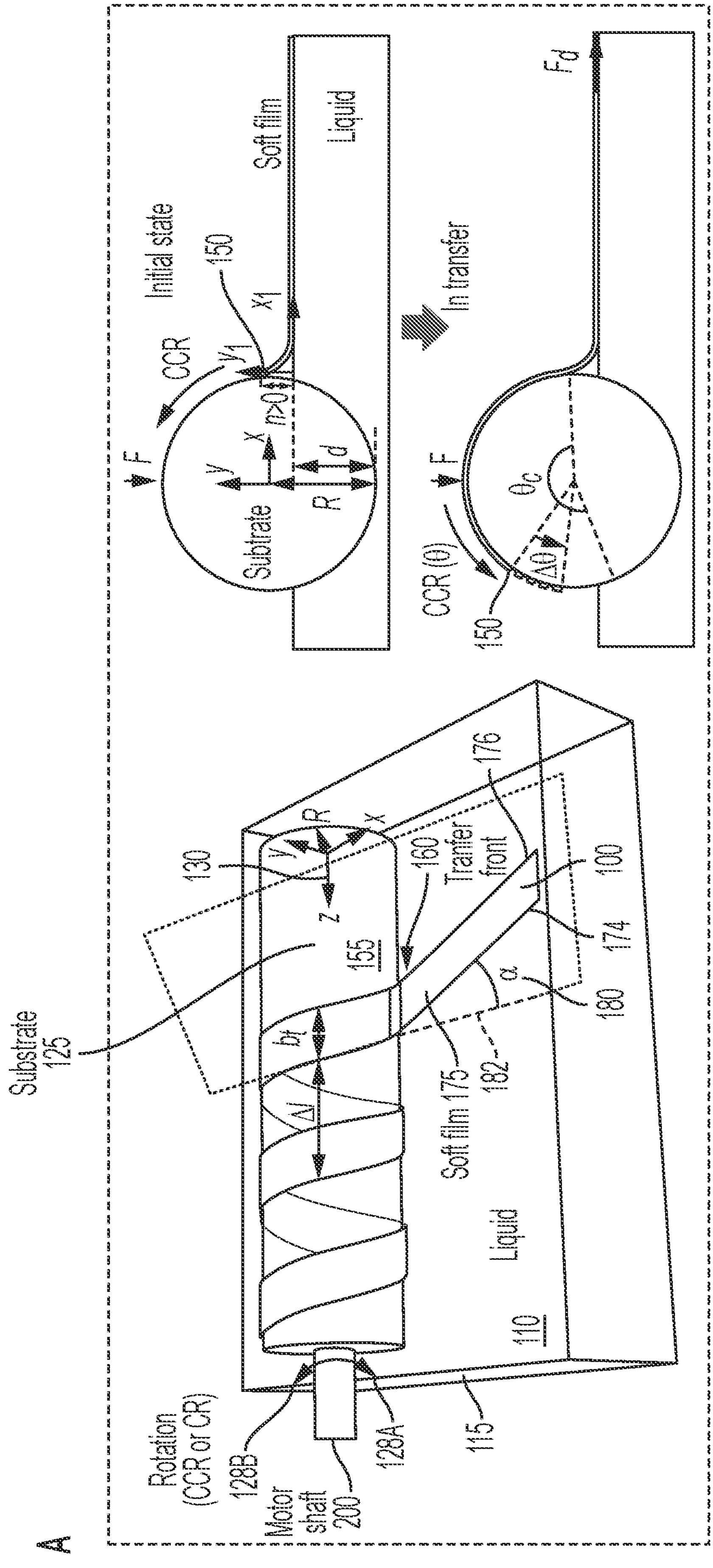
A
Substrate 125
130
R
y
x
z
155
160
Tranfer front
176
100
174
180
α
182
Soft film 175
b_t
Δl
Liquid
110
115
Rotation (CCR or CR)
128B
128A
Motor shaft 200
Initial state
Soft film
Liquid
150
CCR
y_1
x_1
F
y
x
R
d
Subtrate
In transfer
F_d
F
θ_c
CCR (θ)
Δθ
150

FIG. 1A

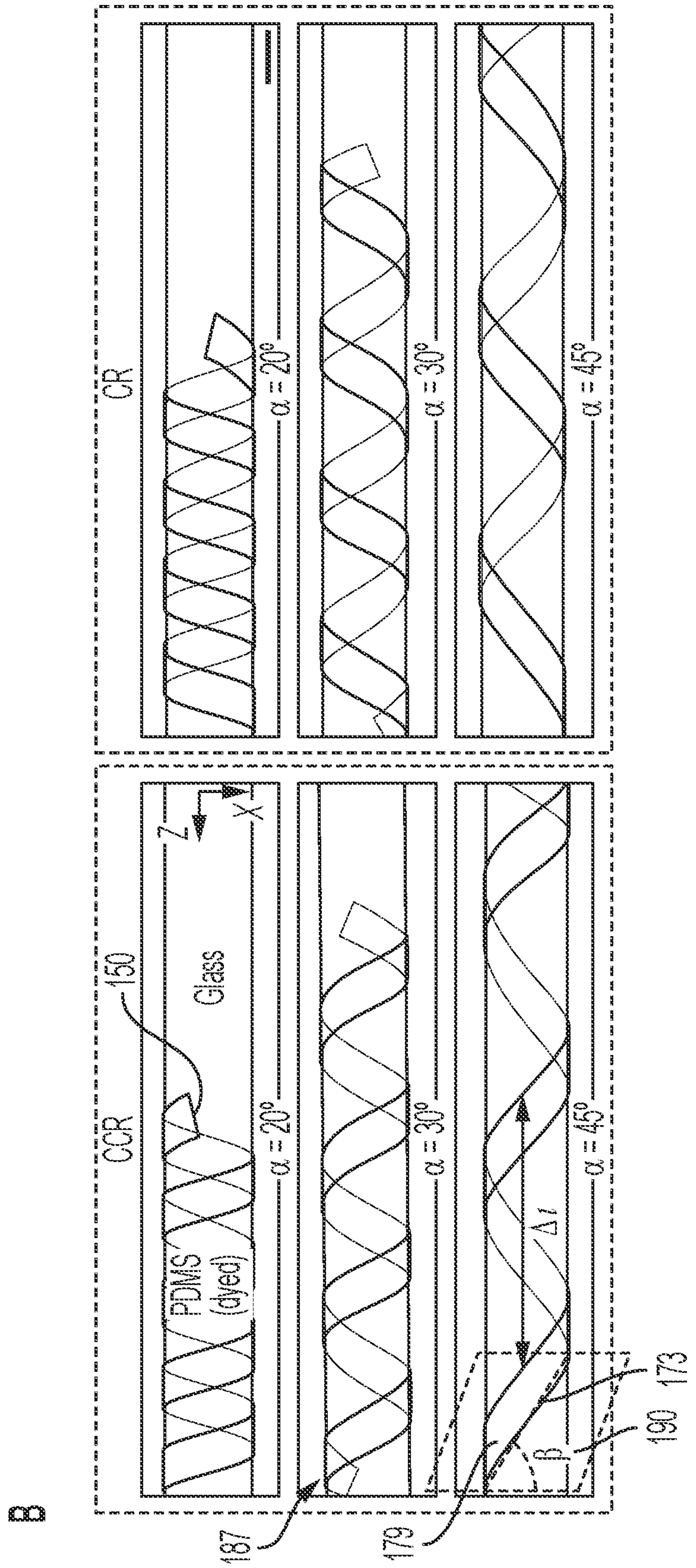

FIG. 1B

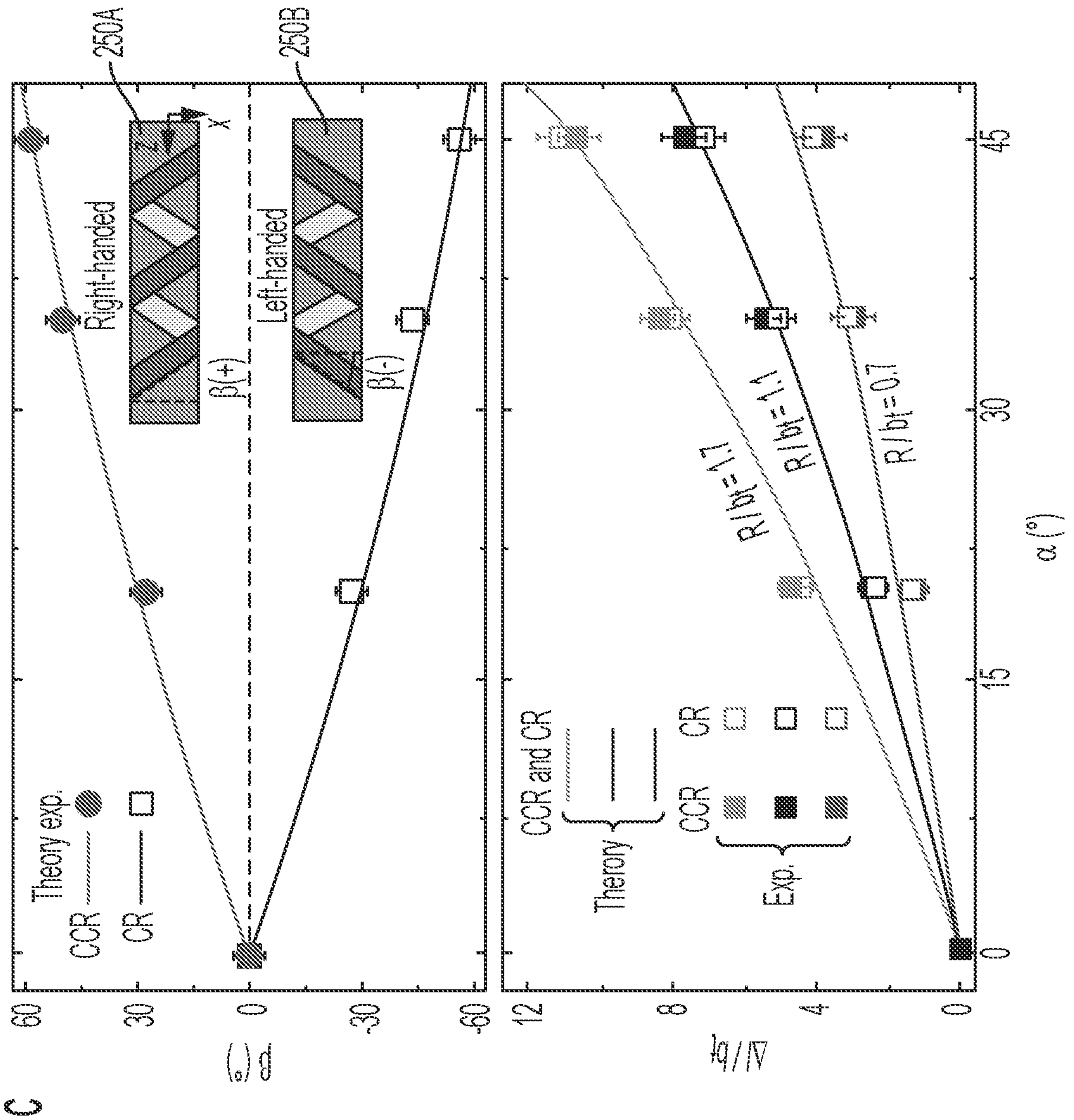
C
Theory exp.
CCR
CR
Right-handed
Left-handed
250A
250B
β(+)
β(-)
Z
X
β (°)
60
30
0
-30
-60
Δl / bt
12
8
4
0
Therory
Exp.
CCR and CR
CCR
CR
R / bt = 1.7
R / bt = 1.1
R / bt = 0.7
0
15
30
45
α (°)

FIG. 1C

D

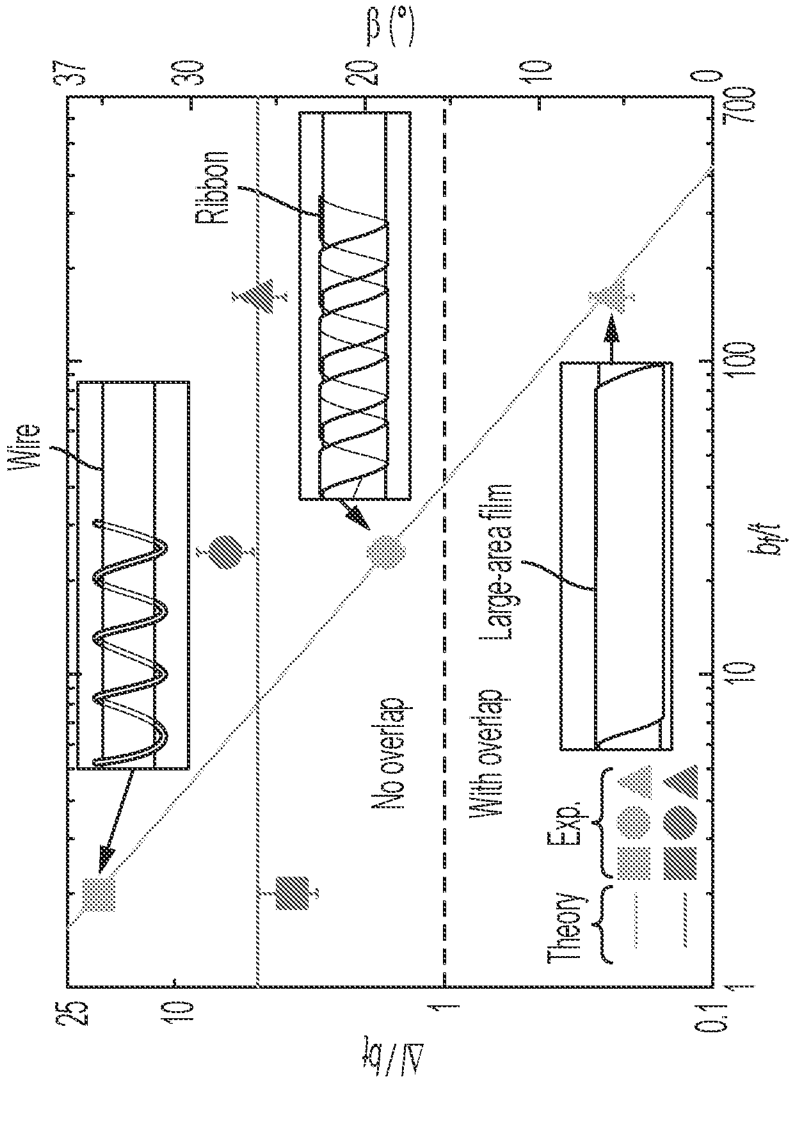

FIG. 1D

E

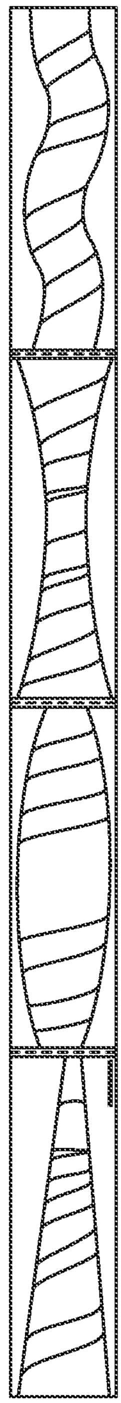

FIG. 1E

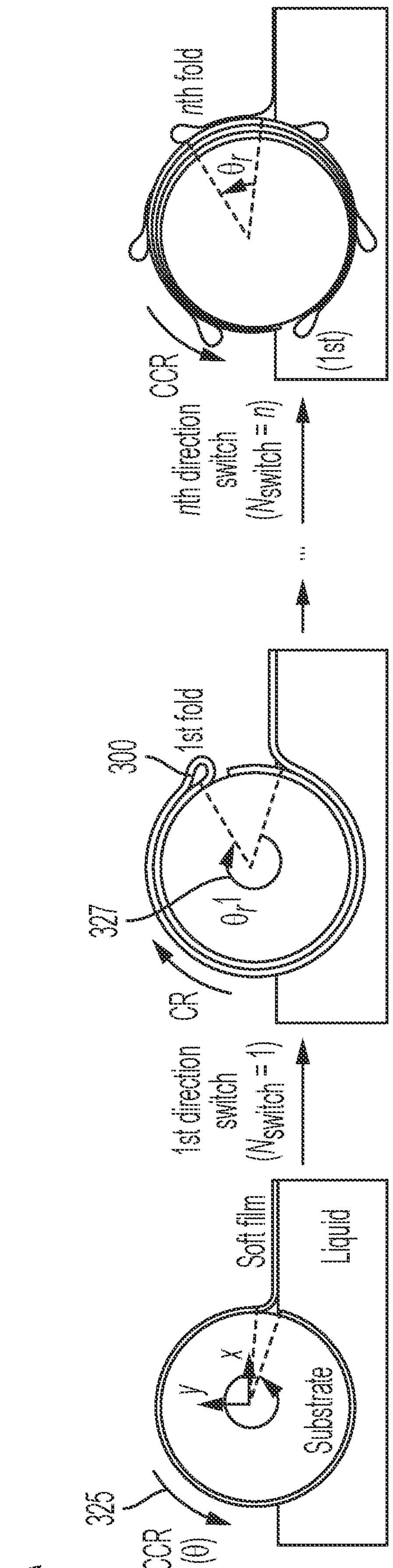
A
CCR
(θ)
325
y
x
Substrate
Soft film
Liquid
1st direction
switch
(Nswitch = 1)
CR
327
θr1
300
1st fold
...
nth direction
switch
(Nswitch = n)
CCR
(1st)
θr
nth fold

FIG. 2A

B

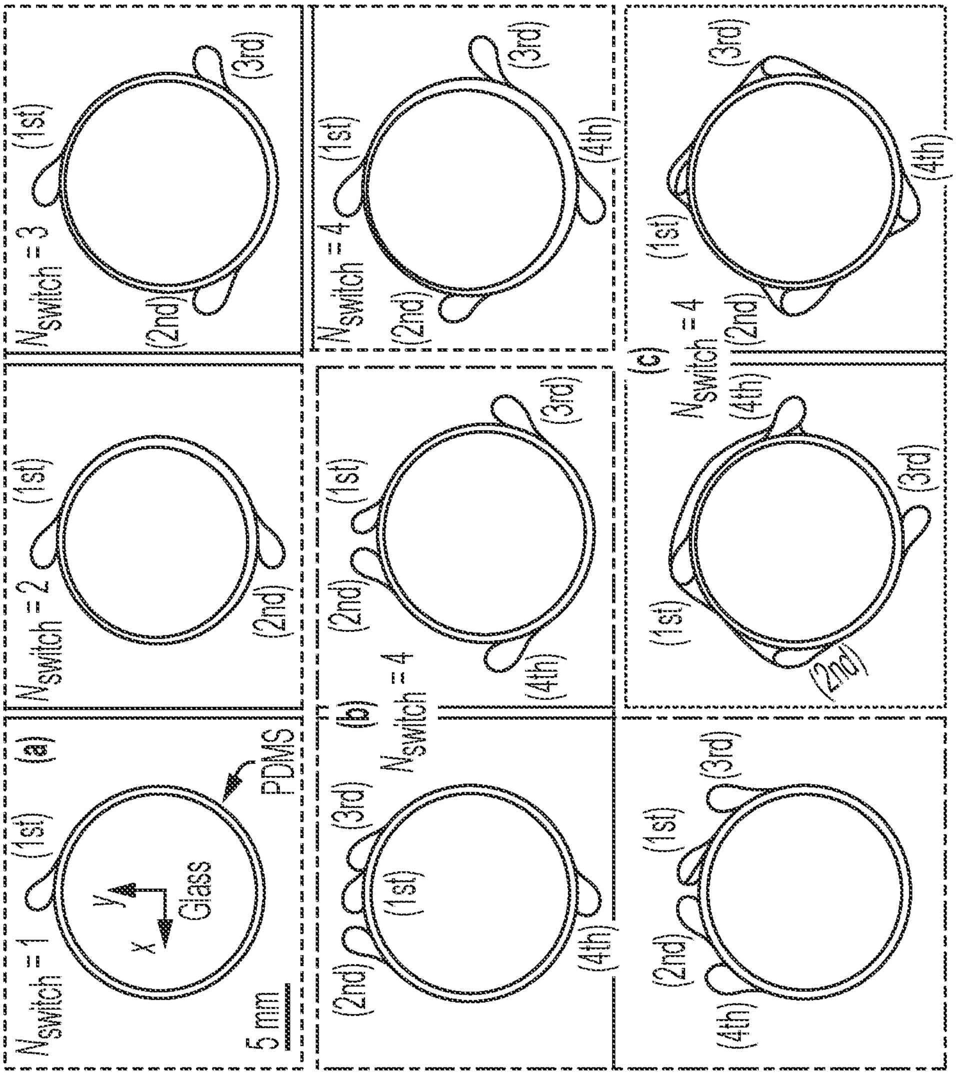
(a)
N_{switch} = 1
(1st)
y
x
Glass
PDMS
5 mm
N_{switch} = 2
(1st)
(2nd)
N_{switch} = 3
(1st)
(2nd)
(3rd)
(b)
N_{switch} = 4
(1st)
(2nd)
(3rd)
(4th)
(c)
N_{switch} = 4
(1st)
(2nd)
(3rd)
(4th)

FIG. 2B

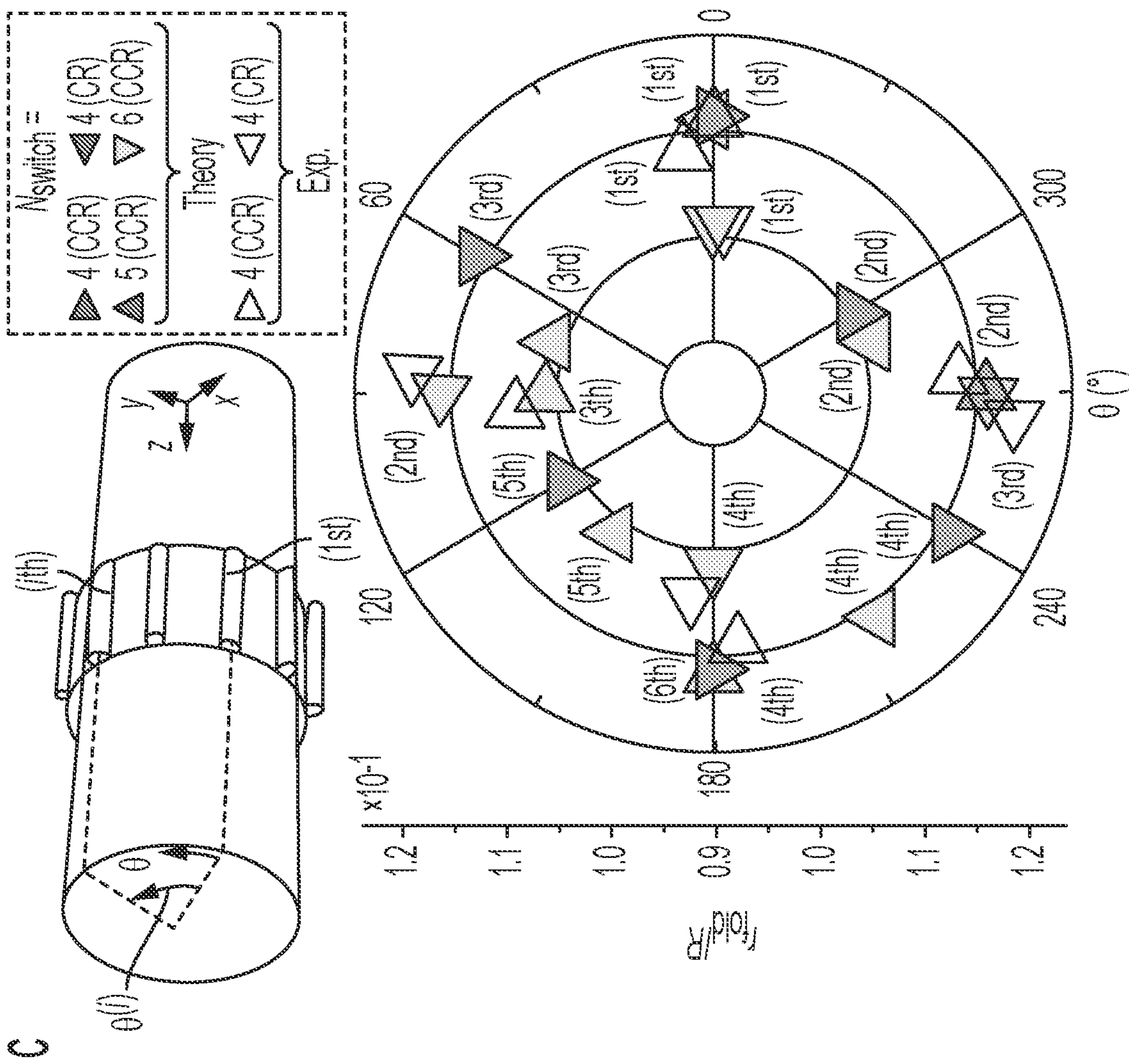
C
θ(i)
θ
(ith)
(1st)
z
y
x
Nswitch =
4 (CCR)
4 (CR)
5 (CCR)
6 (CCR)
Theory
4 (CCR)
4 (CR)
Exp.
x10-1
1.2
1.1
1.0
0.9
1.0
1.1
1.2
r_fold/R
0
60
120
180
240
300
0 (°)
(1st)
(2nd)
(3rd)
(4th)
(5th)
(6th)

FIG. 2C

D

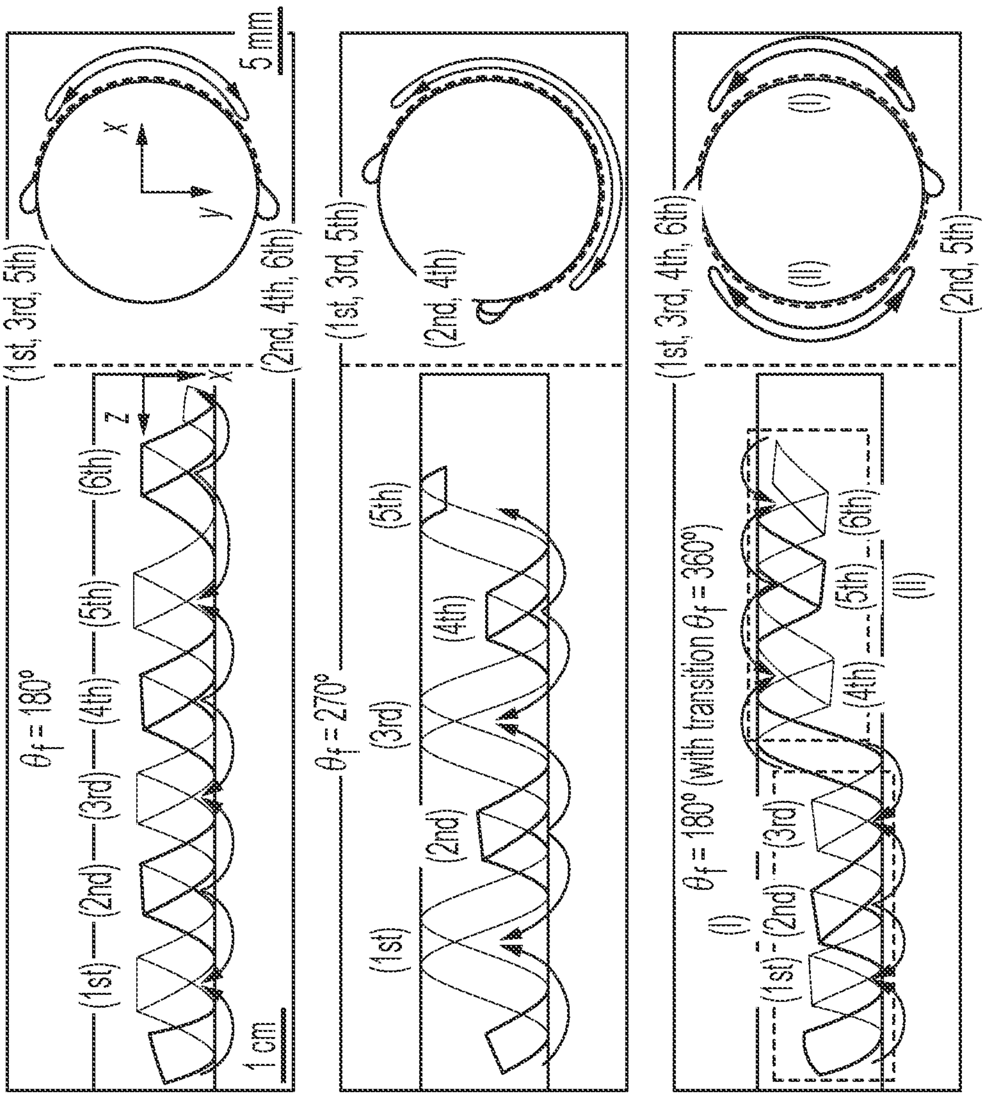

$\theta_f = 180°$
(1st)
(2nd)
(3rd)
(4th)
(5th)
(6th)
1 cm
5 mm
x
y
z
(1st, 3rd, 5th)
(2nd, 4th, 6th)
$\theta_f = 270°$
(2nd, 4th)
$\theta_f = 180°$ (with transition $\theta_f = 360°$)
(I)
(II)
(1st, 3rd, 4th, 6th)
(2nd, 5th)

FIG. 2D

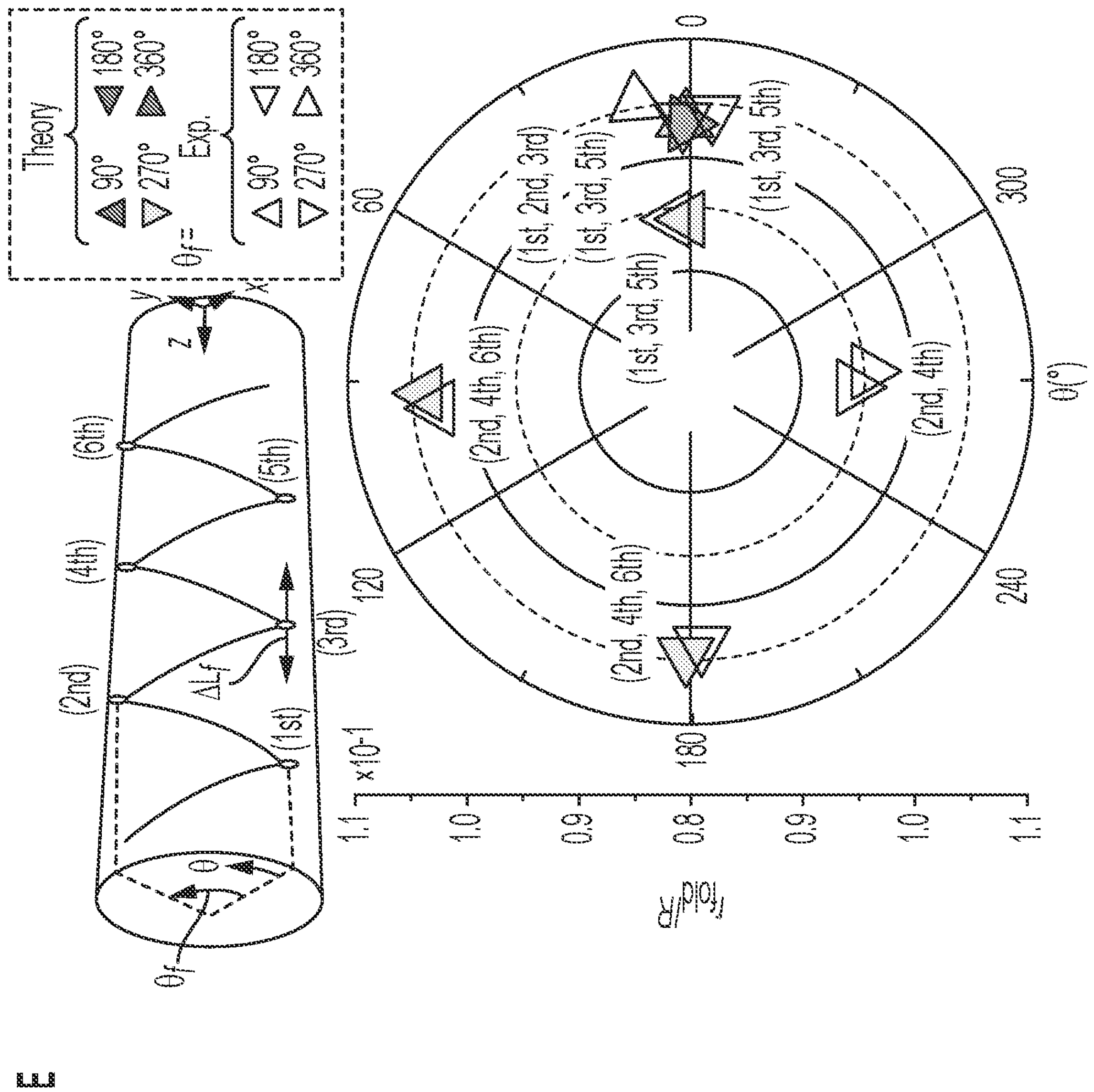
Theory
90°
180°
270°
360°
Exp.
90°
180°
270°
360°
θf =
y
x
z
(2nd)
(4th)
(6th)
(1st)
(3rd)
(5th)
ΔLf
θf
θ
60
0
300
120
180
240
θ(°)
(1st, 2nd, 3rd)
(1st, 3rd, 5th)
(1st, 3rd, 5th)
(1st, 3rd, 5th)
(2nd, 4th, 6th)
(2nd, 4th, 6th)
(2nd, 4th)
1.1
1.0
0.9
0.8
0.9
1.0
1.1
x10-1
rfold/R
E

FIG. 2E

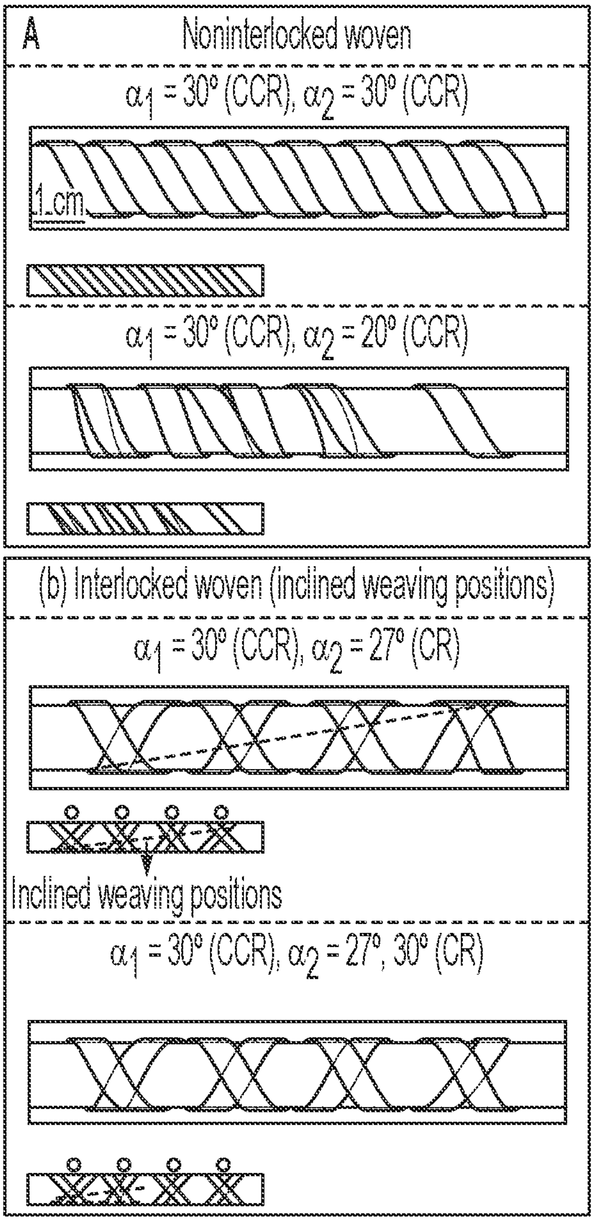
A
Noninterlocked woven
α1 = 30° (CCR), α2 = 30° (CCR)
1 cm
α1 = 30° (CCR), α2 = 20° (CCR)
(b) Interlocked woven (inclined weaving positions)
α1 = 30° (CCR), α2 = 27° (CR)
Inclined weaving positions
α1 = 30° (CCR), α2 = 27°, 30° (CR)

FIG. 3A

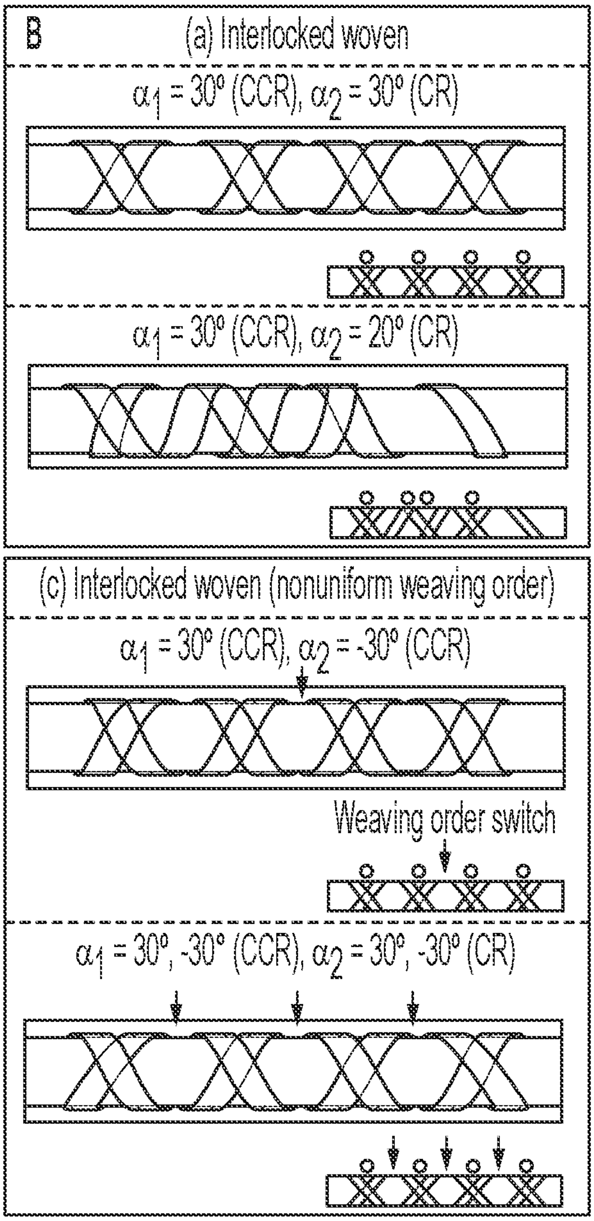
B
(a) Interlocked woven
α1 = 30° (CCR), α2 = 30° (CR)
α1 = 30° (CCR), α2 = 20° (CR)
(c) Interlocked woven (nonuniform weaving order)
α1 = 30° (CCR), α2 = -30° (CCR)
Weaving order switch
α1 = 30°, -30° (CCR), α2 = 30°, -30° (CR)

FIG. 3B

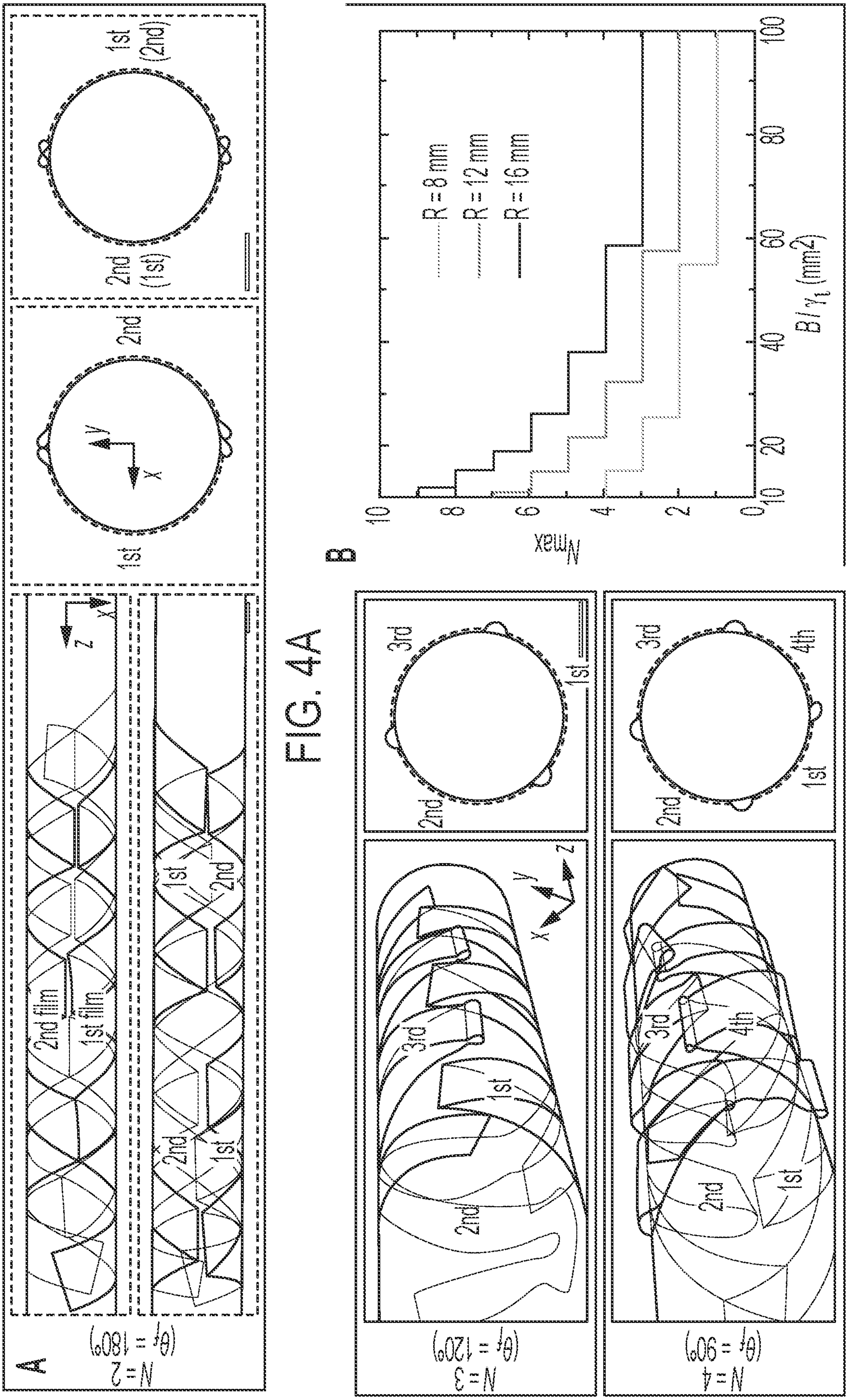

FIG. 4A

FIG. 4B

FIG. 4A Continued

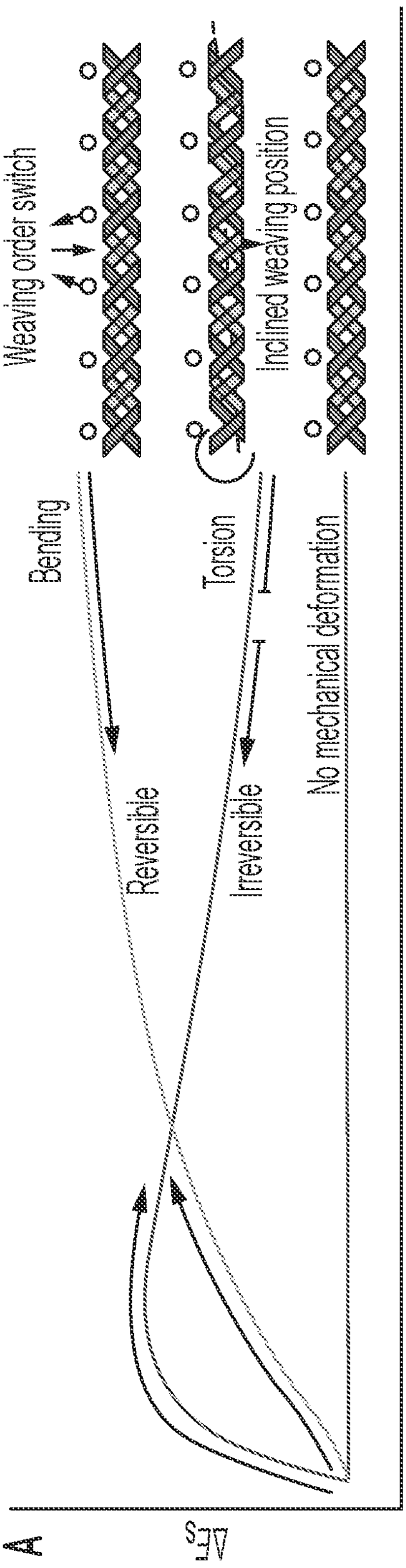

A
ΔEs
ΔT
Bending
Torsion
No mechanical deformation
Reversible
Irreversible
Weaving order switch
Inclined weaving position

FIG. 5A

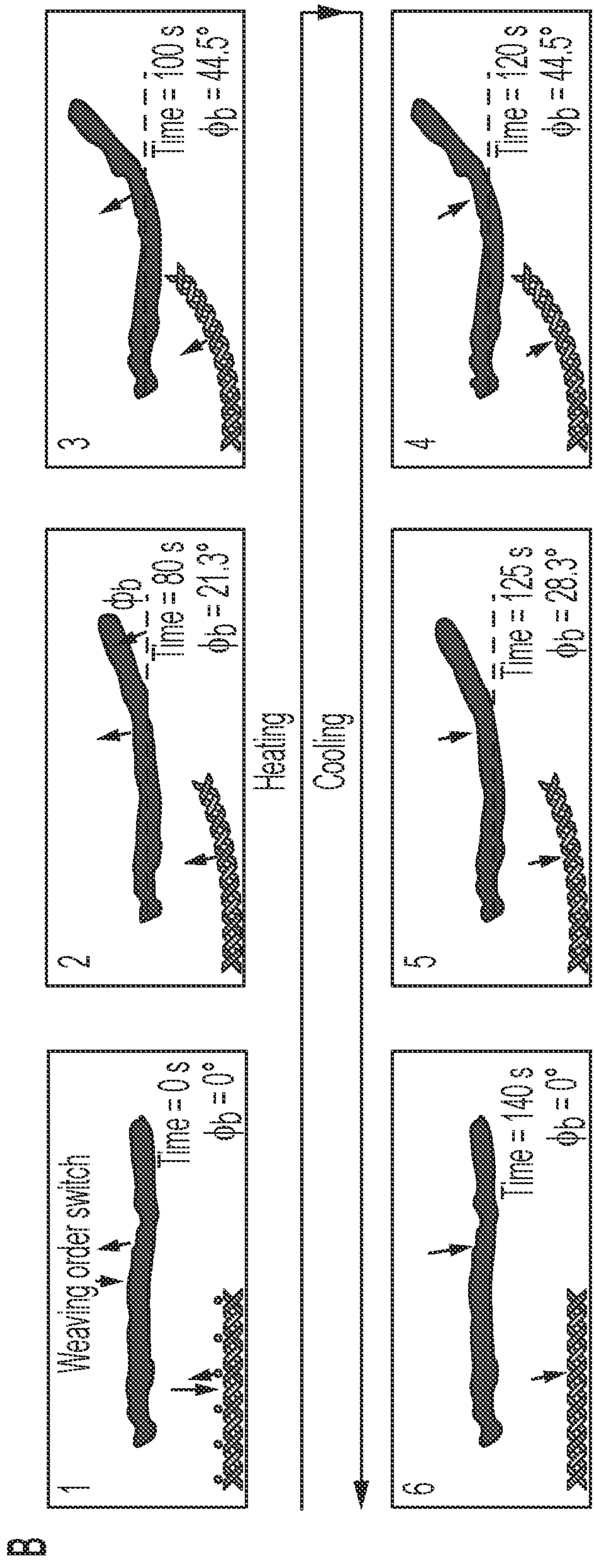

B
1
Weaving order switch
Time = 0 s
ϕb = 0°
2
ϕb
Time = 80 s
ϕb = 21.3°
3
Time = 100 s
ϕb = 44.5°
Heating
Cooling
4
Time = 120 s
ϕb = 44.5°
5
Time = 125 s
ϕb = 28.3°
6
Time = 140 s
ϕb = 0°

FIG. 5B

C

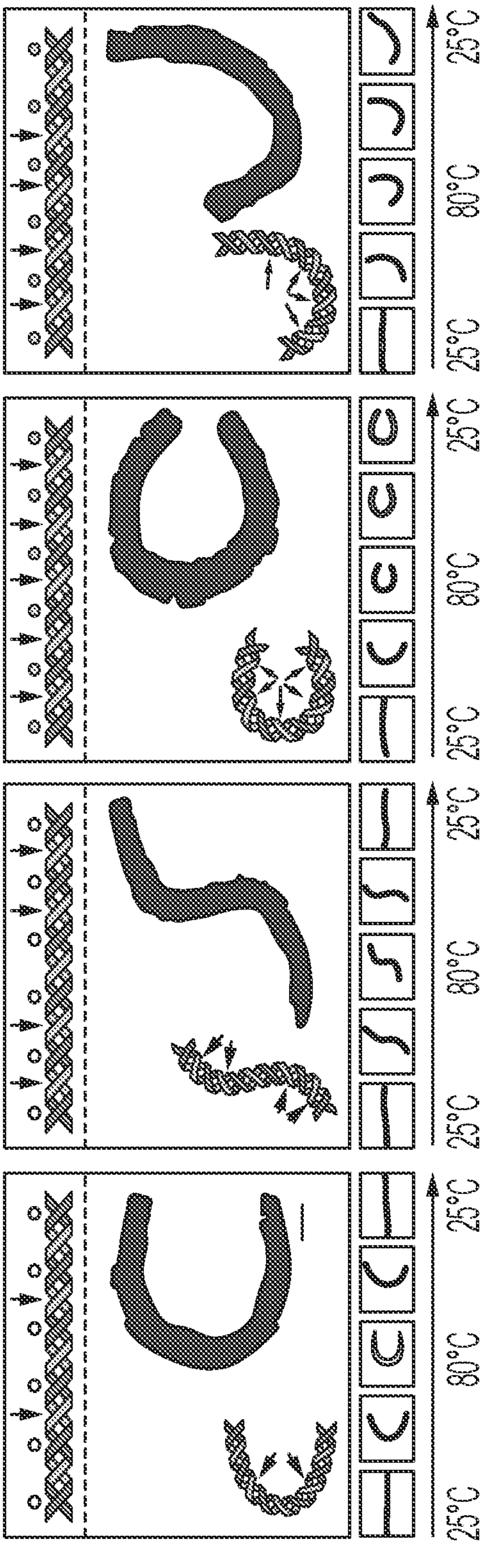

FIG. 5C

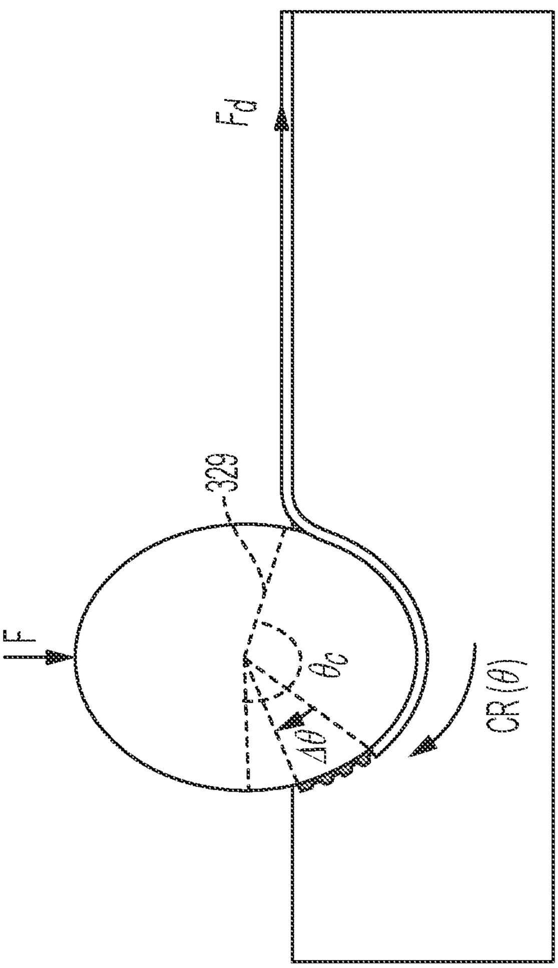

FIG. 7

a

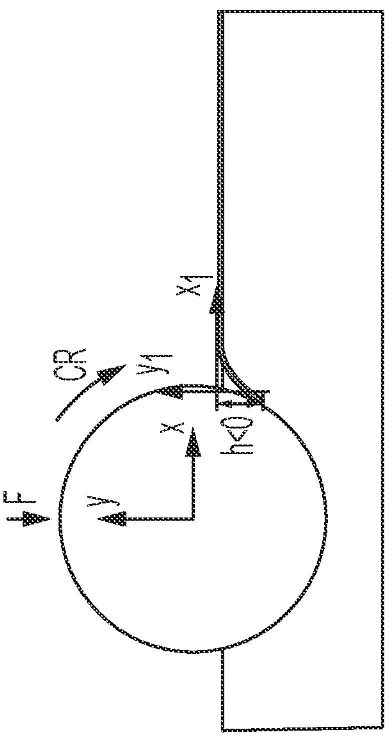

FIG. 6A

b

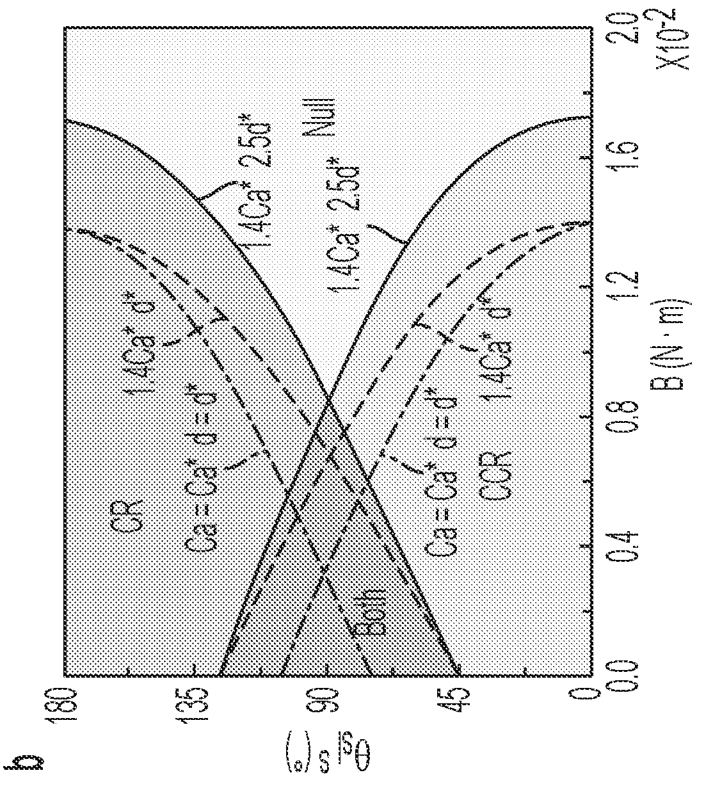

FIG. 6B

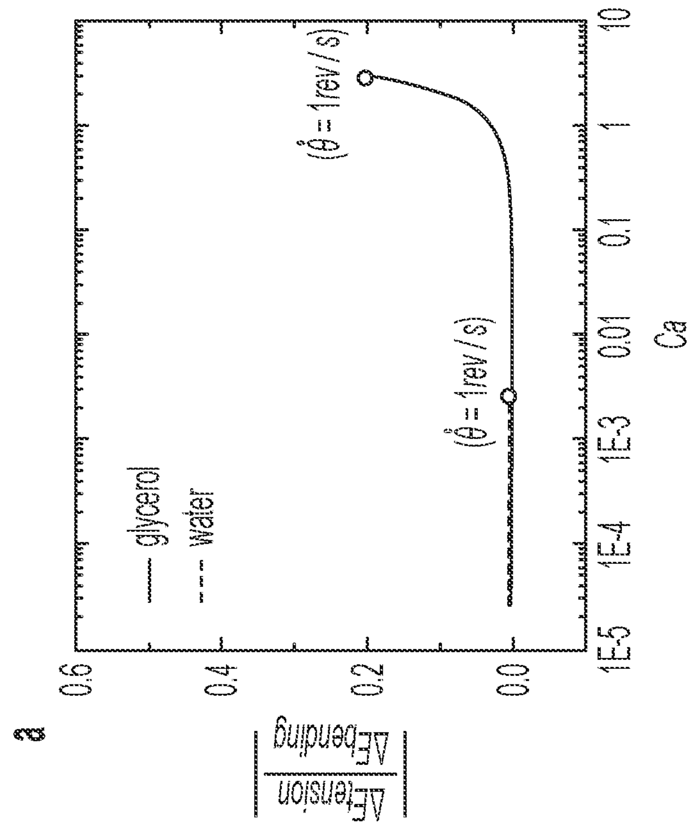
a
|ΔE_tension / ΔE_bending|
0.6
0.4
0.2
0.0
1E-5
1E-4
1E-3
0.01
0.1
1
10
Ca
glycerol
water
(θ̇ = 1rev / s)
(θ̇ = 1rev / s)

FIG. 8A

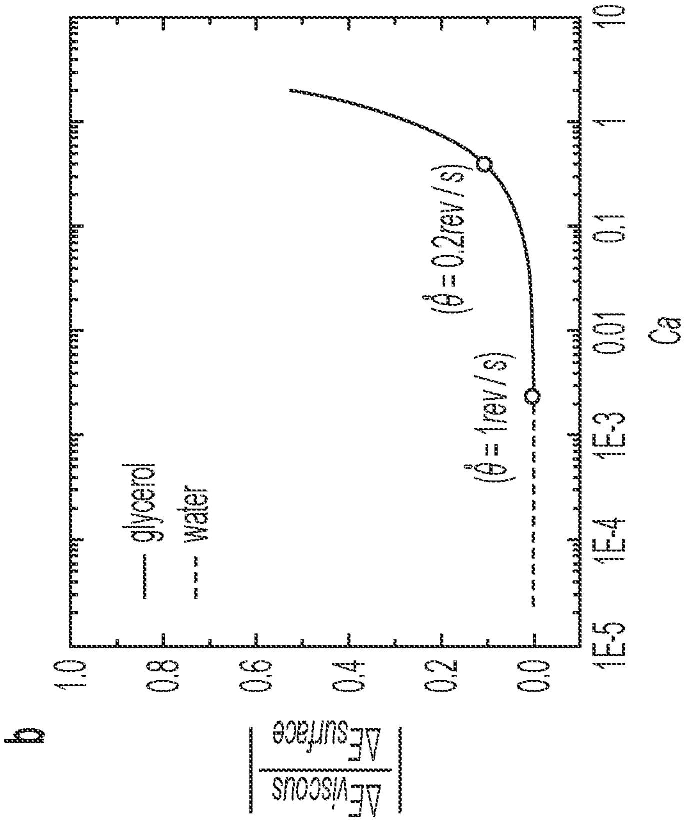
b
|ΔE_viscous / ΔE_surface|
1.0
0.8
0.6
0.4
0.2
0.0
1E-5
1E-4
1E-3
0.01
0.1
1
10
Ca
glycerol
water
(θ̇ = 1rev / s)
(θ̇ = 0.2rev / s)

FIG. 8B

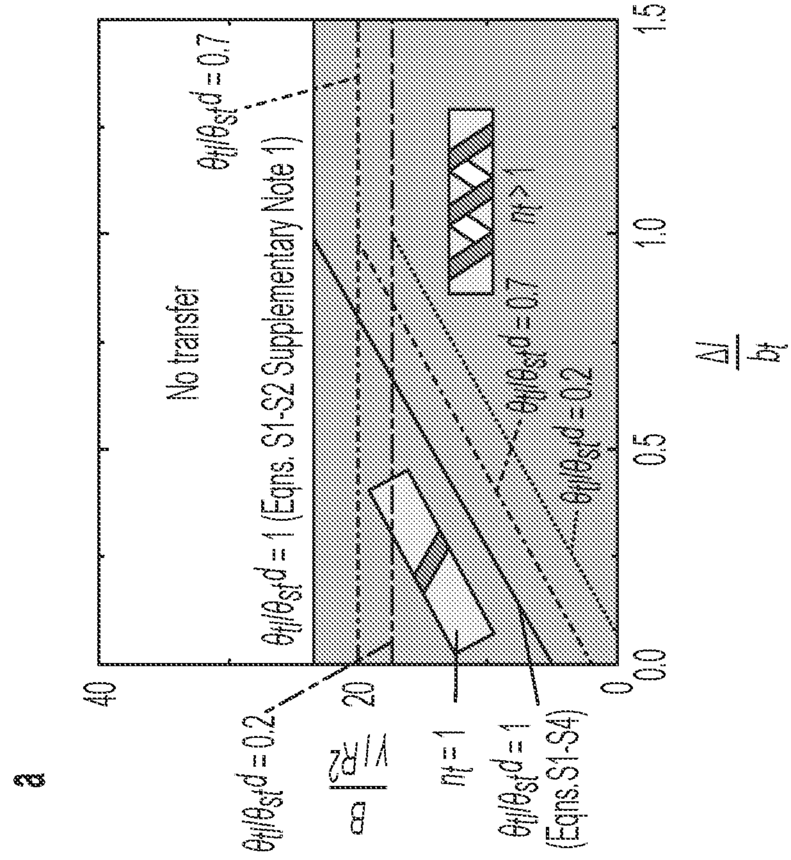
a
No transfer
θtl/θstd = 1 (Eqns. S1-S2 Supplementary Note 1)
θtl/θstd = 0.7
θtl/θstd = 0.2
nt = 1
nt > 1
θtl/θstd = 1
(Eqns. S1-S4)
ω/R2
Δl/bt
0.0
0.5
1.0
1.5
0
20
40

FIG. 9A

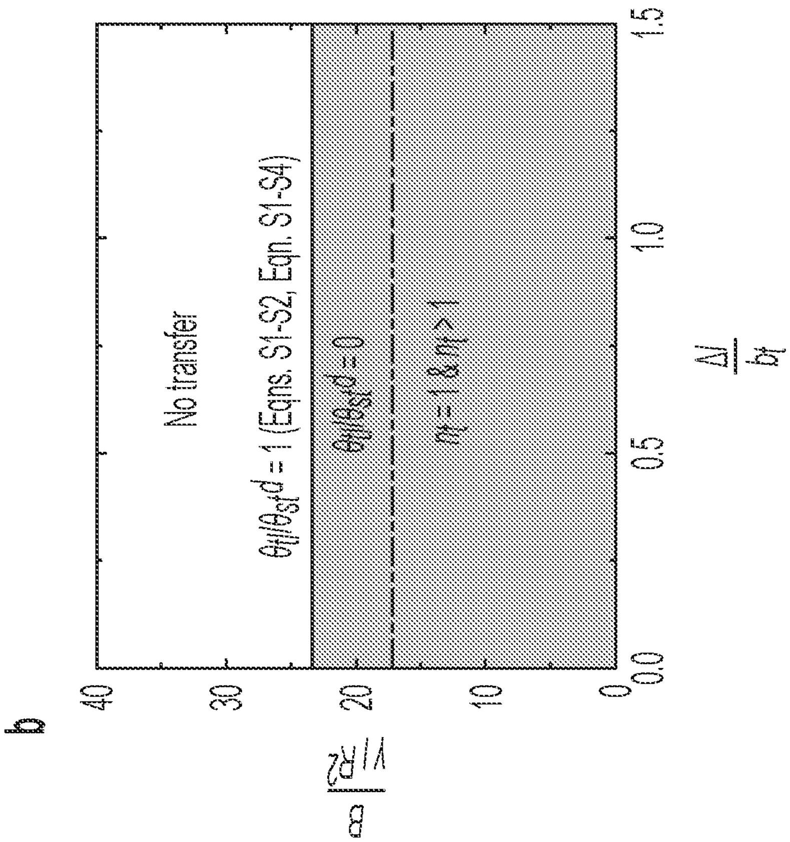
b
No transfer
θtl/θstd = 1 (Eqns. S1-S2, Eqn. S1-S4)
θtl/θstd = 0
nt = 1 & nt > 1
ω/R2
Δl/bt
0.0
0.5
1.0
1.5
0
10
20
30
40

FIG. 9B

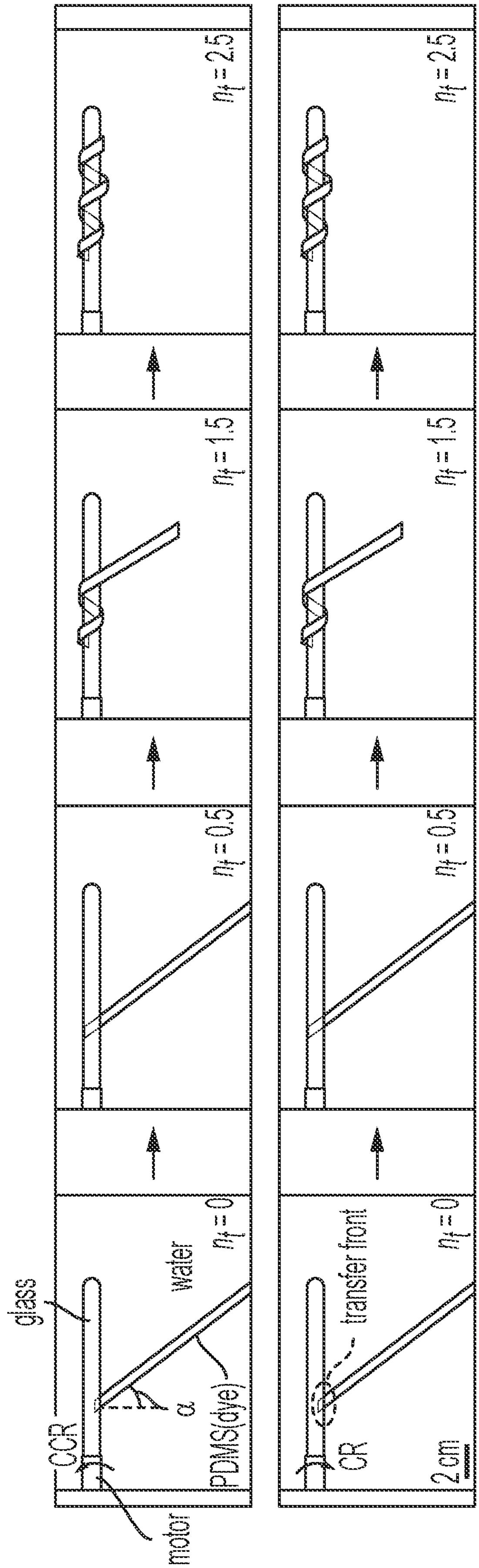
glass
water
CCR
α
PDMS(dye)
motor
n_t = 0
n_t = 0.5
n_t = 1.5
n_t = 2.5
transfer front
CR
2 cm

FIG. 10

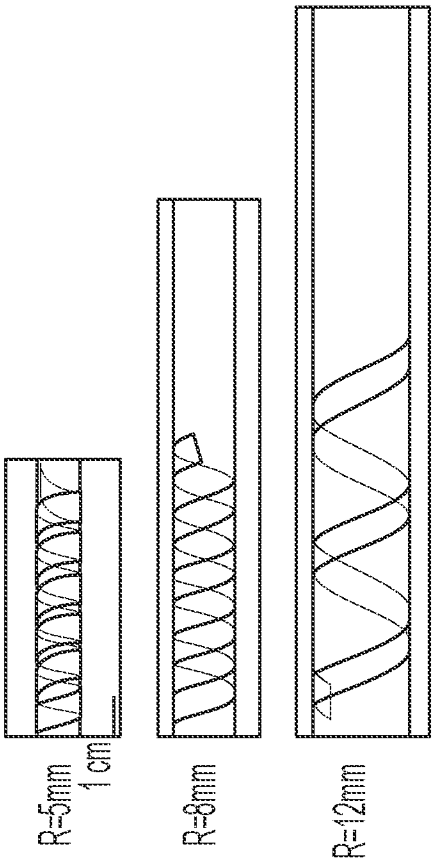

FIG. 12

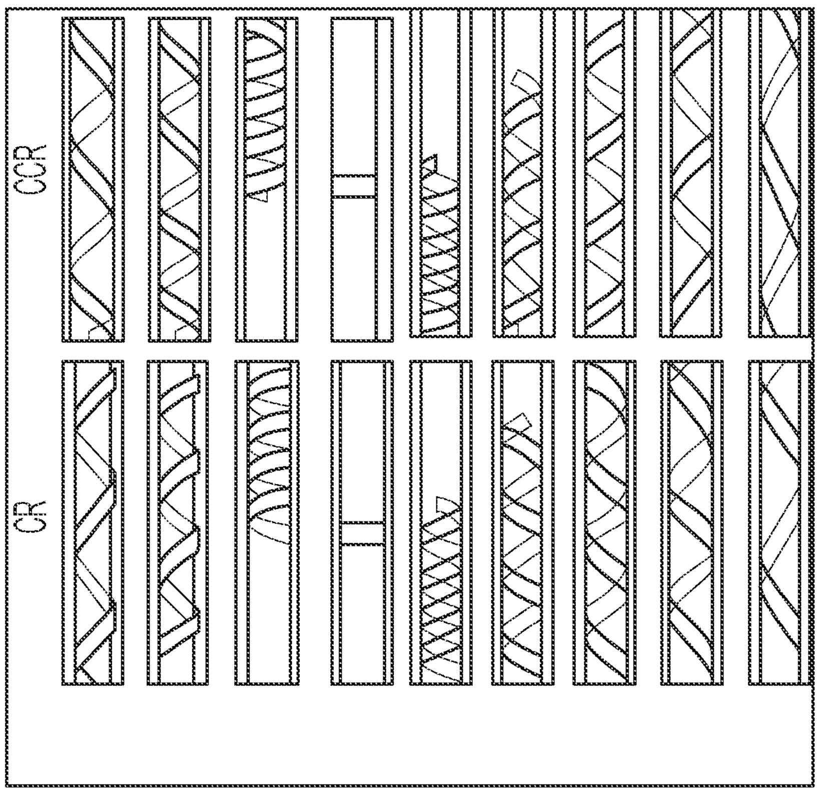

FIG. 11

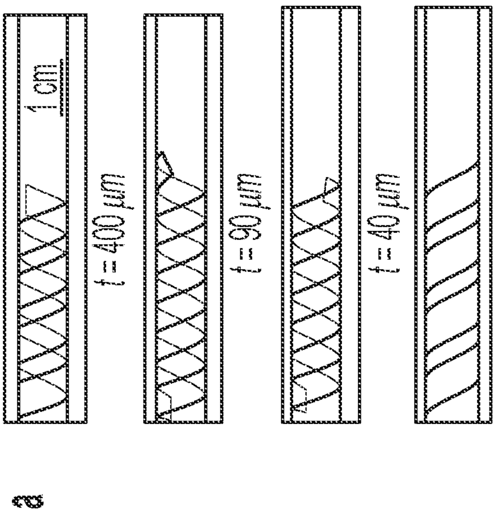

FIG. 14A

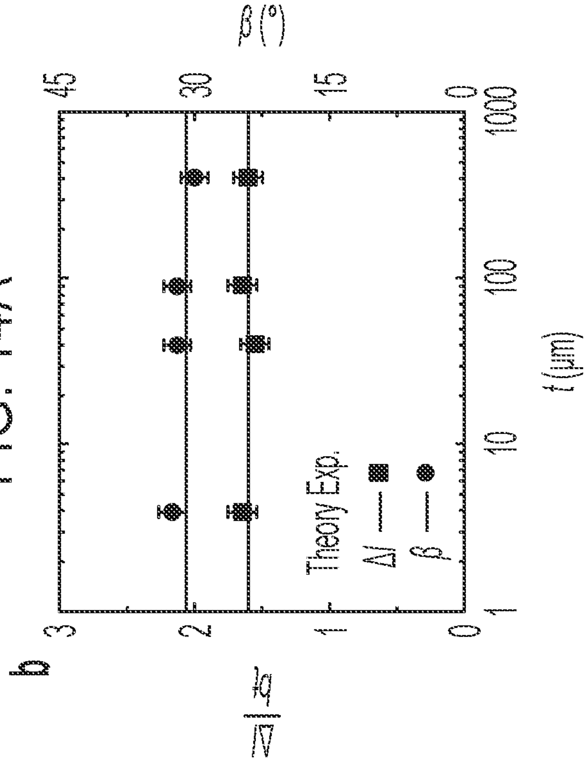

FIG. 14B

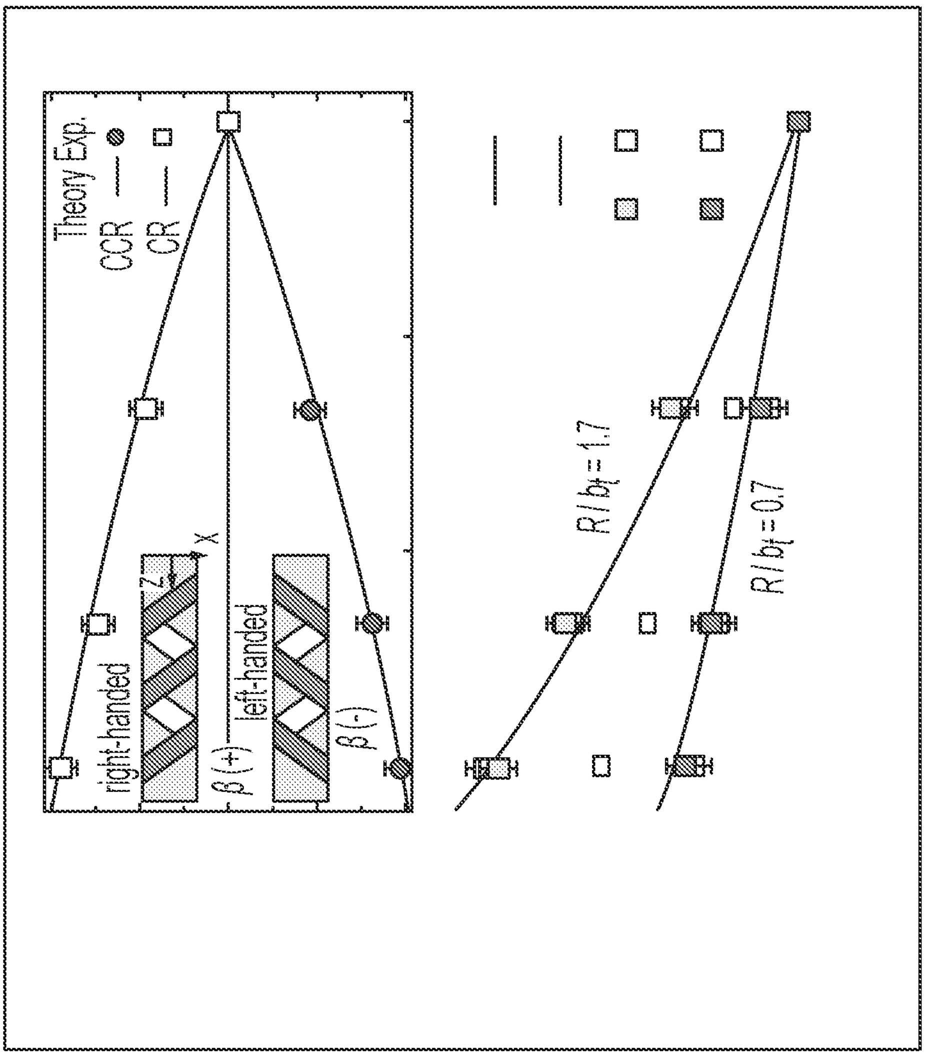

FIG. 13

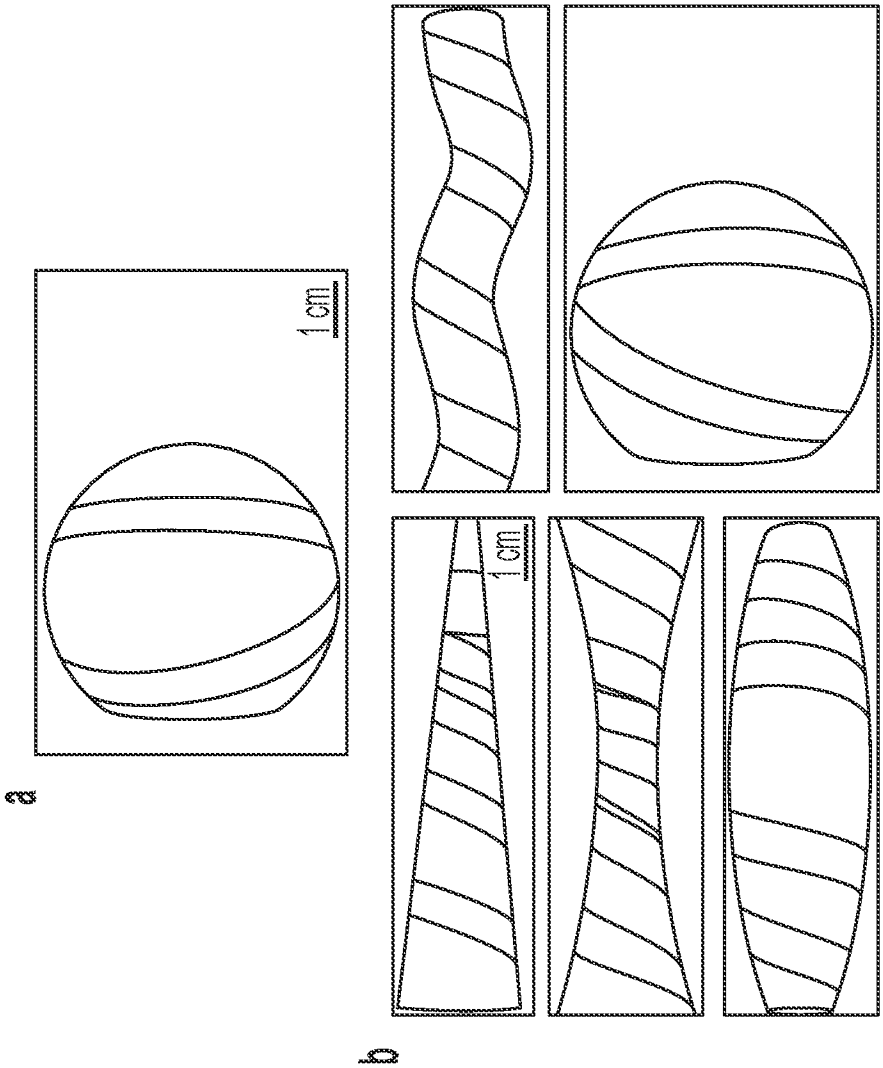

FIG. 15

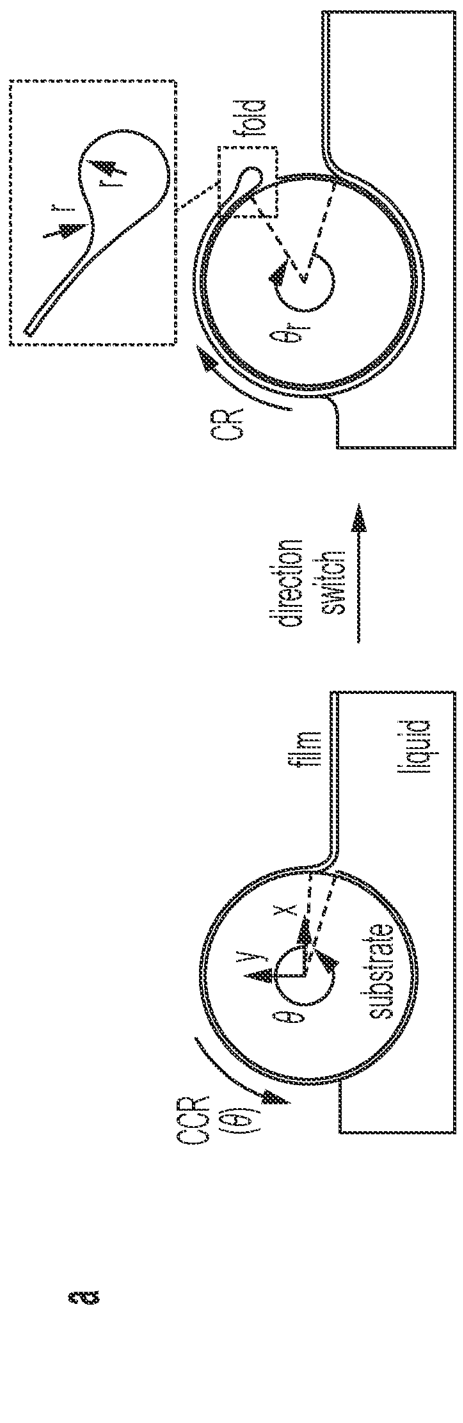

FIG. 16A

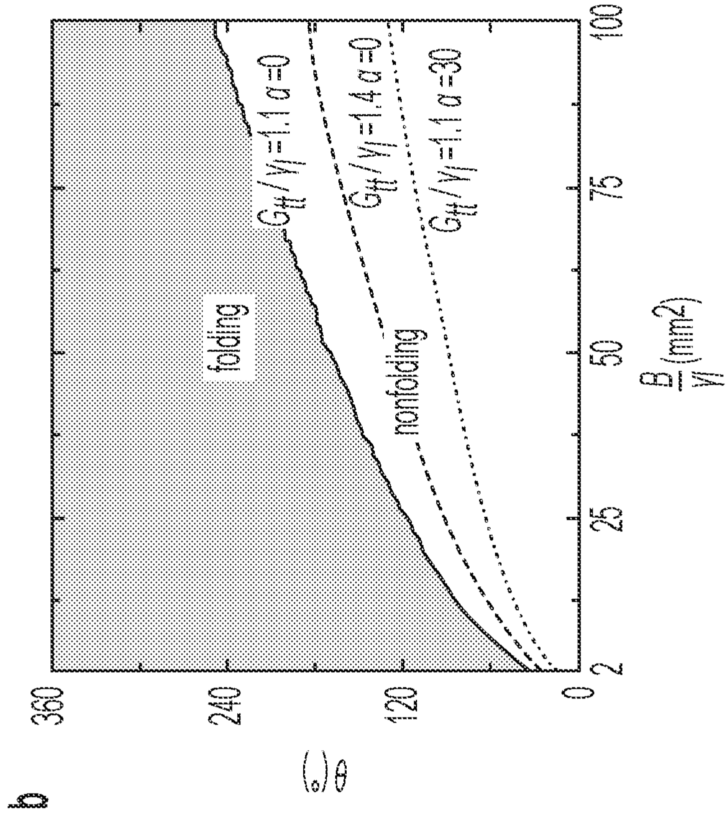

FIG. 16B

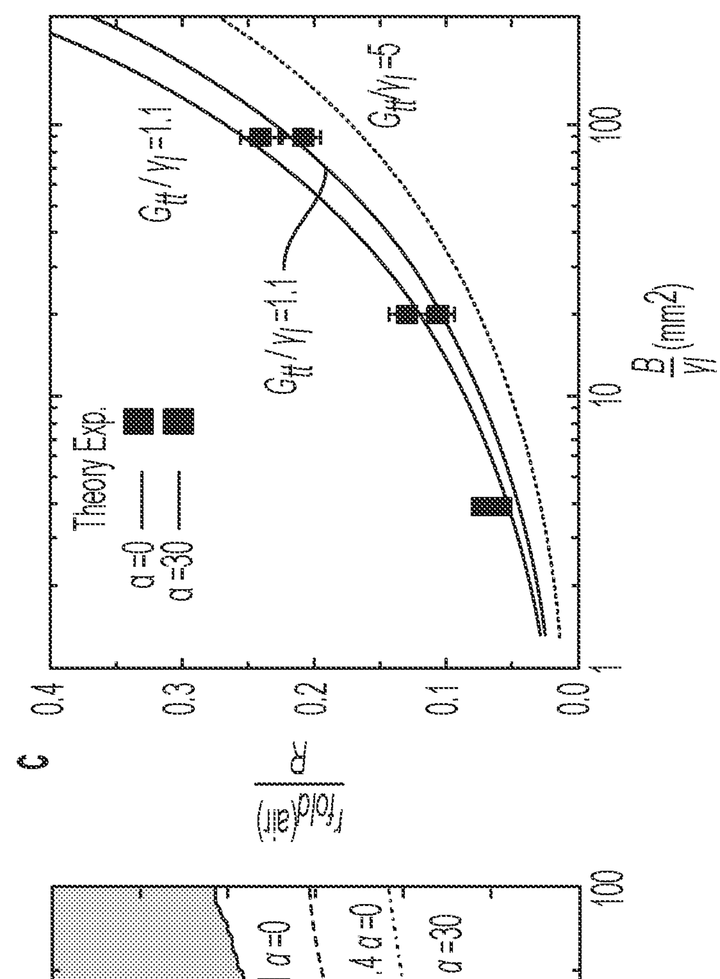

FIG. 16C

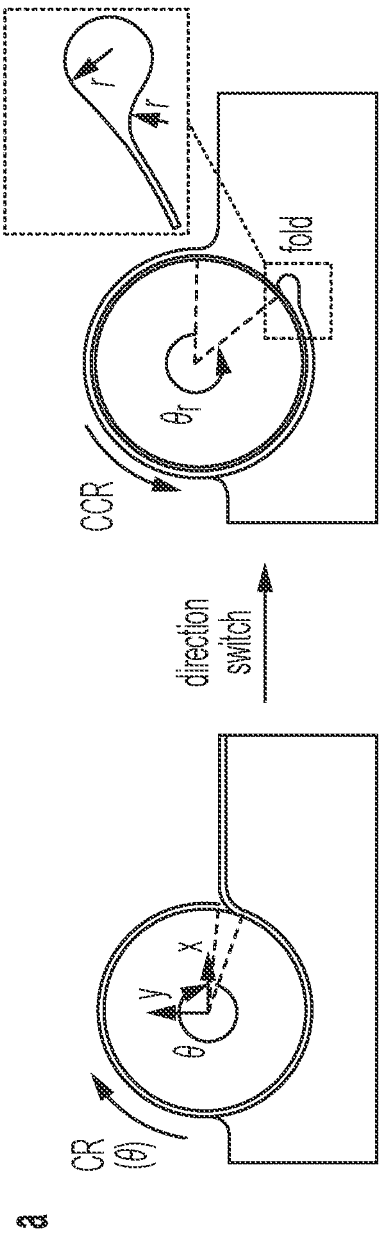

FIG. 17A

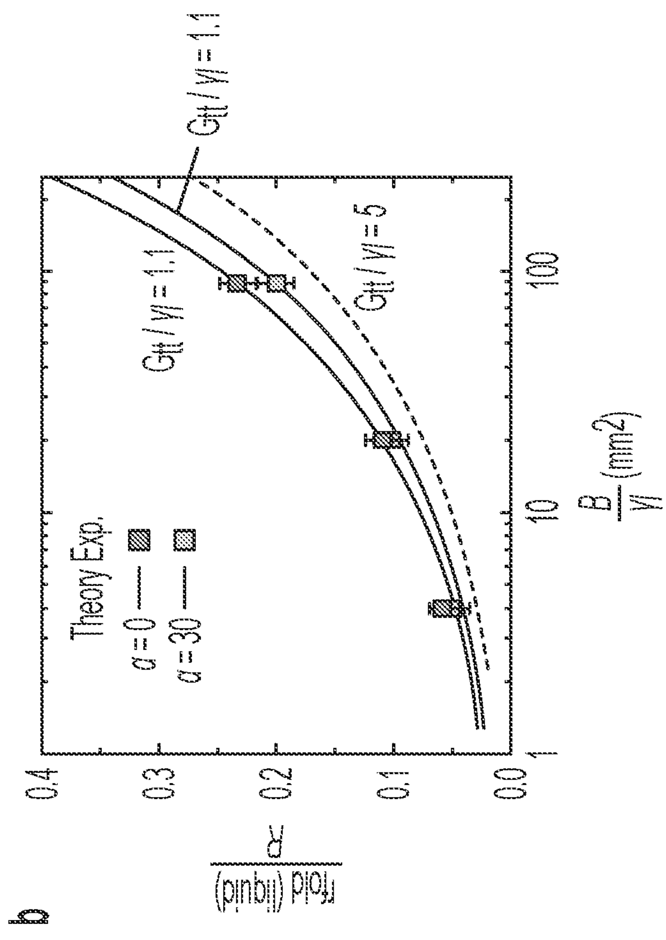

FIG. 17B

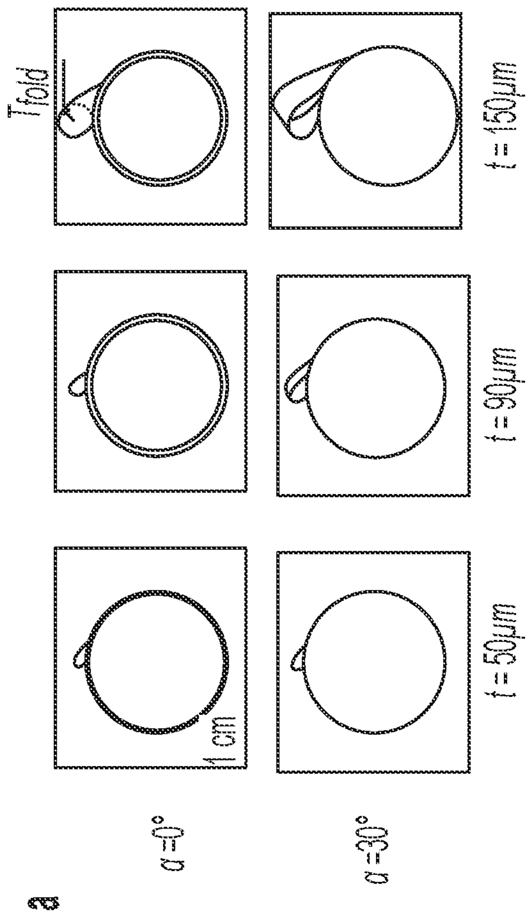

FIG. 18A

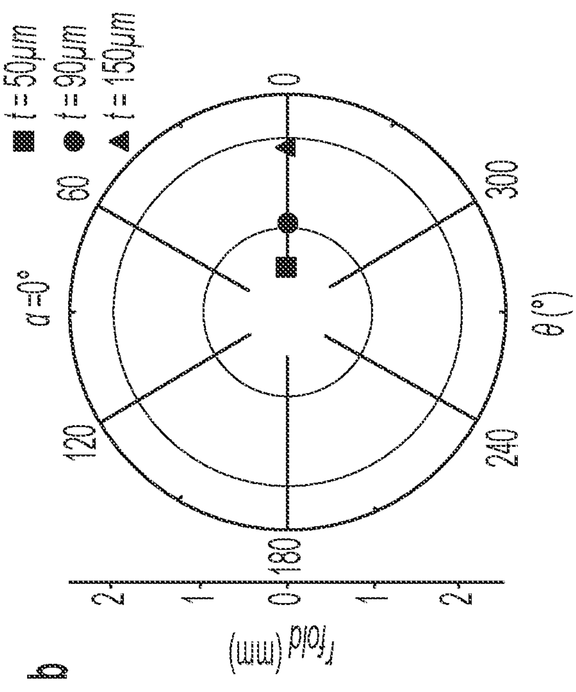

FIG. 18B

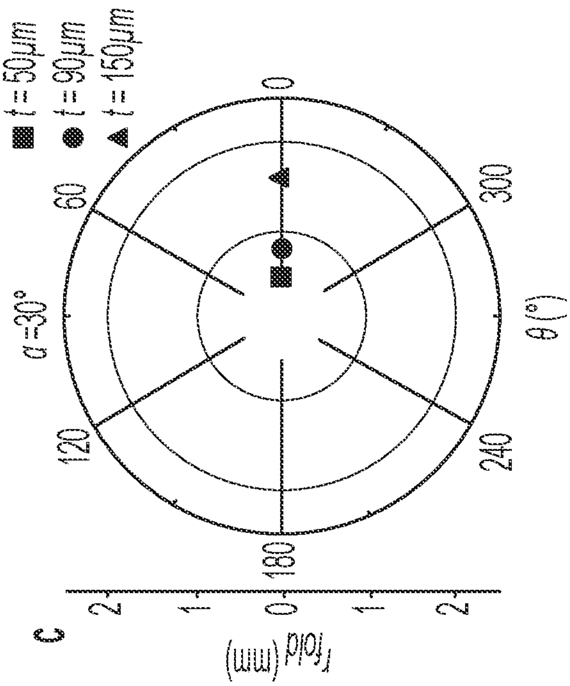

FIG. 18C

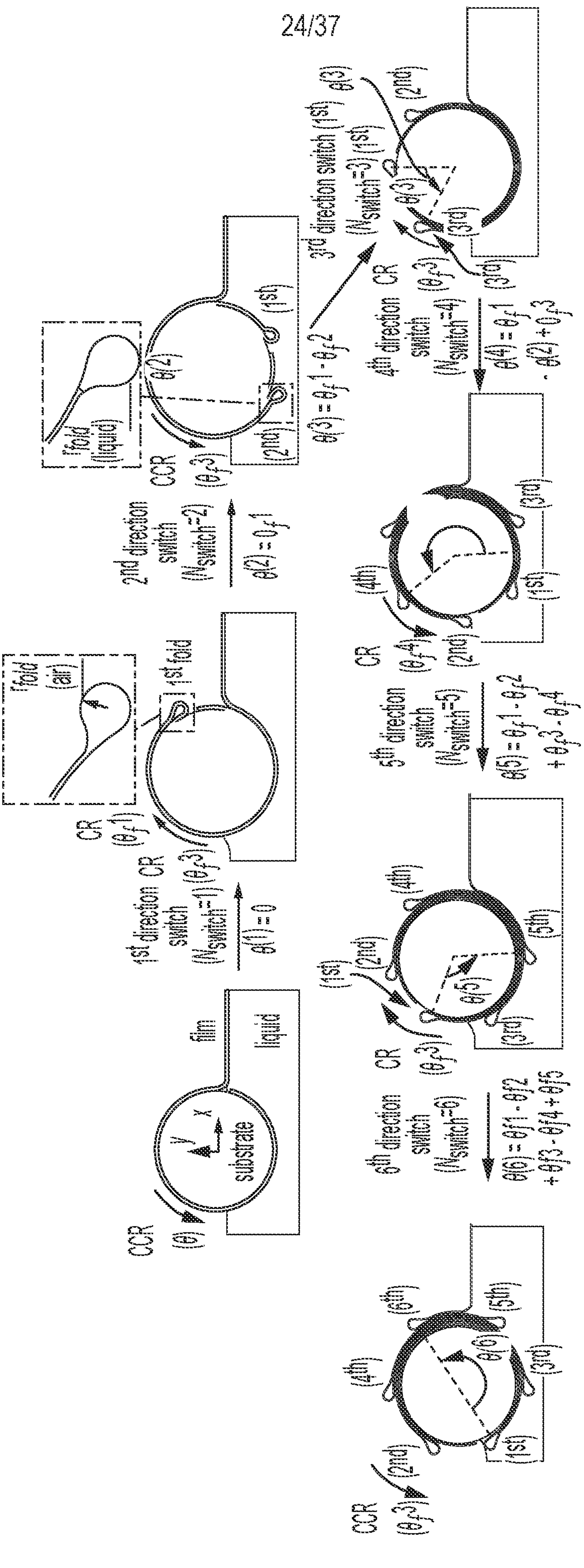

CCR
substrate
film
liquid
1st direction switch
CR
1st fold
fold (air)
2nd direction switch
fold (liquid)
3rd direction switch
4th direction switch
5th direction switch
6th direction switch
(1st)
(2nd)
(3rd)
(4th)
(5th)
(6th)

FIG. 19

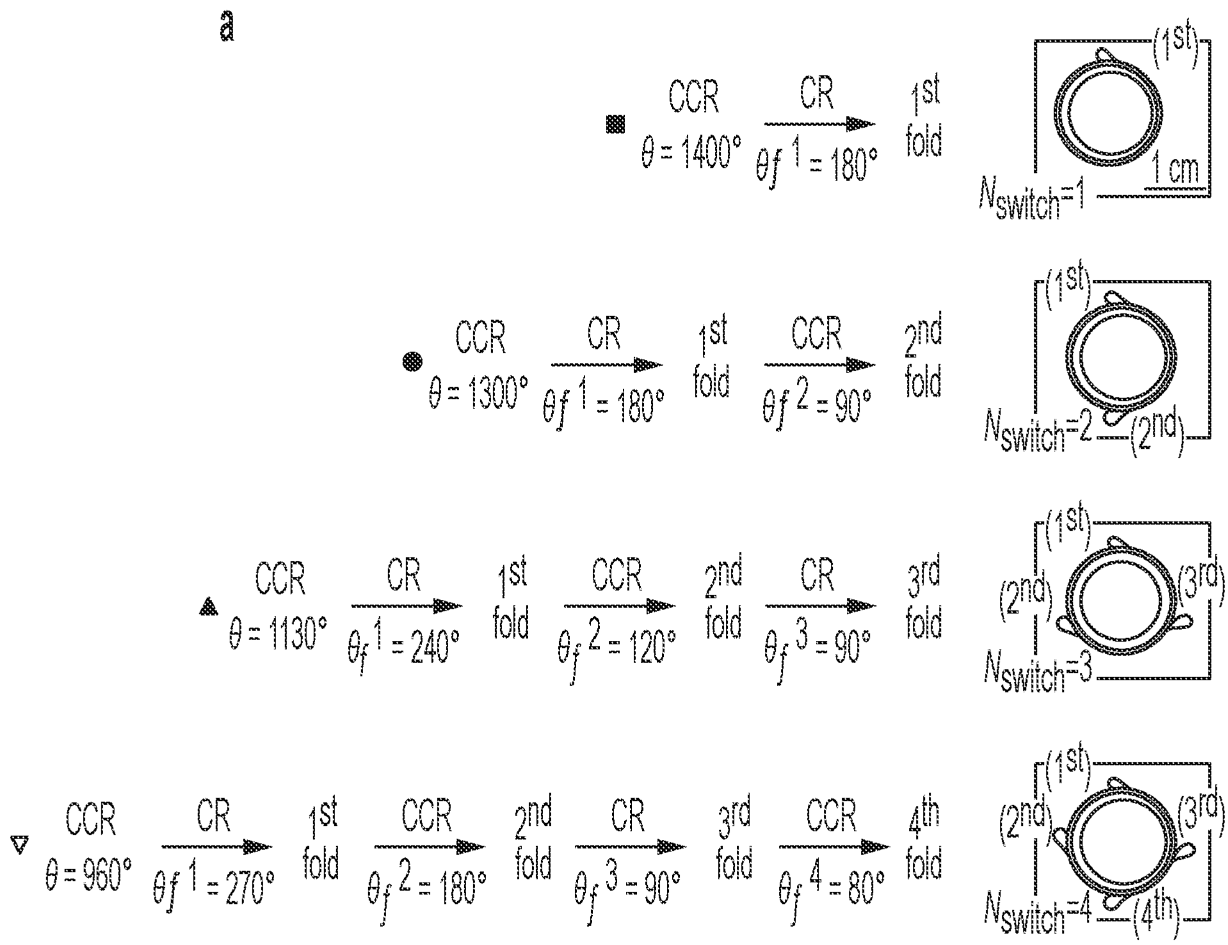

FIG. 20A

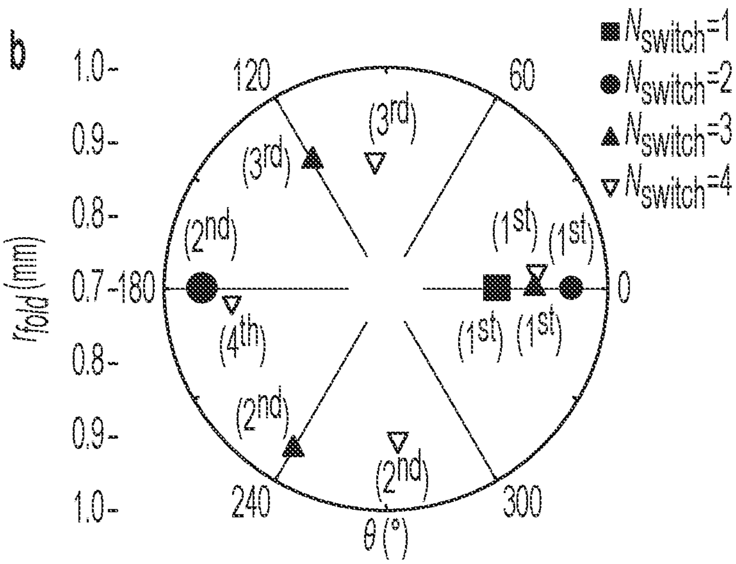

FIG. 20B

26/37

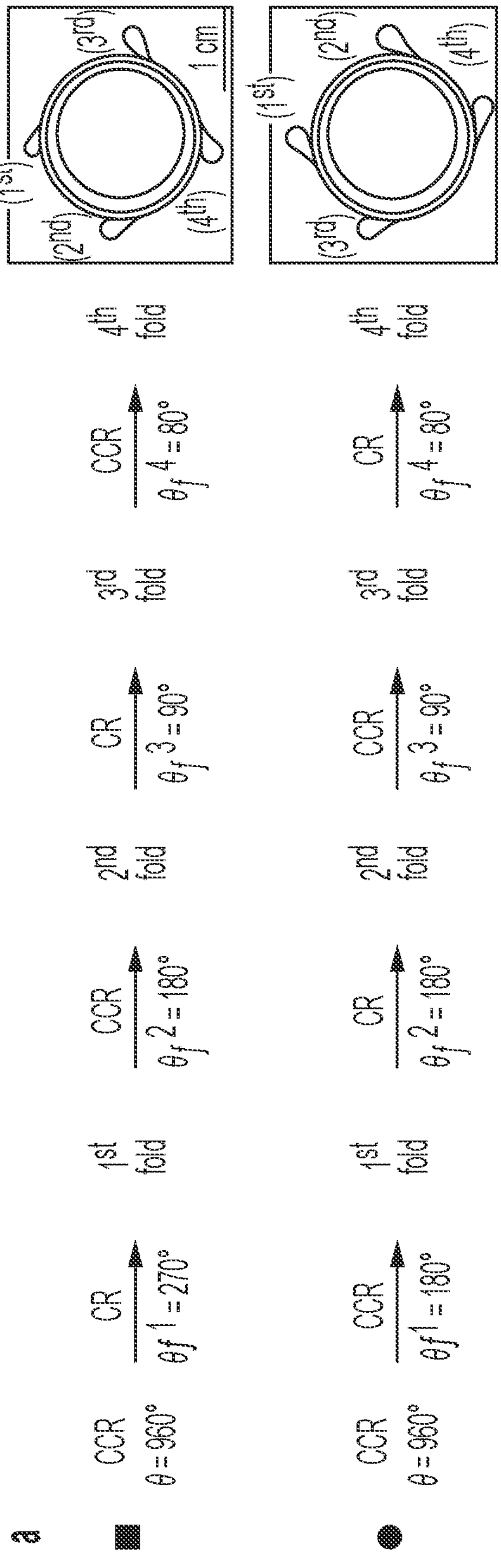

FIG. 21A

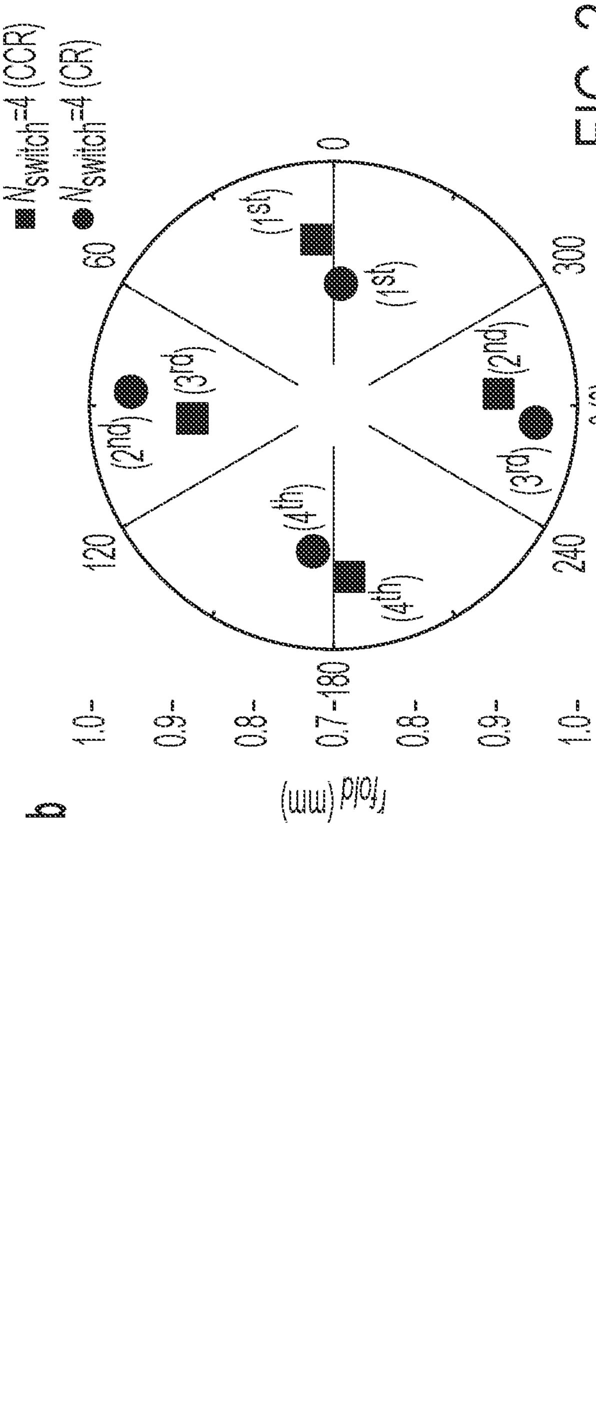

FIG. 21B

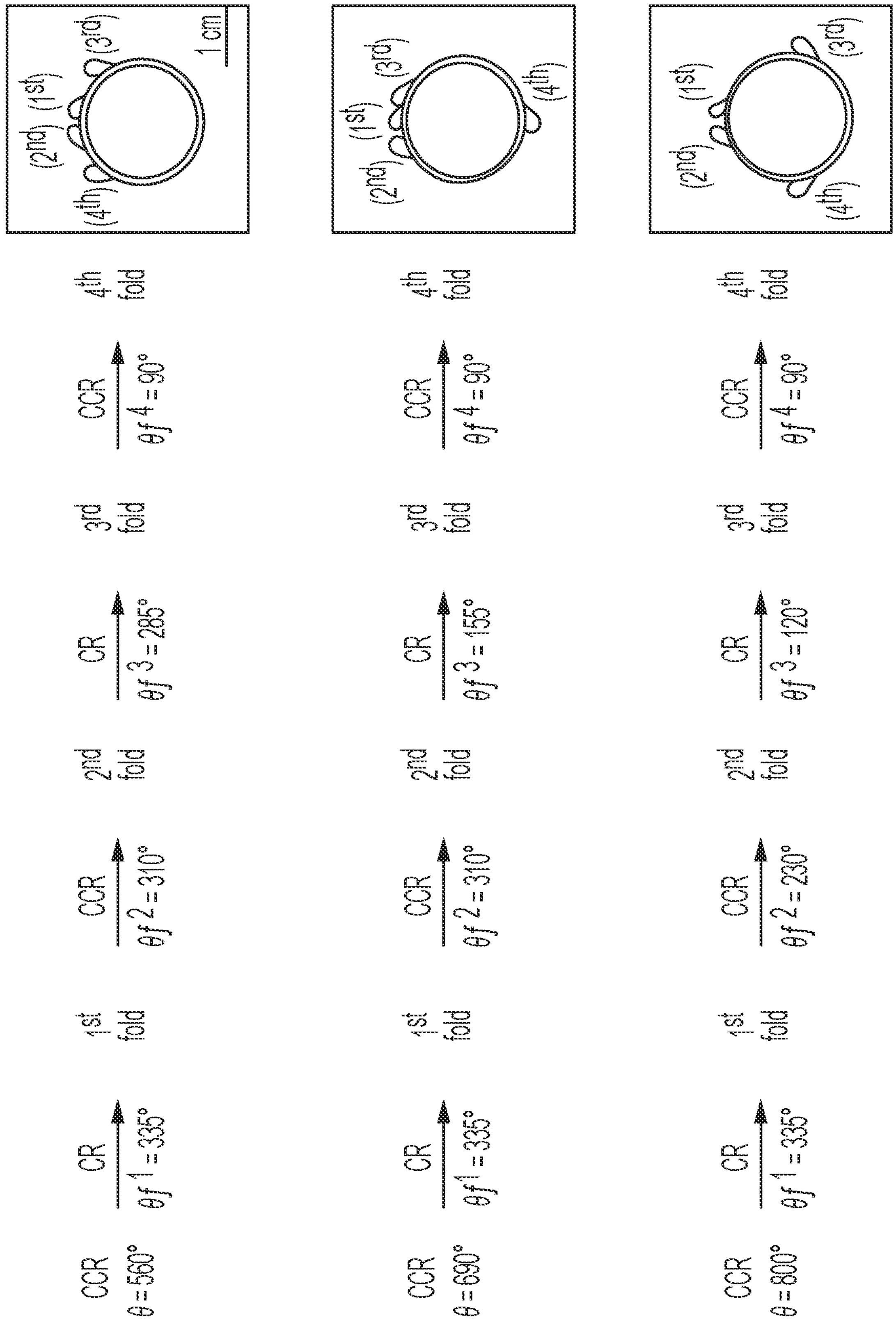
CCR
θ = 560°
CR
θf 1 = 335°
1st fold
CCR
θf 2 = 310°
2nd fold
CR
θf 3 = 285°
3rd fold
CCR
θf 4 = 90°
4th fold
(1st)
(2nd)
(3rd)
(4th)
1 cm
CCR
θ = 690°
CR
θf 1 = 335°
1st fold
CCR
θf 2 = 310°
2nd fold
CR
θf 3 = 155°
3rd fold
CCR
θf 4 = 90°
4th fold
CCR
θ = 800°
CR
θf 1 = 335°
1st fold
CCR
θf 2 = 230°
2nd fold
CR
θf 3 = 120°
3rd fold
CCR
θf 4 = 90°
4th fold

FIG. 22

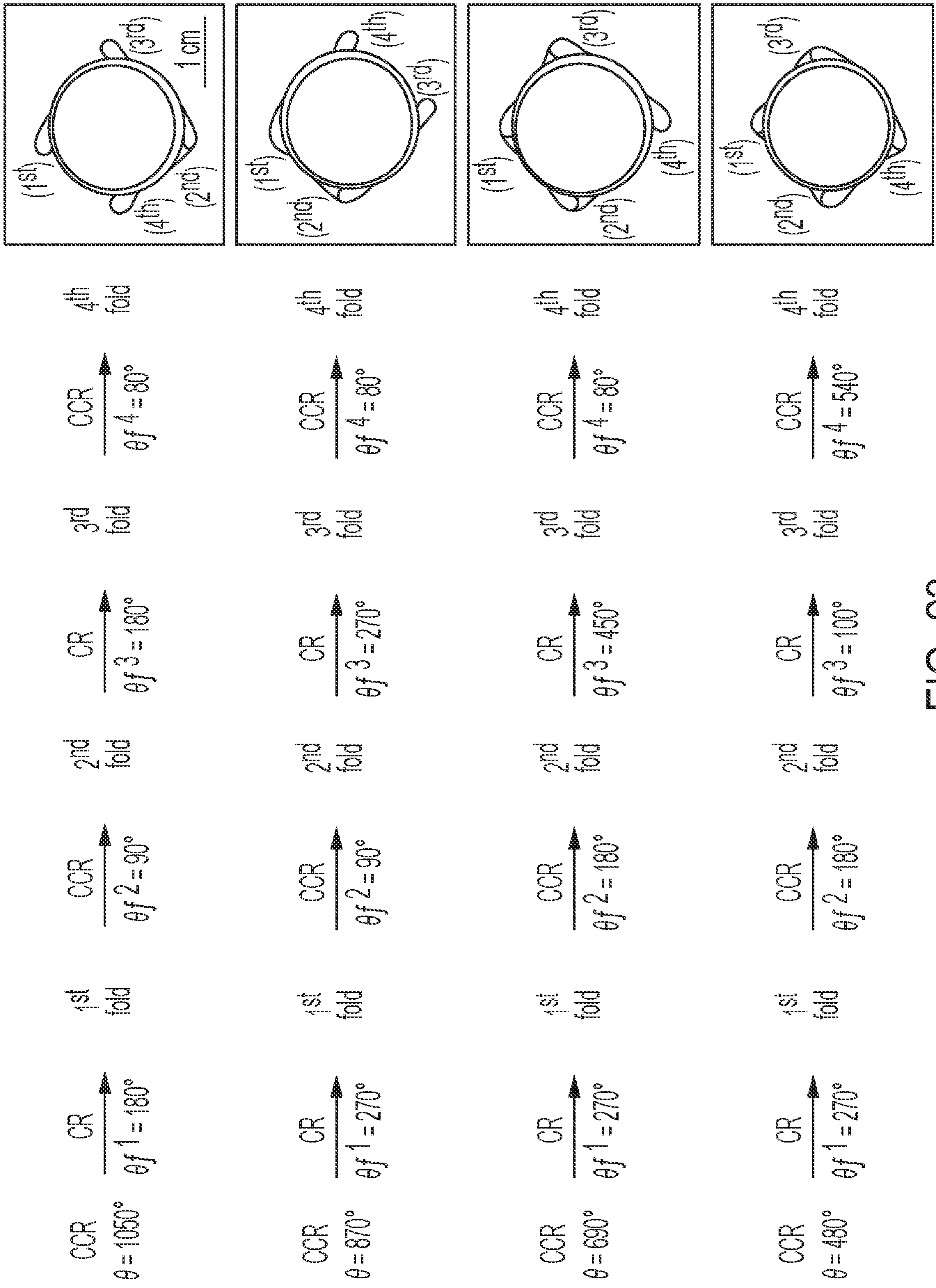
CCR θ = 1050°
CR θf 1 = 180°
1st fold
CCR θf 2 = 90°
2nd fold
CR θf 3 = 180°
3rd fold
CCR θf 4 = 80°
4th fold
(1st)
(2nd)
(3rd)
(4th)
1 cm
CCR θ = 870°
CR θf 1 = 270°
1st fold
CCR θf 2 = 90°
2nd fold
CR θf 3 = 270°
3rd fold
CCR θf 4 = 80°
4th fold
(1st)
(2nd)
(3rd)
(4th)
CCR θ = 690°
CR θf 1 = 270°
1st fold
CCR θf 2 = 180°
2nd fold
CR θf 3 = 450°
3rd fold
CCR θf 4 = 80°
4th fold
(1st)
(2nd)
(3rd)
(4th)
CCR θ = 480°
CR θf 1 = 270°
1st fold
CCR θf 2 = 180°
2nd fold
CR θf 3 = 100°
3rd fold
CCR θf 4 = 540°
4th fold
(1st)
(2nd)
(3rd)
(4th)

FIG. 23

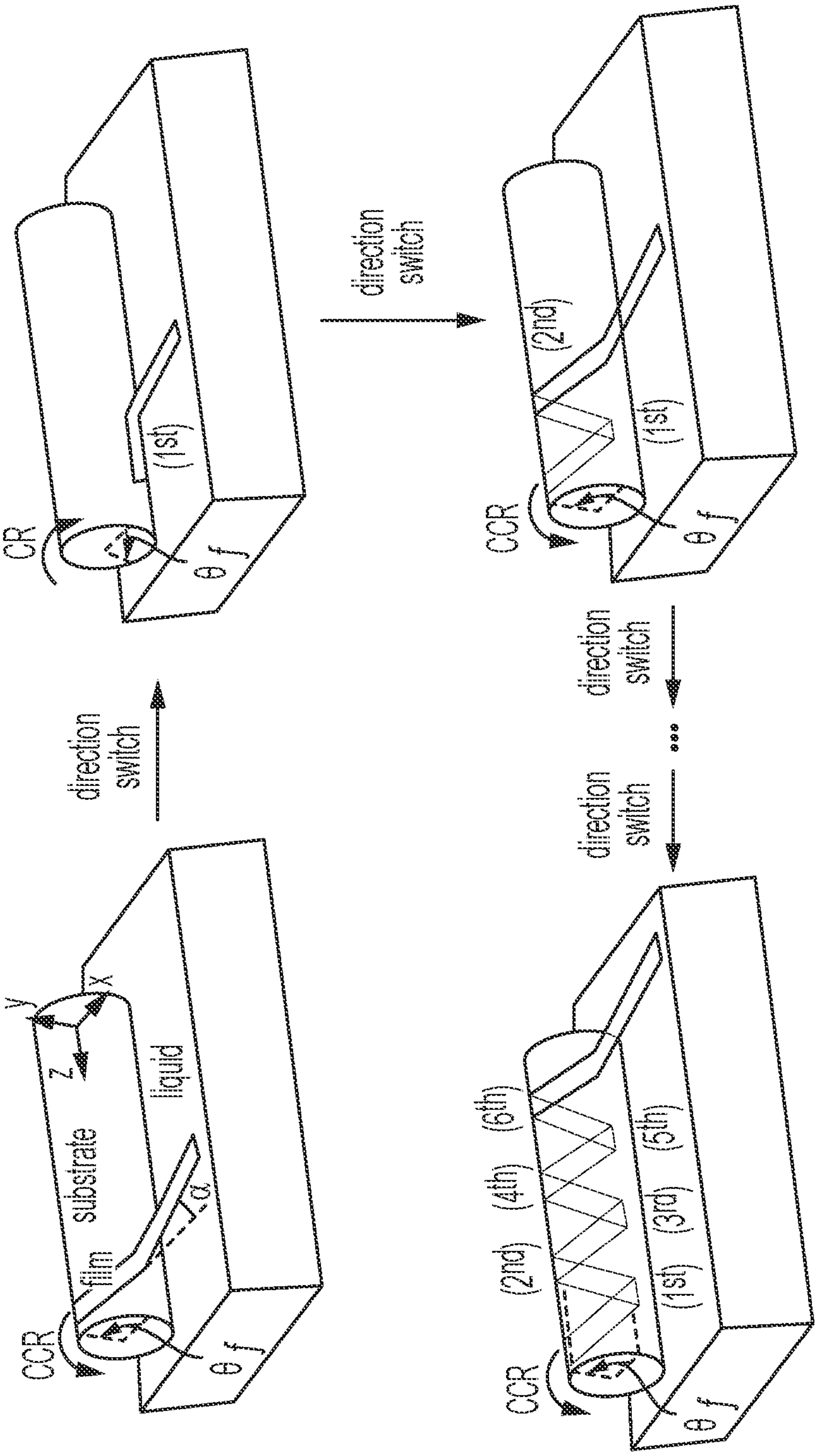
CCR
film
substrate
liquid
z
y
x
α
θ
f
direction switch
CR
(1st)
(2nd)
(3rd)
(4th)
(5th)
(6th)
...

FIG. 24

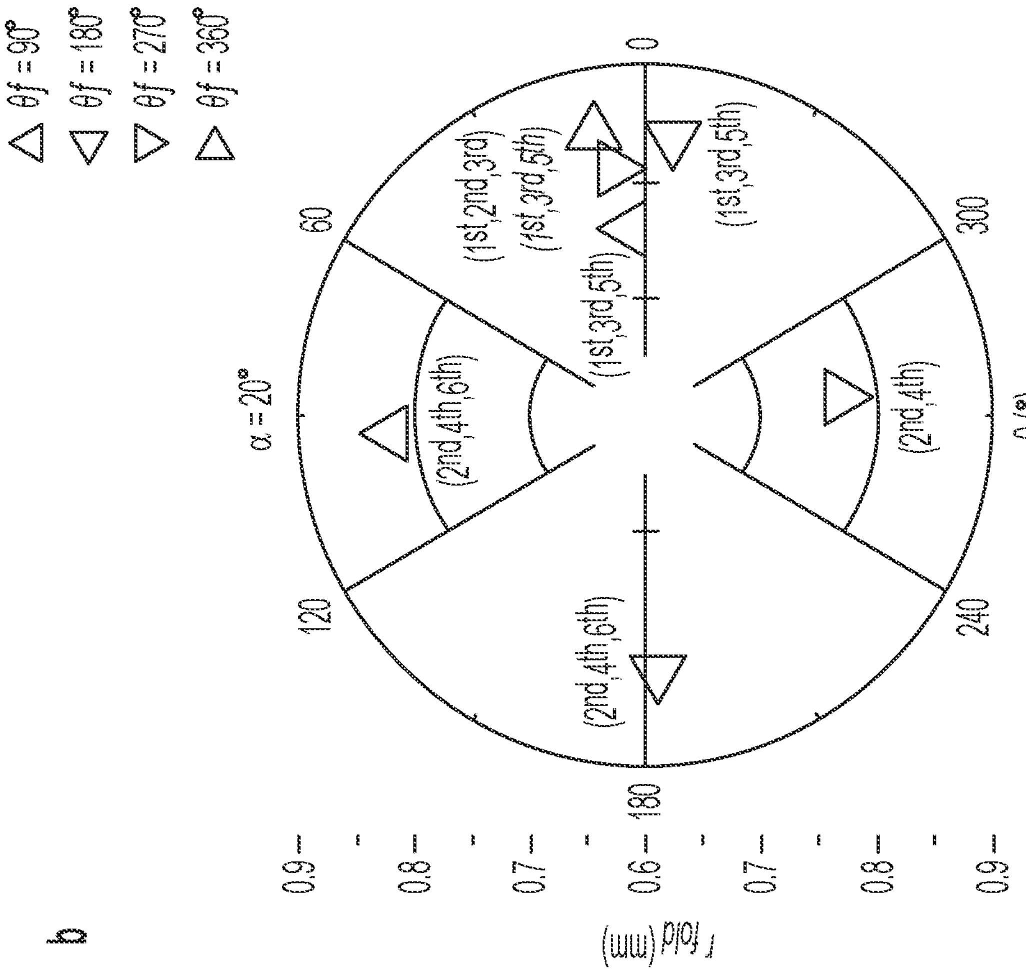

FIG. 25B

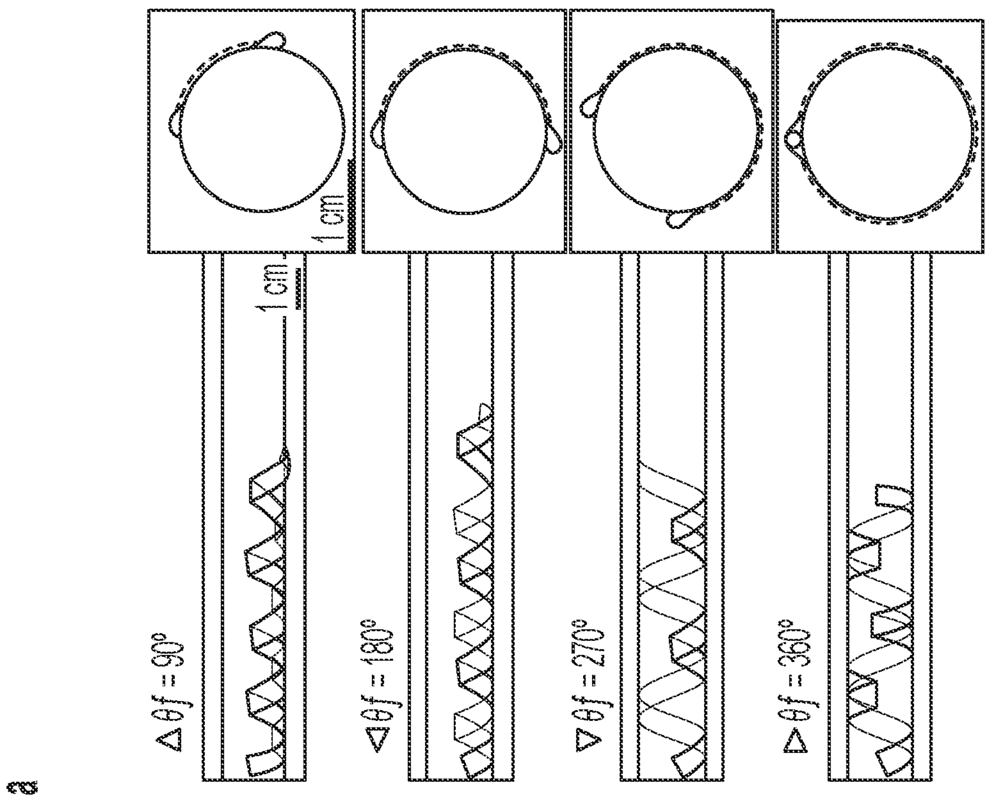

FIG. 25A

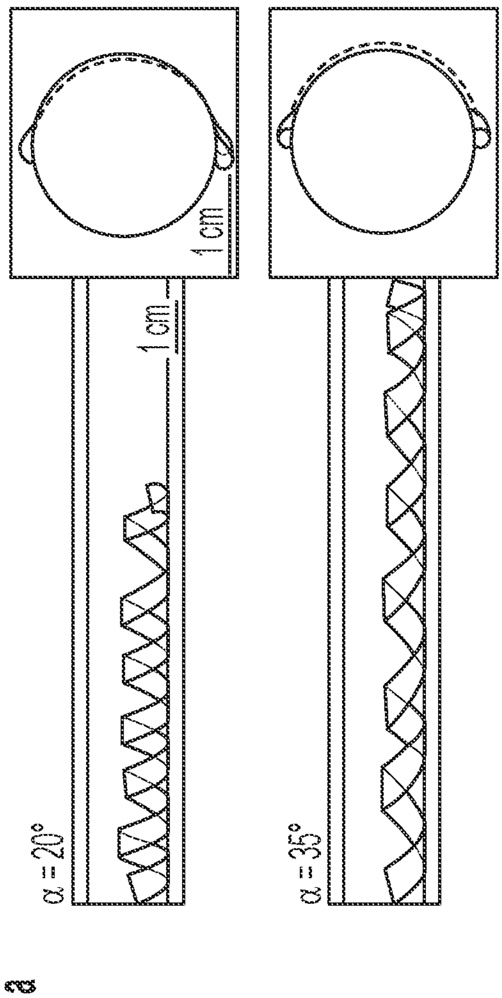

FIG. 26A

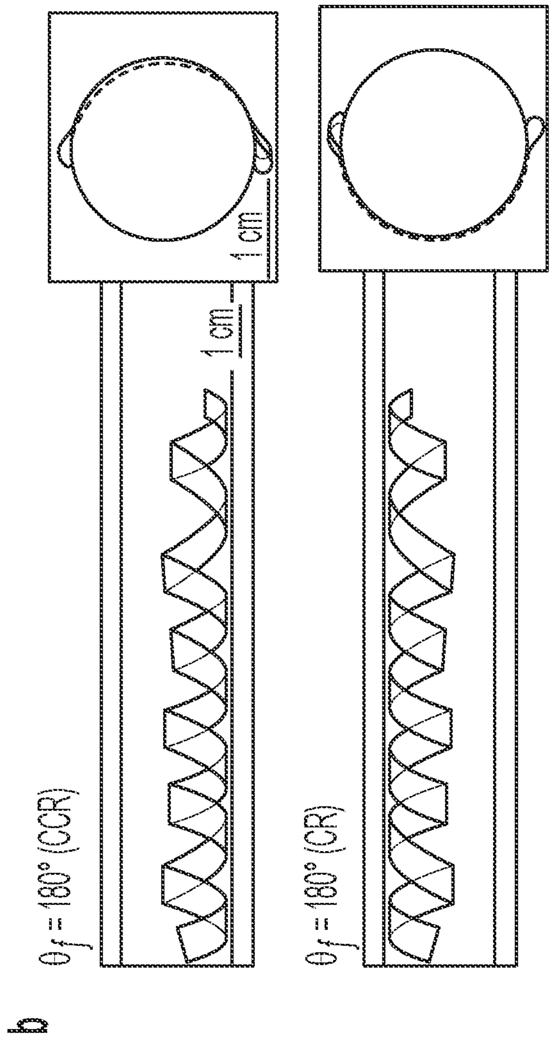

FIG. 26B

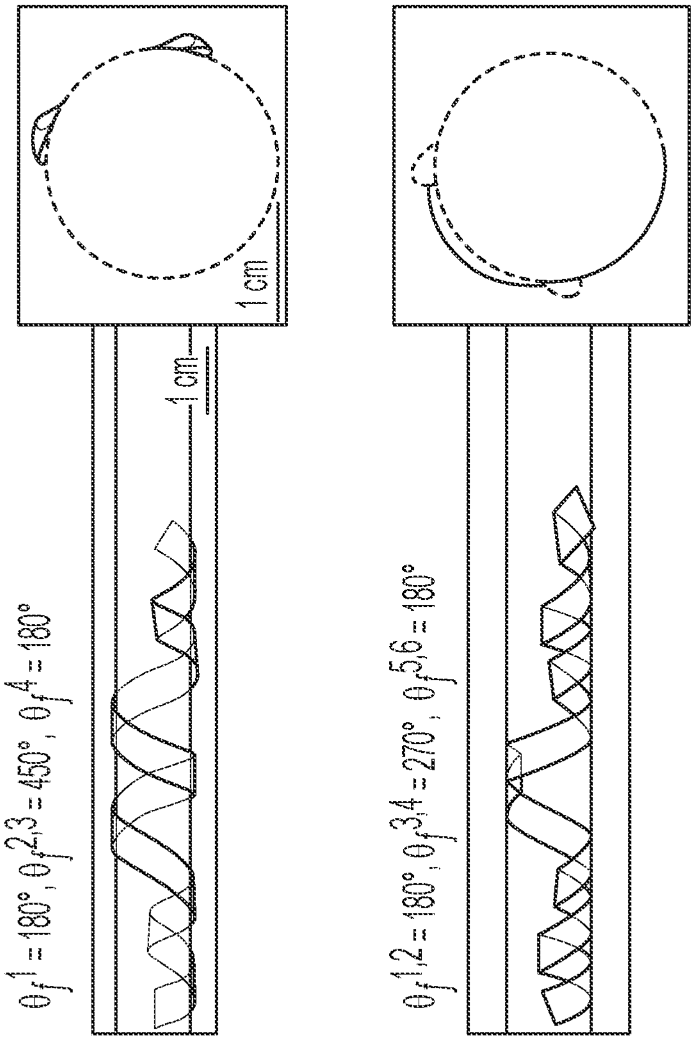
$\theta_f^1 = 180°, \theta_f^{2,3} = 450°, \theta_f^4 = 180°$
$\theta_f^{1,2} = 180°, \theta_f^{3,4} = 270°, \theta_f^{5,6} = 180°$
1 cm
1 cm

FIG. 27

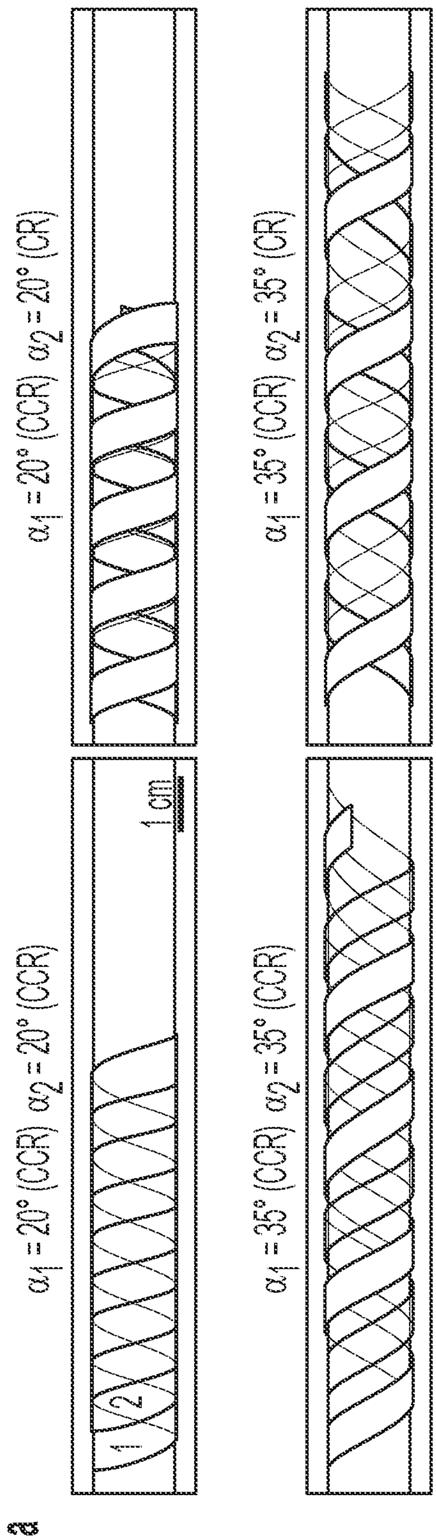

FIG. 28A

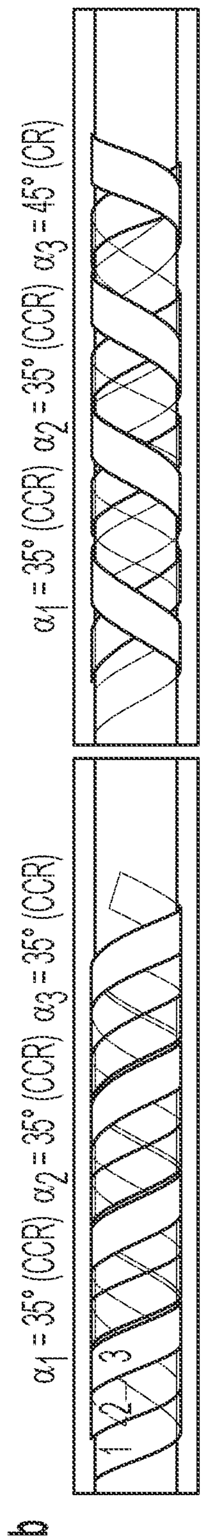

FIG. 28B

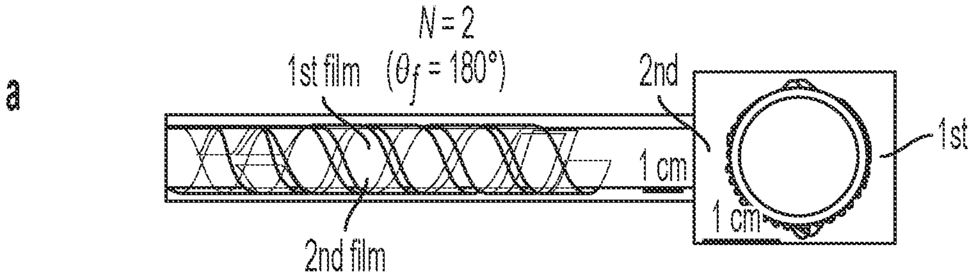

FIG. 29A

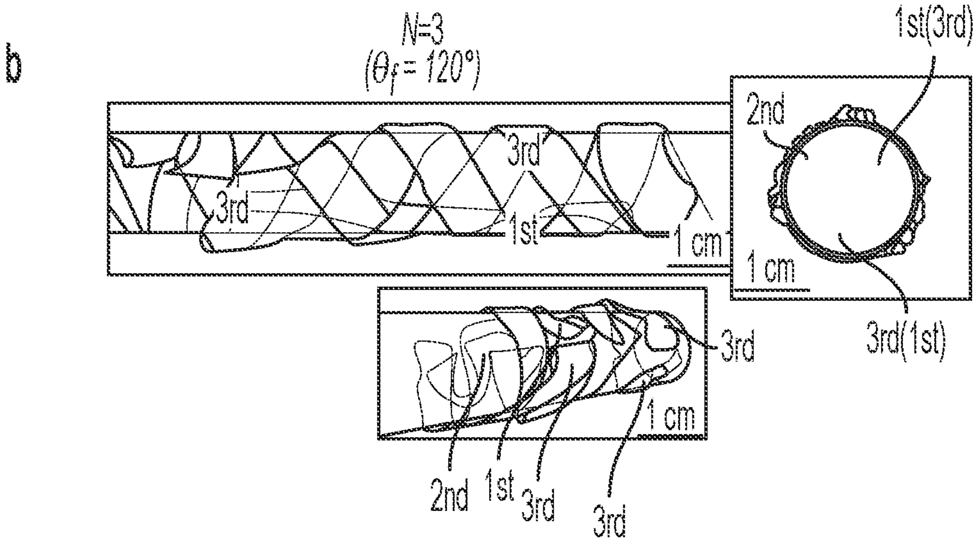

FIG. 29B

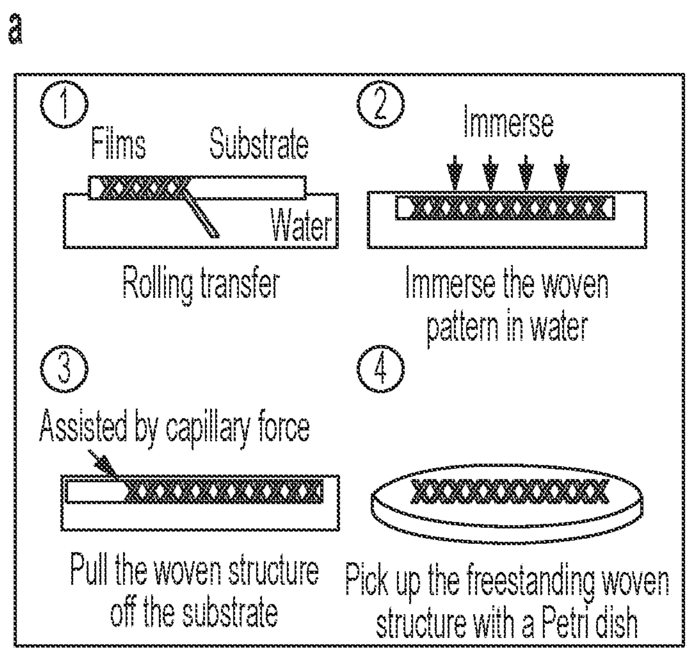

FIG. 30A

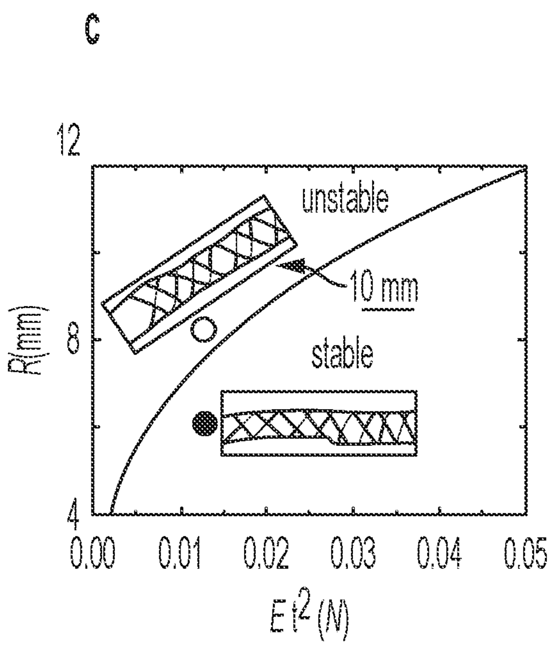

FIG. 30C

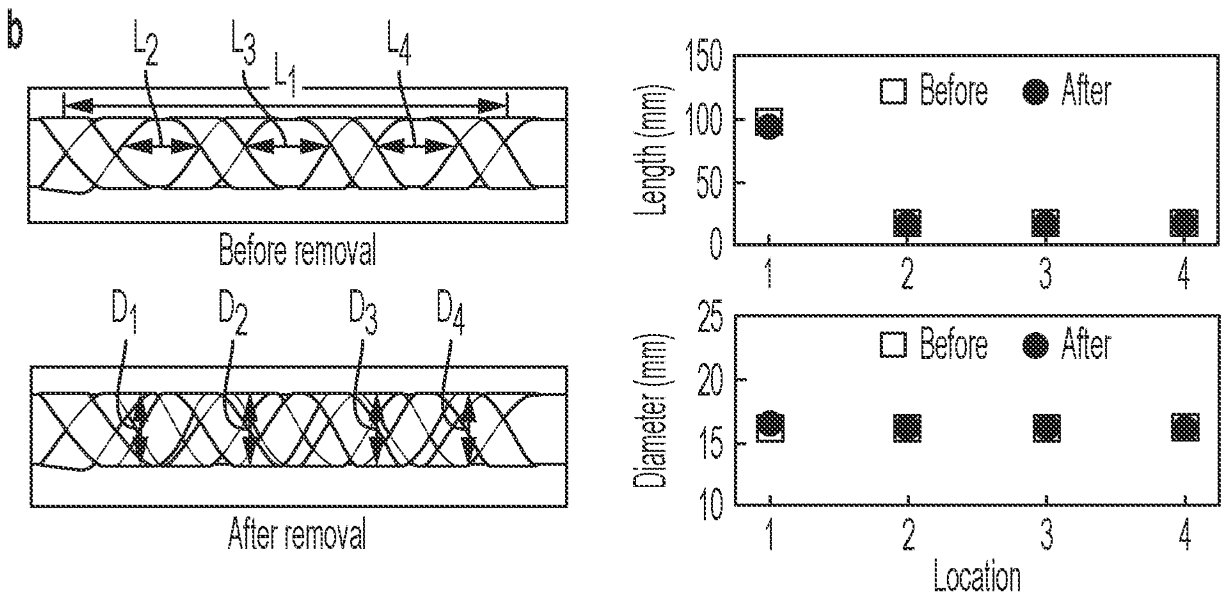

FIG. 30B

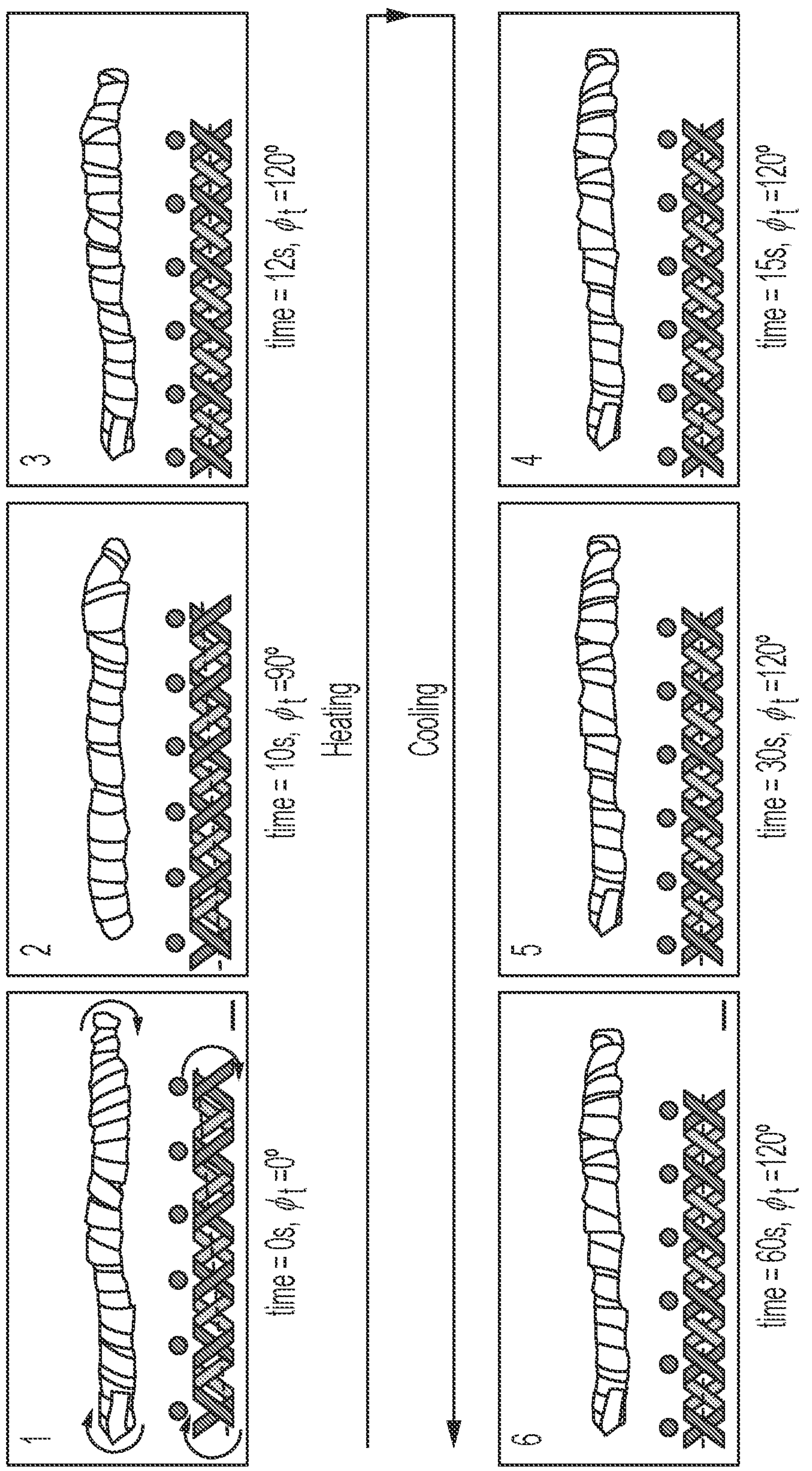
1
time = 0s, ϕ_t =0°
2
time = 10s, ϕ_t =90°
3
time = 12s, ϕ_t =120°
Heating
Cooling
4
time = 15s, ϕ_t =120°
5
time = 30s, ϕ_t =120°
6
time = 60s, ϕ_t =120°

FIG. 31

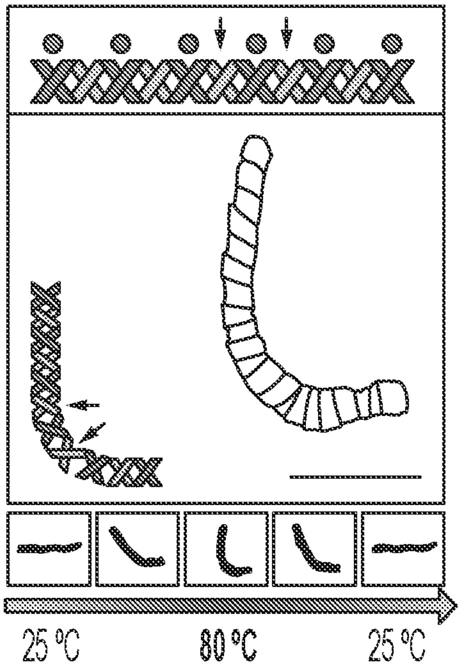

FIG. 32